# Model Predictive Controller for a Battery Energy Storage System to reshape the energy demand curve of an office.

**Case study: office in the Netherlands.**

## Master Thesis

K.J.H. Reinders

Monday 31st October, 2022

**Supervisor information:**

| | |
|---|---|
| Chair of Committee: | Prof. ir. W. (Wim) Zeiler |
| Second Committee Member: | Dr. ir. S. (Shalika) Walker |
| Third Committee Member: | ir. J. (Joep) van der Velden |
| Institution: | Eindhoven University of Technology |
| Place: | Faculty of Building Physics and Services |
| Specialisation: | Building Services |
| Project duration: | February 2022 - October 2022 |
| Company: | Kropman Installatietechniek |

**Final version**

# Model Predictive Controller for a Battery Energy Storage System to reshape the energy demand curve of an office.

---

Case study: office in the Netherlands.

**Author:**
K.J.H. Reinders
1461680

**General information:**
University: Eindhoven University of Technology
Department: Built Environment
Master program: Architecture, Building and Planning
Track: Building Physics and Services

**Course information:**
Course code: 7S45M0
Study Load: 45 EC
Date of graduation: 31-10-2022

**Graduation supervision committee:**

| | |
|---|---|
| Chair of Committee: | Prof. ir. W. (Wim) Zeiler |
| Second Committee Member: | Dr. ir. S. (Shalika) Walker |
| Third Committee Member: | ir. J. (Joep) van der Velden |

This thesis is open to the public and has been carried out in accordance with the rules of the TU/e Code of Scientific Integrity.

_ _ _ _ _ _ _ _ _ _ _ _ _ _ _ _ _ _ _

Signature Chairperson

# Preface

I hereby present my thesis for the master's programme Building Physics & Services at Eindhoven University of Technology. This thesis is a cooperation between Kropman Installatietechniek and the department of Building Services at the faculty of the Built Environment. Practising my skills in energy systems, building services and data science during courses led me towards an amazing opportunity of doing my thesis research at one of the office buildings of Kropman. This challenging project broadened my knowledge as before I started my thesis I had little knowledge of control systems and electrical engineering. The practical implementation of my results motivated me to learn and understand the procedures and triggered my curiosity within these fields.

I would like to express my gratitude to all people who have assisted me during these past nine months. First of all, I would like to thank prof. W. (Wim) Zeiler of the TU/e and ir. J.A.J. (Joep) van der Velden from Kropman for providing me with the opportunity to do my graduation project at a real office of Kropman. The suggestions and knowledge provided triggered my thoughts and pushed my results to the next level. I would also like to thank my supervisor Dr. ir. S.S.W. (Shalika) Walker for the generous feedback, the time she invested in the development of my skills and for connecting me with people from her network to share knowledge on topics of interest.

Furthermore, I would like to thank Shobhit Chitkara for helping me define the scope of my research and my planning. Special thanks to Jan-Willem Dubbeldam and Mark Lambert for their time and assistance with the implementation of my controllers within the BMS. Regarding the practical knowledge of the office building and the BESS, I would like to thank Roel Vos and John Verlaan for their time and hands-on explanation. I would like to thank Bram Hermans from TU/e and Nanda Panda MSc from TU Delft for assisting me with the mathematical equations and optimization, and I want to thank Ward Somers from TU/e for his suggestions, time and feedback regarding the forecasting models.

I would like to thank my friend Luc van Koelen from TU Delft for his insights and suggestions regarding my thesis. I want to thank my friends from Utrecht for providing me with ideas for my thesis outside the field of engineering. I would like to thank my girlfriend for her patience during days when I worked late and her continued support in me chasing my dreams. Lastly, I want to thank my parents for always having my back and supporting my educational journey from Mbo engineering to Technical University.

Koen Reinders

Utrecht, October 2022

# Nomenclature

## Abbreviations

| Abbreveration | Definition |
|---|---|
| AP | Atmospheric pressure |
| B4B | Brains4Buildings |
| BESS | Battery energy storage system |
| BMS | Building management system |
| CMS | Continuous monitoring system |
| CV_RMSE | Coefficient of variance of the root mean square error |
| DSM | Demand-side management |
| EV | Electric vehicle |
| FDD | Fault detection & diagnosis |
| FF | Flexibility factor |
| FI | Flexibility index |
| GHI | Global horizontal irradiance |
| HVAC | Heating, ventilation and air-conditioning |
| KPI | Key performance indicators |
| MAPE | Mean average percentage error |
| MCDA | Multi criteria decision analysis |
| ML | Machine learning |
| MPC | Model predictive control |
| PID | Proportional-integral-derivative |
| PMV | Predictive mean vote |
| PPR | Power peak reduction |
| PPRP | Power peak reduction percentage |
| PV | Photovoltaic (generation) |
| PWAT | Precipitable water |
| RES | Renewable energy sources |
| RH | Relative humidity |
| RPC | Remote procedure call |
| SC | Self-consumption |
| SHAP | Shapely additive explanations |
| SOC | State of charge |
| SRI | Smart readiness indicator |
| SS | self-sufficiency |
| TEMP | Temperature |
| ToU | Time of use |
| VIF | Variance inflation factor |
| WS | Wind speed |

# List of Figures

# List of Tables

# Abstract

On a global scale, the transition from fossil fuels to renewable energy sources introduces new challenges for the real-time balancing of supply and demand of the electricity grid. As buildings are responsible for approximately 35% of the energy use worldwide, demand for energy saving measures and smart control strategies increases. This research contributes to the development of smart control strategies using model predictive control (MPC) to optimally schedule the battery energy storage system (BESS) with locally produced PV electricity. Most MPC applications within the literature only focus on simulations and practical implementation is often not considered. Therefore, the added value of this study is the development of a simplified MPC and real-time implementation of the controller within the building energy management system of an office building to identify general challenges during the implementation. For the simulation study, along with BESS and PV, the effect of EV load is also included. Real-time implementation was performed to optimally balance the building electricity load with PV production while taking charging and discharging currents of the BESS as the controlled signals from the MPC. Within this research, machine learning forecasting models are created to predict the building load and Solargis was used to obtain the solar generation predictions. The added benefit of MPC is emphasized and compared with flexibility KPIs developed by IEA Annex 81 and with the smart readiness indicator. This study successfully demonstrates the possibility of implementing MPC within the built environment. Moreover, implementing MPC significantly increases the smart readiness of a building with regards to electricity, however, the building as a whole and the comfort of its users are nevertheless as important.

# Contents

# 1. Introduction

Chapter 1 presents an introduction to the thesis topic. Paragraph 1.1 presents a short introduction to the relevance of the topic as well as the research motivation. Paragraph 1.2 provides the research approach, objective, and questions for this thesis. Last, paragraph 1.3 provides the thesis outline.

## 1.1 Research Motivation

Buildings are expected to have an important role in future scenarios as buildings in 2020 were responsible for approximately 35% of the global energy use [1]. In addition, more than 50% of the existing residential buildings and 40% of the offices were built before 1970 [2]. Since older buildings use more energy, energy saving measures are becoming even more important. On a global scale, greenhouse gas emissions are rising and if no significant changes are made, this trend is estimated to continue. The Netherlands has introduced energy transition strategies to reduce these emissions [3]. However, it is expected that the energy transition will bring new challenges for future scenarios. The International Energy Agency states that the contribution of fossil fuels in the total energy mix is approximately 80% in 2021 [4]. However, renewable energy sources (RES) are estimated to provide a dominant share in future scenarios. The introduction of RES such as wind- and solar energy ascends power variation as production is dependent on prevailing weather conditions. This is one of many factors which will affect the stability of the future energy grids [5].

This thesis contributes to work package 2: Intelligent energy flexibility control strategies from the Brains4Buildings (B4B) initiative. B4B is a multi-year, multi-stakeholder project focused on developing methods to harness big data from smart meters, building management systems (BMS), and the Internet of Things devices, to reduce energy consumption, increase comfort, respond flexibly to user behaviour and local energy supply and demand, and save on installation maintenance costs [6]. B4B activities are part of an open innovation methodology wherein students, PhDs and (young) professionals publish work and allow contribution with companies to improve business cases and the built environment as a whole. It is necessary to improve the energy performance of buildings' heating, ventilation, and air-conditioning (HVAC) increases due to its great portion of the total energy demand. HVAC systems are most commonly controlled by rule-based- or proportional-integral-derivative (PID) controllers because of their simplicity to maintain setpoints and requirements of human satisfaction [7]. In contrast to the PID controller, more complex control systems such as model predictive control (MPC) determine actions in a system not only for the current state but also for the actions that a system will have in future states. The development of MPC requires defining a scope and optimization problem which is solved and control outputs are implemented within a specific case.

As research on the topic of complex control strategies increases, this study will contribute to the topic by investigating the development of an MPC to reshape the building energy profile and achieve energy flexibility. The change from momentarily control towards model-based control shifts the challenges of energy reduction from simple renovation towards more complex solutions. Complex control systems introduce variables such as occupancy behaviour and seasonal weather change which all drastically influence building performance. As buildings are known to show little repetition in their characteristics, complex strategies are often tailored to a specific building, making solutions hardly scalable.

This study consists of a simulation and practical implementation where an office is used as a case study. This office has multiple building amenities, such as an on-site weather station, photovoltaic generation (PV), and a battery energy storage system (BESS) that are connected to the building management system (BMS) which allows monitoring and control. The main focus is to develop, simulate, implement and optimize an MPC for the case study. So far, within the literature, MPC has been used to improve energy flexibility and efficiency of building installations. However, the implementation of MPC within the built environment is hardly discussed. Therefore, this thesis mainly focuses on successfully implementing MPC within the built environment, adding knowledge to the literature about the implementation and contributing to work package 2 of B4B as this smart control method addresses increased energy flexibility.

## 1.2 Research Approach, objective and questions

As MPC comes in many forms and has a wide variety of applications, different strategies are investigated.

This research should give insights into the practical added value and implementation possibilities of MPC for energy flexibility in office buildings. A research question for this thesis is formulated, based on the literature review and query given by the company:

**How to implement model predictive control to optimize the interaction between building services and reshape the energy demand profile of an office?**

The following sub-research questions support the main question:

1. How to formulate the optimization problem?
2. What can be gained in terms of energy flexibility and process efficiency from implementing MPC within the built environment?
3. What are rule-based control strategies which can be implemented in comparison to using MPC?

## 1.3 Outline

The global outline of this thesis is presented as follows: Chapter 1, introduces the research problem. The objectives and research questions are presented. Chapter 2, gives an exploratory literature study and describes the applied method of this research for all components. The case study office is explained and an overview of all developed models is presented. The results of the different models in this research are presented in Chapter 3. The discussion of the results is discussed in Chapter 4, where the meaning, importance, and limitations of the results are presented. Chapter 5, concludes the research findings and recommendations for future research.

# 2. Methodology

The methodology of this thesis consists of four main paragraphs. First, in paragraph 2.1 a literature study is executed to introduce smart buildings and the theoretical background of MPC. Second, paragraph 2.2 describes the case study and the building characteristics. Third, in paragraph 2.3 the development process of all models within this research is presented. Lastly, evaluation methods are described in paragraph 2.4 and 2.5.

## 2.1 Literature study

### 2.1.1 State-of-the-art

Improving the corporation between buildings and their HVAC systems is essential in order to meet future requirements regarding energy savings and energy flexibility. As it is hard to specify a generic building, the universal term for a building that has sufficient cooperation with its systems is considered a smart- or intelligent building. These smart buildings work at their highest capacity in relation to the structure, system, service and management [8]. This can be achieved by ensuring a clever interaction between operations, user demand and behaviour. Smart buildings use sensors and actuators to monitor the weather and generate input data for the systems to rely on. With this data the building creates opportunities for learning capabilities to improve its performance and a proper interconnection with the electricity grid [9]. Ultimately, a building that meets user needs with as less human interference and energy consumption as possible, while maintaining a safe and high-quality indoor climate in combination with learning capabilities, is considered a smart building [10].

Multiple variables are to be considered in smart buildings. Modelling strategies are the bridge between theory and implementation [12]. Data-driven modelling and control of systems are currently undergoing a revolution, driven by the application of big data, advanced algorithms in machine learning (ML), and modern computational hardware [11]. Typically, MPC works by solving control problems on a certain horizon by taking given constraints into account and producing the next control action in a system. This optimization is repeated at each new timestep where the model sends feedback to itself to update the control law and learn from possible misjudgments. MPC is therefore considered to be one of the more powerful model-based control strategies due to the flexibility in objective definition and the ability to add constraints. In Figure 2.1, the light blue line shows the control input sequence which is optimized over the con-

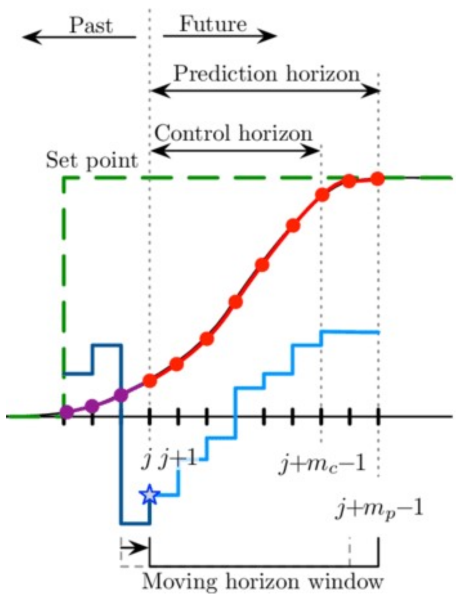


**Figure 2.1.** Schematic overview of MPC where an input value is iteratively optimized over a receding horizon. Figure obtained from: [11].

trol horizon based on the predicted future outputs (red line) to ultimately achieve the system driver (green line). The start of the sequence is demonstrated as the blue star where the purple- and dark-blue lines show past measurements of the system. The strength of MPC lies in its versatility as reinforcement- and ML models are improving rapidly over the years and computational power becomes less of an issue.

The mathematical principle of an MPC system consists of a prediction model, an objective function and obtaining the control law. The objective function of an MPC is also known as the cost function which is solved by using a mathematical model where it is subjected to constraints. This cost function is solved over a certain time horizon where time-varying parameters are added to the mathematical model. Typical time-varying parameters used in MPC are energy price, comfort criteria, occupancy presence and weather predictions. In summary, the goal of the control problem is to minimize the overall cost while satisfying various constraints [13]. This problem is in generality expressed as:

$$\min_{u_k} J \sum_{k=1}^{N} (x, u) \tag{2.1}$$

Where $x$ contains the state of the system, $u$ contains the control decisions to be made, and $(x, u)$ are the various costs and penalties which should be minimized.

Important to note is that when MPCs are implemented, the prediction horizon $N$

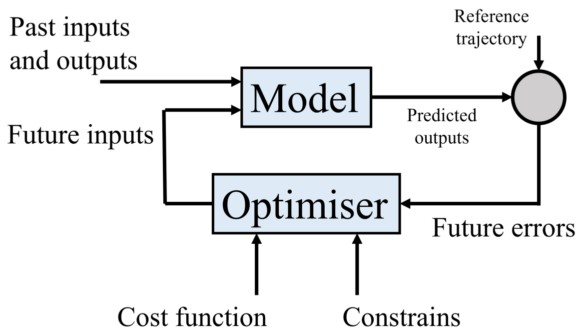


**Figure 2.2.** Overview of MPC relationships.

is added within the mathematical model where only the first control step of this time horizon is employed. This horizon is receded step-by-step over the total duration of time. Here a prediction is made, and the optimization problem is solved again resulting in an iterative process.

### 2.1.2 MPC strategy evaluation

MPC is widely applied in numerous fields. In this study, building-related review papers exploring MPC are investigated to overview multiple strategies.

The beginning of MPC can be traced back to the work of Kalman in the early 1960s and was mostly applied in the oil- and chemical sector in the 1980s [14]. In more recent years, due to its rapidly increasing popularity, MPC found its usefulness in the power- and energy sector. Problem-solving with MPC within the built environment is known to exist since the 21st century. Research by Mossoly et al. compared conventional HVAC control with fixed setpoints and temperatures with two control strategies. In these strategies supply temperature, fresh air amount, air supply rate and predicted mean vote (PMV) were included [15]. The objectives of MPC in relation to buildings are focused on optimisation purposes such as management of on-site renewables and the interaction with HVAC- and energy storage systems [16]. Algorithms such as MPC can have an average energy saving potential of 15 to 20%. An essential first step when MPC is implemented in a building is to generate a control-orientated building model which demonstrates the physics and interaction between all building services, measurements and connections. This step clarifies disturbances such as weather influences, occupant behaviour and time-of-use (ToU) regarding energy consumption. Maintaining occupant comfort while minimizing the energy costs of all systems is the challenge where ultimately these performance indicators are achieved with the least amount of computational time. Therefore, challenges for implementing MPC strategies are in the interconnection of complex systems and models to building operations. Therefore, one of the main challenges for MPC in buildings lies within the integration of the algorithm in the application of the building services.

In literature, a distinction between different theoretical approaches of MPC is addressed as white-box, black-box and grey-box approach [17]. White-box models describe the physical knowledge dynamics of a building. They are based on principles of physical processes such as heat-, energy- and mass transfer. Accordingly, input parameters for white-box models are obtained from technical documentation regarding geometry, material properties and equipment. In contrast to white-box models, black-box models learn dynamics from measured data without prior knowledge regarding physical relationships. Black-box models require extensive training data and become more uncertain when working with small samples of data. The grey-box models represent a combination between simplified physical relationships and measured data. However, compared to white- and black-box models, their development costs are usually lower [18]. The physical aspects of grey-box models are often simplified, or reduced to save development time and costs. A general methodology for modelling, design and implementation of MPC is given in 2.3.

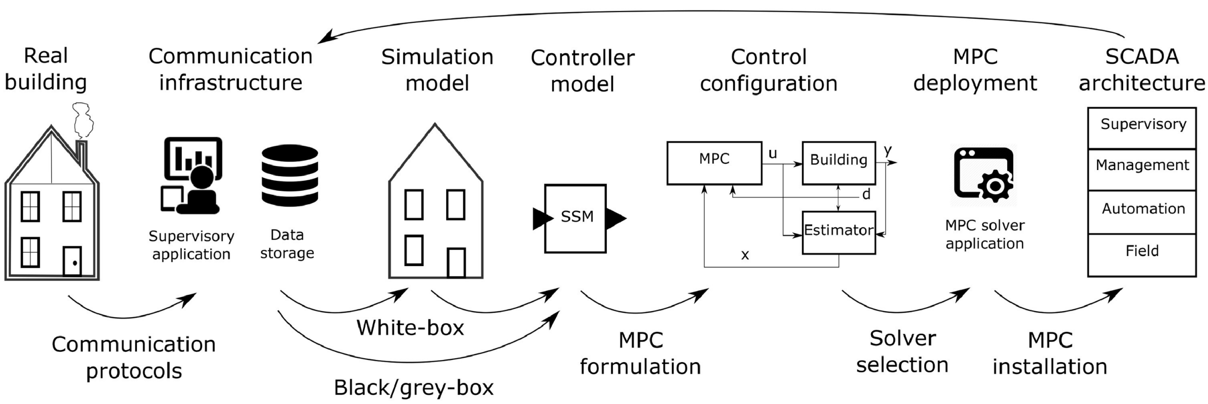


**Figure 2.3.** A general step-wise methodology for MPC in buildings obtained from: [17].

These three different model approaches are all forms of MPC and have a challenge as the frequency of the input variables is often not identical. Different measurement- or sampling times are present inside the building which typically range between intervals of 5 to 60 minutes. For each of the MPC strategies to succeed, the investigation and manipulation of data are of major importance. It should be noted that data manipulation introduces uncertainties in the final model and therefore validation is key. Another challenge associated with MPC is determining which of the approaches is most suitable for a specific building. An example suggested in the literature is using multi-criteria decision analysis (MCDA) which could support this decision-making process [19]. Another challenge is the sensitivity of the MPC. As MPC is often tailored to a specific case study, a broad range of factors such as computational time, forecasting uncertainty and soft- and hardware availability make objective comparison difficult.

### 2.1.3 Previous application of MPC

To complement the strategy evaluation, case studies were evaluated based on search criteria in scientific journals, being: *model predictive control; model-based optimization; energy saving; control of HVAC; building management strategies; smart buildings.* The structure of this paragraph consists of a brief historical timeline of MPC within the built environment.

As discussed in the previous section, conventional control strategies in buildings are based on maintaining required temperatures in zones by varying parameters of a building's HVAC. Individual performance indicators such as indoor air quality and thermal comfort are therefore the most important drivers regarding the energy consumption of the building services. Work by Mossoly et al. showed two control strategies where conventional control is compared with variable control strategies [15]. Their paper proved the enhancement of evaluating multiple variables in order to improve indoor air quality and thermal comfort to demonstrate a change of thinking about how control strategies can be used.

Recently, other applications for HVAC control systems, such as demand-side management (DSM) and fault detection & diagnosis (FDD) are widely discussed in combination with MPC [20]. Due to computational power becoming less of an issue, data-driven solutions are becoming more accessible. Research by Putta et al. states that incorporating information such as weather forecasts and occupancy profiles in combination with real-time decision-making makes MPC highly advantageous [21]. As previously mentioned, there are three different model approaches for MPC, being: white-, black and grey box. For each model approach, an application to buildings is given.

First, a white-box model is used by Salakij et al. to foresee and evaluate energy utilization in non-residential buildings in the beginning phase of building development [22]. Their research showed a simple mathematical approach to creating a white-box model. However, the white-box model is embedded to optimize design parameters and shapes rather than using it as a control strategy and only one specific climate region was considered.

Second, a black-box model was executed by Fan et al. [23]. Data-driven ML solutions were implemented in a case study where a control system synchronizes the HVAC, BESS and renewable energy generation. Trade-offs between different ML models include model complexity and interpretability. Moreover, the importance of prediction performance accuracies with black-box models is emphasized. An important side note in their research is that they did not include thermal comfort models inside the building. Their optimization was focused solely on solving the synchronization problem.

Third, in literature by Merema et al., a grey-box model is used to control an all-air system for an educational building [24]. Inside this building, CO2 is monitored in combination with operative temperature. The building has an extensive BMS and it uses its own measurements of weather data as a weather station is located on the roof of the building. This paper presents a method to implement a predictive control for a smart controlled ventilation system in an educational building.

Besides different model approaches for MPC, MPC can also be categorised in regard to energy flexibility. Three main categories are presented below;

1. On-site energy generation in combination with energy storage are used to facilitate peak load shaving- or shifting. The majority of the literature aims to optimize energy systems and demand response of buildings using MPC [25].

2. Using MPC to optimize the use of building mass by activating mass- and heat storage of the building's construction [26].

3. Thermal comfort of occupants in buildings can be optimized. Especially MPC is a powerful solution as thermal comfort optimisation requires multiple constraints and MPC is typically known for its versatility as many constraints may strengthen the model [27].

Almost all of the previous applications of MPC mentioned are simulations and not practical implementations. Therefore, a need to contribute research towards practical implementation is desirable.

## 2.2 Case study: Office building

### 2.2.1 Schematic overview and data acquisition

Defining the specification of the office is an important first step, which is done by mapping all relevant meta information. The building is built in 1993 and has a floor area of approximately 1500 $m^2$. Figure 2.4 presents a schematic overview of all the different building services as well as the control software applications of the office. This section will elaborate on the interaction between all systems.

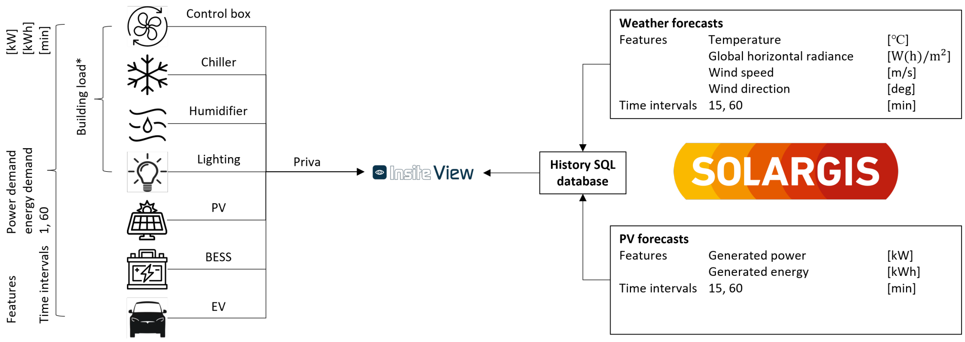


**Figure 2.4.** Schematic overview of the office building.

The case study is using weather forecasting models provided by the company Solargis.

The forecast contains estimations of diffuse and global irradiance, PV generation, temperature, wind direction and wind speed with a 15 or 60 minute interval. The case study has a maximum occupancy count of 35 people. Data is perceived using the building management system and continuous monitoring system of the case study building. The continuous monitoring system (CMS) which is named InsiteSuite can be used for multiple building automation purposes such as real-time monitoring of building performance, data analysis and reporting, fault detection, remote control and various forms of demand prediction to allow buildings to self-operate. As InsiteSuite is the central data collection element of the case study, the Priva BMS processes all data obtained from meters in the building to the CMS. Moreover, weather data measurements are obtained by the weather station on the roof of the building. The 65 PV panels on the roof generate electricity which is used in the building up to a maximum capacity of 16.9 kWp. When generation exceeds usage, the electricity is transferred back to the electricity grid using net metering. The case study building has four charge parking spots for electric vehicles (EVs). Furthermore, the building contains a Nilar NiMH BESS with a maximum storage capacity of 57.6 kWh. This BESS can be operated by either charging or discharging using surplus electricity from the PV panels or the electricity from the grid. The interconnection of the electricity microgrid is visualized in Figure 2.5.

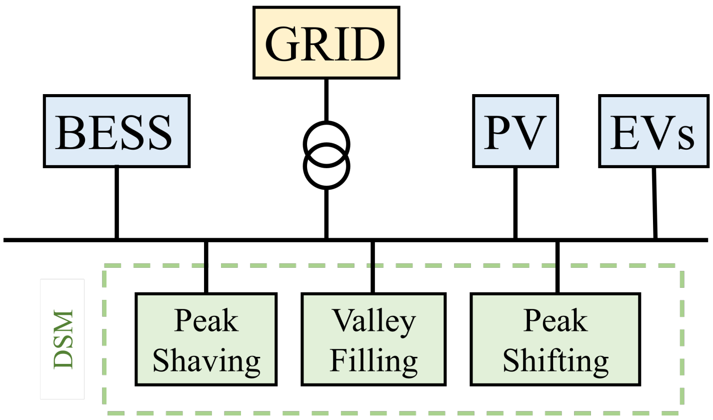


**Figure 2.5.** Visualization of the electricity microgrid.

## 2.2.2 Model objective identification

To implement an MPC for this case study it is of major importance to identify the objective function. In this study, the interest is developing an MPC which optimizes the BESS by reshaping the building's energy profile and achieving energy flexibility.

### Reshape the energy demand profile

A variety of techniques are known to reshape the energy demand profile [28, 29]. Six general demand side management strategies are shown in Figure 2.6 where three classic forms of load management are further discussed.

1. Peak clipping or peak shaving represents the reduction of peak loads by using active load control and reducing peak hours of electricity demand.

2. Valley filling involves electricity demand stimulation during off-peak hours of a building.

3. Load shifting involves shifting a load from on-peak to off-peak periods.

These three strategies, MPC in combination with BESS provides the system with the capability to purchase and store extra power during off-peak pricing time. The use of stored power can be used during peak price times smoothing out the power fluctuations in grid supply power or PV generation [30]. Considering office buildings, in particular, peak shaving is especially interesting as this reduces their energy costs significantly [31]. These various DSM strategies all contribute towards a more generic solution of building energy efficiency [32].

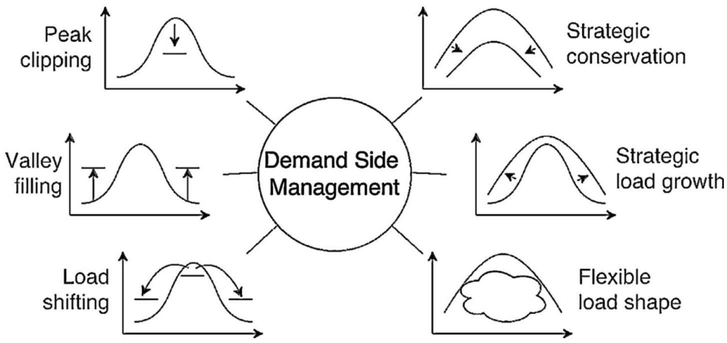


**Figure 2.6.** Strategies for DSM.

### Smart readiness indicator (SRI)

SRI is defined to evaluate not only cost-effective measures but also reduce carbon impact and RES integration problems while providing healthy and comfortable living conditions for building occupants. Thus, future-proof objectives should contain the building performance as a whole and achieve energy flexibility rather than DSM strategies. As discussed, the objective function of MPCs often embodies minimizing the energy purchase cost and applying on-site RES as efficiently as possible [20]. Considering the case study, a balance between energy flexibility and smart readiness is key. Table 2.1 summarises various objectives which appear in reviewed articles [30]. The findings of this paragraph and the goal of the research concentrate on developing MPC which focuses on the energy purchase cost. Not only is this objective most widely applied within the literature, which makes result comparison more accessible, but the focus is also on energy which adds to the energy flexibility goal. Nevertheless, additional objectives can be interesting, however, developing a simplified MPC and achieving implementation are the most important goals of this research. As almost all of these studies are simulations, not practical implementations, the added value of this research is to take a step towards successful implementation.

Table 2.1. Objective functions discussed within literature.

| Objective | Details | Number of papers |
|---|---|---|
| Energy purchase cost | Total cost of energy purchased from the power grid | 29 |
| Operational cost | Cost of operating DGs including fuel costs | 18 |
| Maintenance cost | Cost of maintaining DGs | 10 |
| Battery ageing cost | Penalty applied to limit the number of charge/discharge cycles a battery undergoes | 8 |
| Emissions cost | Cost of GHG emissions of DG | 6 |
| Comfort penalty | Penalty applied to limit temperature violations | 5 |
| Demand response cost | Penalty applied to limit total load curtailment time | 2 |

## 2.3 Model development

### Overview

This research consists of the development, testing and implementation of several models. This section gives an overview of the different models that are developed. Figure 2.7 shows the step-wise process of model development. First, a forecasting model of the building load for the MPC model is developed. Second, prior to the rule-based DSM models, a test is executed manually. This manual test is named 'Naïve control' as it would refer to doing operations manually based on human knowledge. This test was done also with the aim of making and checking the hardware and software connections and communication towards the BMS. Third, the rule-based DSM models MeanControl and Adapted-MeanControl are developed and implemented within the InsiteView environment. Lastly, an MPC model is developed, simulated and tested.

The reasoning behind the rule-based algorithms that are developed is to first learn about the InsiteSuite environment in order to have a more smooth implementation of the final product, the MPC. In addition, an intercomparison between algorithms and models gives the option to scientifically show improvements in later stages when key performance indicators (KPIs) are compared.

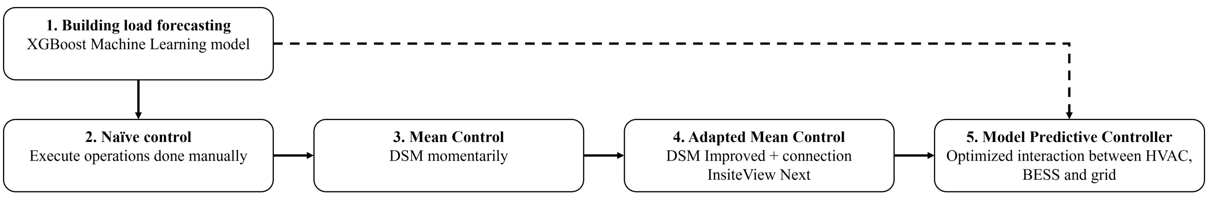


Figure 2.7. Overview of algorithm phases.

### 2.3.1 Forecasting models

In this section, the process and methods for developing a forecasting model for the building load will be explained. Four different subsections will elaborate on different phases within the development. For ML applications such as forecasting model development, the Python library Sci-kit Learn (SKLearn) is applied [33].

#### Data aquisition

It is important to identify the input- and output variables as they form the base of the setup of the forecasting model. Mapping all input variables gives insight into whether to in- or exclude a certain parameter as it might not be relevant to include. Moreover, the dependency of the variables is important to consider. The use of external forecasting models and data reduces development time as additional models do not have to be developed. The forecasting model will be one of the two main input variables for the final MPC. Typical ML models use historical data for training in order to create forecasts. For this research, an overview of the available input variables is shown in Table 2.2. The historical data available for this research dates from the year 1992 until today. However, for this forecasting model, only recent years are used. Therefore, the start and end dates for this forecasting model are from 2016 until 2021 to forecast for the year 2022.

**Table 2.2.** Input variable for the case study obtained from InsiteSuite.

| Variable | Type | SI notation | Dependency | Frequency [min] |
|---|---|---|---|---|
| Air handling unit | Measurement | [kW] | Kropman | 1 |
| Battery | Measurement | [kW] | Kropman | 1 |
| Chiller | Measurement | [kW] | Kropman | 1 |
| Diffuse irradiance | Forecast | [W/m²] | Solargis | 15 or 60 |
| EV demand | Measurement | [kW] | Kropman | 1 |
| EVs | Measurement | [kW] | Kropman | 1 |
| Humidifier | Measurement | [kW] | Kropman | 1 |
| Lighting | Measurement | [kW] | Kropman | 1 |
| Power demand* | Measurement | [kW] | Kropman | 1 |
| PV generation | Measurement | [kW] | Kropman | 1 |
| PV generation | Forecast | [kW] | Solargis | 15 or 60 |
| Solar irradiance | Forecast | [W/m²] | Solargis | 15 or 60 |
| Temperature | Forecast | [ºC] | Solargis | 15 or 60 |
| Wind angle | Forecast | [º] | Solargis | 15 or 60 |
| Wind speed | Forecast | [m/s] | Solargis | 15 or 60 |

∗ Power demand is a summation of the power used and generated by the air handling unit, chiller, humidifier, PV panels, Battery and both EV charging spots.

An overview of the meters placed in the Kropman office is presented in Appendix A. Each individual meter is indicated with an E-xx notation. Table 2.2 shows that forecasting models by Solargis are an important input dependency for the MPC as they provide PV generation forecasts. Together with the building load forecast, this data will be the input for the final MPC.

#### Data pre-processing

After data acquisition, data manipulation and cleaning are essential. As table 2.2 showed, the frequency varies per variable and might contain *Nan-values*. Therefore, data cleaning and pre-processing are required. As data pre-processing is executed using Python

Programming Language, all data from the table is added to one *Pandas DataFrame*. Additional time-gap features (i.e. temporal features) such as *Week*, *Day*, *DayOfWeek*, *Hour* and *Month* are added to the *DataFrame*. The final features which are added are measurement dependant features (i.e. lag features). As the building load is the feature of interest, yesterday's demand and the demand of the previous week for that day are also added. Lastly, the Dutch holidays are added to the *DataFrame* to visualize whether holidays are occurring on certain days in the data set. The final *DataFrame* containing all features includes temporal features, lag features, energy demand features and weather data from Solargis.
Continuing, the DataFrame is resampled to a 15-minute time interval to match the time interval of the Solargis data. After cleaning the data set the data is split into a train and test set using SKlearn libraries for Python. The train-test split applied in this case is 80% training and 20% testing for all variants of model development discussed in Chapter 3. Furthermore, it is essential to evaluate multicollinearity between the features in the data set. Multicollinearity ensures that features are not independent and therefore influence each other. Ultimately, this can affect the robustness of the forecasting model. To evaluate the multicollinearity, the variance inflation factor (VIF) is introduced. This factor gives the ratio between the variance for a given regression coefficient with only that variable in the model versus the variance for a given regression coefficient with all variables in the model [34]. A VIF value of 1 indicates no multicollinearity, whereas a value of 1-5 or higher indicates moderate or high multicollinearity. Features with such high VIF values are removed from the *DataFrame* making the VIF analysis an iterative process. Below, the equation used to calculate the VIF value is given.

$$VIF_i = \frac{1}{1 - R_i^2} \tag{2.2}$$

Where:
$VIF_i$ = Variance inflation factor of a specific feature
$R_i^2$ = Residual value of a specific feature

To conclude the data pre-processing part after the VIF is executed, the data is retrained and split using the train-test split. The cleaned *DataFrame* can be used in the next steps of selecting an ML model, training the model and ultimately optimizing the model.

**Model training and optimization**

In this research, a forecasting model for the building load is developed which will be one of the inputs for the MPC. The main focus of the forecasting model is therefore not to find the best model, however, a sufficient and fast forecasting model is desired. A comparison of prediction models is not in the scope of this research, therefore a widely used ML algorithm which is XGBoost is used for the prediction. Moreover, the XGBoost model is developed due to its relatively fast computational time and feature scaling is not required [35]. Continuing, the hyperparameters of the XGBoost model are to be optimized. XGBoost comes with a set of nine default hyperparameters of which an overview is given in table 2.3.

For hyperparameter optimization, GridSearchCV and RandomizedSearchCV are the two main approaches. GridSearchCV evaluates all possible combinations for the given hyperparameters, therefore this method is time-consuming if a lot of hyperparameters are present. RandomizedSearchCV finds appropriate combinations for the hyperparameters through random selection. Thus, RandomizedSearchCV is prefered as XGBoost has a large number of hyperparameters and computational time can be reduced significantly without compromising on performance [36]. Moreover, cross-validation is included within the RandomisedSearchCV function of SKlearn. Cross-validation avoids overfitting by continuously using a different fold as test data by splitting the train- and test set differently while maintaining the eighty and twenty per cent.

**Evaluation**

The evaluation of the performance and accuracy of the created forecasting model is done by using selected error metrics. The error metrics are calculated for all individual variants of forecasting models where ultimately the best performing model is selected. Two main error metrics are evaluated in this research. The Mean Average Percentage Error (MAPE) is used as a mean of comparison between several algorithms for electricity consumption predictions [37]. The MAPE is the mean percentage error of the predictions versus the actual data for the total sample size $N$.

$$MAPE = 100 \cdot \frac{1}{N} \sum_{i=1}^{N} \frac{|\hat{y}_i - y_i|}{|y_i|} \tag{2.3}$$

The second error metric is the Coefficient of Variance of the Root Mean Square Error (CV-RMSE). This error metric is mentioned in the ASHRAE Guideline for the measurement of energy demand. The CV-RMSE will be the main focus of evaluation as a value below 0.3 (i.e. 30%) is sufficiently close to physical reality and is therefore deemed suitable for engineering purposes [38, 39].

$$CV - RMSE = \frac{RMSE}{Mean(observations)} \tag{2.4}$$

$$RMSE = \sqrt{\frac{\sum_{i=1}^{N} (\hat{y}_i - y_i)^2}{N}} \tag{2.5}$$

$$Mean = \frac{\sum_{i=1}^{N} y_i}{N} \tag{2.6}$$

Lastly, in addition to the error metrics, the importance of the selected features is evaluated using Shapely Additive Explanations (SHAP). This gives insight per feature on the importance and influence of the feature on the final model [40]. The final model will be used to create building demand predictions for the year 2022 as one of the inputs for the MPC. All findings are presented in Chapter 3.

**Table 2.3.** XGBoost hyperparameter selection with description.

| Hyperparameter | Default value | Limit | Description |
|---|---|---|---|
| learning rate ($\eta$) | 0.3 | (0,1] | Shrinks feature weights to make the boosting process more conservative. Lower values result in a more conservative model. |
| n_estimators | 100 | (0,$\infty$] | Number of gradient boosted trees. Equivalent to the number of boosting rounds. |
| gamma | 0 | (0,$\infty$] | Minimum loss reduction required to make a further partition on a leaf node of the tree. The larger gamma is, the more conservative the algorithm will be. |
| max depth | 6 | (0,$\infty$] | Maximum depth of a tree. Increasing this value will make the model more complex and more likely to overfit. |
| min child weight | 1 | (0,$\infty$] | Minimum sum of instance weight needed in a child. If the tree partition step results in a leaf node with the sum of instance weight less than the min child weight, then the building process will give up further partitioning. The larger min child weight is, the more conservative the algorithm will be. |
| subsample | 1 | (0,1] | The ratio of the training instances. It means that XGB would randomly sample the specified ratio of the training data prior to growing trees, which will prevent overfitting. Subsampling will occur once in every boosting iteration. |
| colsample by tree | 1 | (0,1] | The subsample ratio of columns when constructing each tree. Subsampling occurs once for every tree constructed. |
| lambda | 1 | (0,$\infty$] | L2 regularization term on weights. Increasing this value will make the model more conservative. |
| alpha | 0 | (0,$\infty$] | L1 regularization term on weights. Increasing this value will make the model more conservative. |

### 2.3.2 Demand-side management (DSM) models

As part of the research process in developing an MPC, rule-based DSM algorithms are created to understand the behaviour of the office building and learn about the digital environment InsiteSuite. Three different DSM model approaches are proposed and implemented. The DSM models are rule-based control models which use little to no calculated values or ML. The reasoning for the rule-based approach is to learn about the implementation procedure of InsiteSuite as soon as possible and the development of a simplified rule-based controller gives sufficient outcomes in little development time. These model approaches are all executed real-time in the office. The results of these experiments are described in Chapter 3. The DSM algorithms are compared with the MPC to increase the perspective and provide additional motivation for the added value of implementing an MPC.

#### Naïve control

The first executed DSM control experiment gives an example of the performance of a supervised 'algorithm'. For this experiment, the logic which would ideally be executed by the machines and computers itself is operated manually. For this experiment, a typical spring weekend is used to charge the BESS with excess solar energy. This stored energy is then used to shave off the 'peak' of the Monday morning. Figure 2.8 visualizes the logic of this algorithm. It should be noted that the Naïve control model is not actually a control model. However, it is used to emphasize the benefits of automated algorithms and control strategies. Moreover, actual control strategies have the benefit of being adaptable within different systems and using data to make decisions in contrast to luck. Other than that, this test helped in making and checking the hardware and software connections and communication towards the building management system.

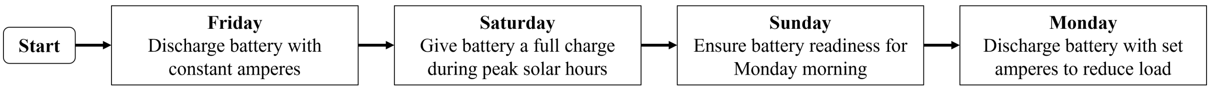


**Figure 2.8.** Visualization of Naïve control algorithm.

#### MeanControl

In contrast to the Naïve control, the MeanControl is an actual algorithm which is created and tested within the InsiteSuite environment. This algorithm is an improvement as it does not require human interaction and it acts based on decisions supported by data. MeanControl is a DSM algorithm capable of peak shaving and valley filling by taking the mean energy demand of a certain day into account. The average energy demand for the day of operation going back five weeks is calculated and added to a report within InsiteReports. This list of seven values is therefore fluctuating to represent seasonal changes in energy demand. In addition, the MeanControl algorithm first checks whether there is excess solar energy to charge the BESS. If this is the case, the amount of excess energy is calculated and will be transferred back into the BESS rather than feeding the energy back to the grid. During the DSM procedure, peak shaving and valley filling currents are set values which are 10 and 5 amperes respectively. Furthermore, the MeanControl algorithm operates on a time sample of 5 minutes. A visualization of the MeanControl algorithm is given in Figure 2.9. Like the Naïve control, the MeanControl algorithm is tested during the spring period of 2022. The actual time period is from May $24^{th}$ until June $6^{th}$.

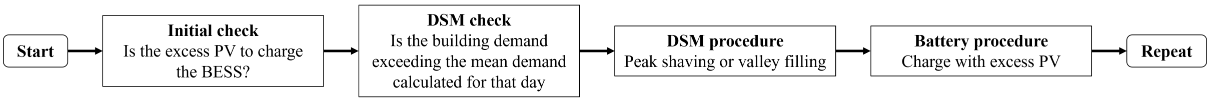


**Figure 2.9.** Visualization of MeanControl algorithm.

### Adapted-MeanControl

During the testing period of the MeanControl algorithm, an upgrade to this algorithm was developed. A separate goal of the MeanControl algorithm was to gain knowledge of the implementation within the InsiteSuite environment. Therefore, during the testing period of the MeanControl algorithm, an upgraded version of this algorithm was developed which would be the final rule-based DSM algorithm. The Adapted-MeanControl algorithm is a more extensive algorithm which operates on a 1-minute time sample. As the MeanControl algorithm, the main objective of this algorithm is to successfully execute DSM operations such as peak shaving and valley filling. However, Adapted-MeanControl has several steps in between decisions which calculate amperes based on thresholds and deviations. Like the MeanControl, the average value per day over a period of five weeks is still active. However, this algorithm examines the current state of the battery. As Figure 2.10 shows, the state of the battery can either be charging, discharging or idle. This allows the algorithm to understand whether the previous input of the system would still be sufficient if a time-sample period is finished and repeated. In addition, the Adapted-MeanControl algorithm calculates the charging current based on the deviation of the energy demand in comparison with the mean. This involves a simple subtraction of the actual demand minus the mean demand in kW which is then transformed into amperes sent to the BESS. The Adapted-MeanControl algorithm was tested during the spring period of 2022. The actual time period is June $9^{th}$ until June $16^{th}$.

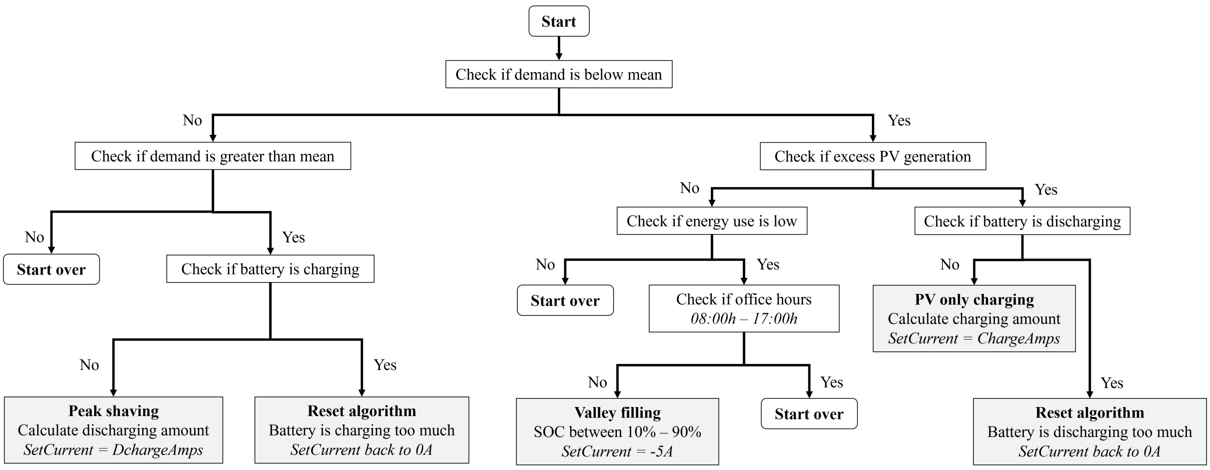


**Figure 2.10.** Visualization of Adapted-MeanControl algorithm.

### 2.3.3 Model predictive controller(s) (MPC)

The next step of the research consists of upgrading from rule-based DSM algorithms toward the development and implementation of an MPC. Surpassing the capabilities of earlier developed DSM algorithms, MPCs have forecasting- and learning capabilities as well as the support of smart constraints. A successful implementation requires an understanding of the building installations, knowledge of the theoretical concept and sufficient understanding of the chosen optimization library in Python.

To have an accurate representation of the physical case study, the electricity network of the office is investigated. Figure 2.11 shows how the building installations and their meters are connected. This electricity network forms the base of operations of the MPC. Typical input variables are the current state of the system, the system model and outside disturbances to the system. Generally, the future state of the system is the models' output [30]. Within this MPC, the battery is the control variable. Therefore, the current state of the system would be the state of the BESS. Outside disturbances to the system are the weather data obtained by Solargis and the outcomes of the building load predictions. These disturbances will be used as input variables for the MPC. The future state of the battery will include charging and discharging power sequences over the total horizon of the model. As all meters are interconnected to the grid, the building load is determined by subtracting all individual components from the *Power* and *Lighting* meters combined. In this research, a distinction is made between MPC simulations and MPC implementation. This distinction relates to the inclusion of EVs in the final building load. As the EV data is historically registered, the MPC simulations have the influence of EVs included in the building load. The inclusion of EVs in the simulations will identify whether the MPC models can respond to the undesired peaks. For the MPC implementation, it is currently impossible to add the influence of EVs as making accurate predictions is not yet achieved. Hence, the influence of EV, PV and the BESS is included in the MPC simulations but excluded in the practical implementation of the MPCs. The building load calculations are formulated as follows:

$$Building\_load_{Simulation} = (Power + Lighting) - (PV + Battery)$$

$$Building\_load_{Implementation} = (Power + Lighting) - (PV + EV + Battery)$$

Ultimately, the MPC minimizes the power exchange with the grid by using the BESS as its control variable by charging and discharging the battery.

#### Electricity network of the office

The electricity network of the office can mathematically be written as a power balance. This power balance contains all power going through the network from- and to the grid. In the power balance, the building load and the generated PV are the disturbance variables that are uninfluenced by the MPC. When generated solar power is exceeding the building load a negative power balance can occur. Therefore, the battery charging and discharging variables are the control variables in the electricity network of the office building for the MPC. This equation is written as follows:

$$p_{grid} + p_{pv} + p_{load} + p_{bat,ch} - p_{bat,dch} = 0$$

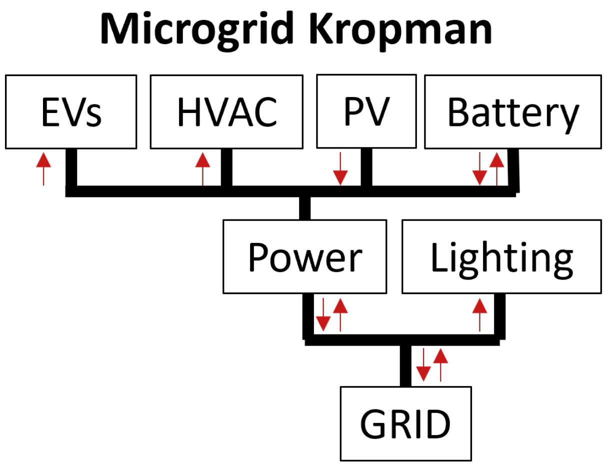


**Figure 2.11.** Simplified visualization of the microgrid of the office.

### Electric vehicle dynamics

Considering the MPC, the influence of the EVs is only present in the MPC simulation scenarios. Stochastic charging patterns, the lack of available SOC values and unknown EV presence, drastically decrease the opportunity [41] to create sufficient forecasting models. Regarding the MPC simulations, historical data of EVs is used and added to the building load to analyse the MPC response to EV peaks. However, within the practical implementation of the MPCs, is thusly excluded.

### Battery

The equation which is essential in the approximation of the battery dynamics focuses on the state of charge (SOC) of the batteries [42]. Linearly, this can be expressed by the following equation:

$$SOC_{k+1} = SOC_k + \frac{\eta \cdot p_{ch,k \cdot \Delta T}}{C_{bat}} - \frac{(\frac{1}{\eta})p_{dch,k} \cdot \Delta T}{C_{bat}}$$

Where $\eta$ is the round trip efficiency, $p_{ch}$ and $p_{dch}$ are the charging and discharging power, $C_{bat}$ is the capacity of the battery system and $\Delta T$ is the time step. Most battery systems enforce "spinning reserves" for both charging and discharging [30]. Typical values for the SOC are $0.2 \leq \text{SOC} \leq 0.8$. Regarding the MPC, the control variable of the battery system is defined as the charging- and discharging power of the BESS. Additionally, the MPC requires the state of the battery which relates back to the SOC. When the initial state of the system is obtained, the future state can be calculated by the MPC. Moreover, the MPC operates on a time interval of 15 minutes. As the SOC is a variable of energy, the control variables are multiplied by a time-sample variable ($T_s$) to ensure the conversion of kW to kWh. In this case, the $T_s$ is equal to 0.25. The full mathematical representation of the battery is as follows:

$$x_{bat} = \begin{cases} x_k^{bat,init} + (\eta^{bat} p_k^{Bat,ch}) - \frac{p_k^{Bat,dch}}{\eta^{bat}} \cdot T_s \; k = 1 \\ x_{k-1}^{bat} + (\eta^{bat} p_k^{Bat,ch}) - \frac{p_k^{Bat,dch}}{\eta^{bat}} \cdot T_s \quad \forall k \geq 1 \end{cases}$$

**Objective**

The objective of the MPC is to minimize the power- and energy through the grid. i.e. $p_{grid}$ is to be minimized. To obtain a global minimum a quadratic term of the grid is created as it can be both positive and negative. This ensures a convex solution and penalises the high values (i.e. it recognises the building load peaks and tries to avoid high values). The cost function of this MPC is the following:

$$\min_{u_k} J \sum_{k=1}^{N} (p_{grid+} - p_{grid-})^2$$

$$\min_{u_k} J \sum_{k=1}^{N} (p_{grid})^2 \tag{2.7}$$

$$s.t. \quad p_{grid} + p_{pv} + p_{load} + p_{bat,ch} - p_{bat,dch} = 0 \tag{2.8}$$

$$x_{bat} = \begin{cases} x_k^{bat,init} + (\eta^{bat} p_k^{Bat,ch}) - \frac{p_k^{Bat,dch}}{\eta^{bat}} \cdot T_s \ k = 1 \\ x_{k-1}^{bat} + (\eta^{bat} p_k^{Bat,ch}) - \frac{p_k^{Bat,dch}}{\eta^{bat}} \cdot T_s \quad \forall k \geq 1 \end{cases} \tag{2.9}$$

$$x^{bat,min} \leq x_k^{bat} \leq x^{bat,max} \qquad \forall k \in N \tag{2.10}$$

$$p^{bat,ch} \leq p^{bat,max} \cdot (u_k) \qquad \forall k \in N \tag{2.11}$$

$$p^{bat,ch} \geq p^{bat,min} \cdot (u_k) \qquad \forall k \in N \tag{2.12}$$

$$p^{bat,dch} \leq p^{bat,max} \cdot (1 - u_k) \qquad \forall k \in N \tag{2.13}$$

$$p^{bat,dch} \geq p^{bat,min} \cdot (1 - u_k) \qquad \forall k \in N \tag{2.14}$$

**Constraints**

In addition to the system dynamics, two constraints are added to include physical limitations of the system.

$$x^{bat,min} \leq x_k^{bat} \leq x^{bat,max}$$

The first constraint focuses on the installed BESS capacity. The SOC cannot be lower than zero, and higher than the capacity of the system. In the case study, the BESS has a maximum capacity ($C$) of 57.6 $kWh$. In order to translate this to the implementation the SOC needs to be included. The lower- and upper limit of the battery capacity is 10% SOC and 90% SOC. i.e. the battery cannot charge above 90% and discharge below 10% SOC.

Thus:

$$x^{bat,min} = C_{bat} \cdot 0.1$$
$$x^{bat,max} = C_{bat} \cdot 0.9$$

Note: $C_{bat}$ is a capacity variable in $J$ or $kWh$.

In addition, the minimum and maximum amperage that the battery can charge or discharge is also limited. Therefore, the control variables $p_{bat,ch}$ and $p_{bat,dch}$ are to be limited to a minimum and maximum. For the implementation, this is equal to a set value in

*Amps*. However, for this MPC the limit is set to $kW$ in order to maintain clarity. To converse $A$ to $kW$ the voltage of the BESS is required. In this MPC the BESS is estimated to have a bank voltage of $600V$.

Thus:

$$\begin{aligned} Amp_{min} &= 5 \rightarrow kW_{min} = 3 \\ Amp_{max} &= 30 \rightarrow kW_{max} = 18 \end{aligned}$$

$$\begin{aligned} 3 \leq p_{charge} &\leq 18 \\ 3 \leq p_{discharge} &\leq 18 \end{aligned}$$

### Optimization library

To translate the mathematical objective and constraints of the MPC to a Python environment, the optimization library Pyomo is consulted. Pyomo is a Python-based open-source package for optimization purposes. Pyomo provides a platform for specifying optimization models that embodies central ideas found in modern Algebraic Modeling Language (AMLs), within a framework that promotes flexibility, extensibility, portability, openness, and maintainability [43]. The final optimization model created with Pyomo can be processed by external solvers. The structure of the Pyomo model can be found in Appendix B where a detailed description is given.

### Implementation

The final MPC is created in a Jupyter Notebook which runs on a local computer. The Jupyter Notebook obtains the forecasting model through a remote procedure call (RPC) stored in the ML wrapper on the InsiteSuite server. The forecasting model is retrained with updated weather data forecasts from Solargis. Hence, the building load for the forthcoming horizon is determined with a time sample of 15 minutes. Next, the Pyomo optimization function is solved and the model determines the most optimal control outputs. The control outputs are converged from $kW$ to amperes to be able to send the output through an RPC to the BESS. As this charging or discharging output is executed in the system, the MPC is re-executed every 15 minutes and the information in the loop is updated. Thus, every 15 minutes a new, updated control output is composed as the time horizon shifts. Figure 2.12 visualizes the flowchart logic of the final MPC. The dash-dotted line indicates all steps which are coded in the Jupyter Notebook.

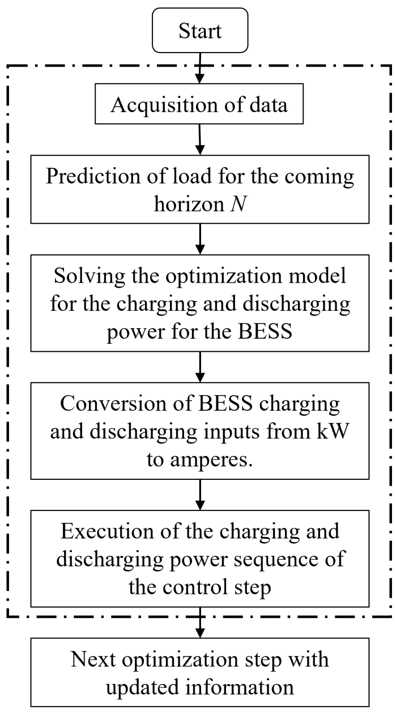


**Figure 2.12.** MPC model flowchart.

## 2.4 Key Performance indicators

The results of the various control algorithms and the final MPC are evaluated using KPIs. Universal KPIs are of major importance as they allow research to be compared with other research and scientific papers. Therefore, six KPIs are used which were developed by the IEA EBC - Annex 81 and are mainly focused on data-driven Smart Buildings and energy flexibility research [44]. These six KPIs all have a relation to the implementation of improved energy control strategies. Therefore, the calculation of most KPIs is in comparison with the case study before improved energy control strategies are implemented to give results based on the change. A detailed explanation of the KPIs is given.

KPI1 - Power peak reduction (PPR): Reduced peak demand due to improved energy control.

$$\Delta P = P_{peak,ref} - P_{peak,ctrl} \ [kW]$$

KPI2 - Power peak reduction percentage (PPRP): PPR in percentage.

$$\Delta P\% = 1 - \frac{P_{peak,ctrl}}{P_{peak,ref}} \ [\%]$$

The PPR and PPRP can be evaluated in multiple ways. Therefore, for this KPI two main components are to be determined. First, the peak period is to be determined as this relates to the time horizon over which the peaks can occur. Second, the amount and calculation method of peaks evaluated are of major importance. For example, one month of data is analysed using the PPR. If this were the case, for this whole month evaluating only one peak will give misleading results. Therefore, the time horizon over which peaks are evaluated is set to one day (i.e. 24 full hours) for all data evaluated. As peaks can occur throughout the day, a distinction between the morning and afternoon during office hours is made. The day is split into a morning and afternoon segment. The morning evaluates peaks occurring from 08:00 am until 12:00 pm and the afternoon evaluates peaks occurring from 12:00 pm until 5:00 pm. Thus, each day includes two peaks that are evaluated and the total sum of all peaks relates to the $P_{peak}$ values which are compared.

KPI3 - Flexibility factor (FF): Relative amount of energy consumed during high-load hours (assumed 8:00 to 17:00) compared to low-load hours.

$$FF = \frac{\int E_{low,load} - \int E_{high,load}}{\int E_{low,load} + \int E_{high,load}} \ [\%]$$

The FF gives an estimation of the load-shifting potential of the evaluated case study. Discharging the battery during peak hours and charging the battery during off-peak hours will reduce the energy required from the grid during peak hours. Please note this peak hour is not to be confused with power-peak shown in KPI1 and KPI2. Moreover, it should be noted that peak hours are no generic term. Therefore, peak hours in this research are set during office hours. Thus, peak hours are from 08:00 am until 05:00 pm. The FF is an indicator of the energy quantity used in a certain load hour. Therefore, the FF would be -100% if the quantity was only during high load hours and 100% if the quantity was only during low load hours.

KPI4 - Self-sufficiency: the degree to which on-site generation is sufficient to fill the energy needs of the building.

$$SS = \frac{\int P_{s,cons}}{\int P_L} \ [\%]$$

KPI5 - Self-consumption: the degree to which on-site generation is consumed by the building.

$$SC = \frac{\int P_{s,cons}}{\int P_s} \ [\%]$$

Two main energy generation and mismatch related KPIs are the SS and the SC. These KPIs present the degree to which solar energy is used directly or fed back to the grid. A high SS relates to a building having enough generation and BESS capacity to compensate for peaks and be little to no dependent on the grid. Moreover, a high SC ratio would involve the amount of on-site (renewable) energy being generated and used in the building without sending it back to the grid. Thus, aiming to be as grid independent as possible, both the SS and SC are to be maximized.

KPI6 - Flexibility index: relative cost reduction. (let $cost_k$ be variable energy cost).

$$FI = \frac{\int cost_k P_{ctrl,k}}{\int cost_k P_{ref,k}} \ [\%]$$

The final KPI focuses on the cost-saving potential of the case studies evaluated. The FI is therefore dependent on the price paid for energy. In this research, the price estimation of energy per kWh is estimated at €0.26 per kWh during off-peak hours. To penalise the peak hours and give an estimation of the price, the base price is enhanced by a factor of 1.3 during office hours. Ultimately, this KPI translates the valley filling and peak shaving potential to a saving component.

## 2.5 Smart readiness indicator (SRI)

The SRI is introduced by the Energy Performance of Buildings Directive (EPBD). In the future, the SRI is estimated to become a cost-effective measure which assists in the development of healthier and more comfortable buildings where low energy use and carbon impact are considered and integration with renewable energy sources is supported. The SRI is prepared for the European Commission where the following definition has been adopted:

*"Smartness of a building refers to the ability of a building or its systems to sense, interpret, communicate and actively respond in an efficient manner to changing conditions in relation the operation of technical building systems or the external environment (including energy grids) and demands from building occupants"* [45].

This research aims to contribute to smart building technologies and functionalities for the three main pillars of SRI. Therefore, the evaluation of the SRI and its underlying methods is included in this section. The SRI calculation methodology is structured amongst three key functionalities and seven impact criteria. A higher SRI score reflects a "smarter" implementation of all services within the building. The SRI thus gives a more generic overview of the building in comparison to the KPI evaluation. The final SRI outcome is a smart readiness score in percentages which represents the ratio between the smart readiness of the building compared to the maximum score that it could reach. Figure 2.13 shows the distribution of the impact of all impact criteria on the final score. Thus, the SRI provides insight and understanding into the concept that focusing solely on one aspect of the building might result in great KPIs, however, the building as a whole and its users are nevertheless as important.

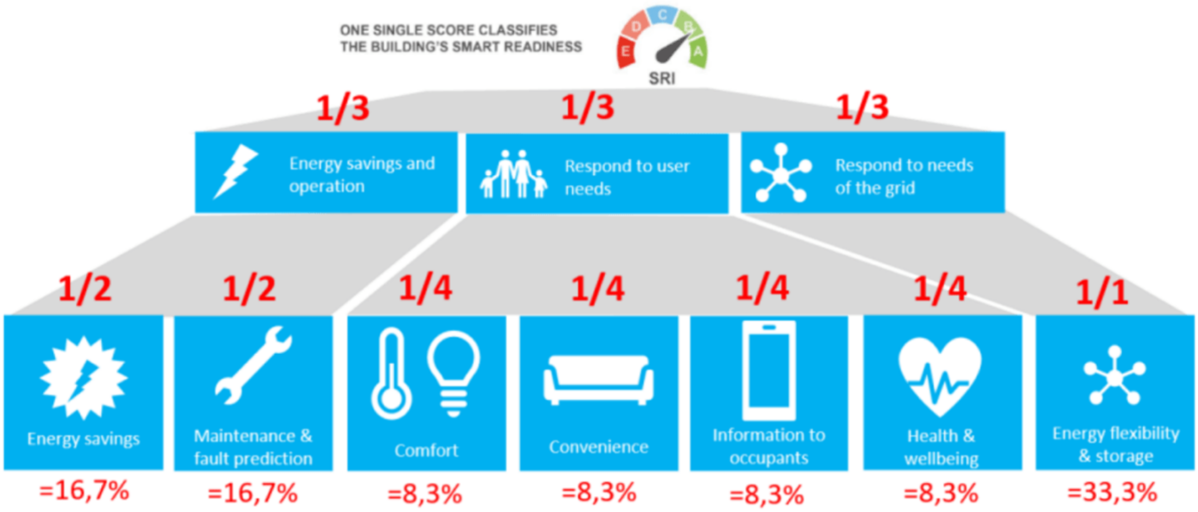


**Figure 2.13.** Weighting factors for impact criteria.

As all buildings are different, the SRI provides three different methods of evaluation. Method A is a simplified evaluation which evaluates 27 services amongst the seven impact criteria. Therefore, method A is considered sufficient for small buildings with low complexity. Method B gives a more detailed result evaluating all 54 catalogue services. Lastly, method C is still under development and would involve the use of metered data to evaluate the performance of the building. As method C is not yet practically available, this research will calculate and compare the results for both methods A and B. Figure 2.14 shows the explanation of the methods. A summary of the findings for both methods will be given in Chapter 3, and the full calculation can be found in Appendix C.

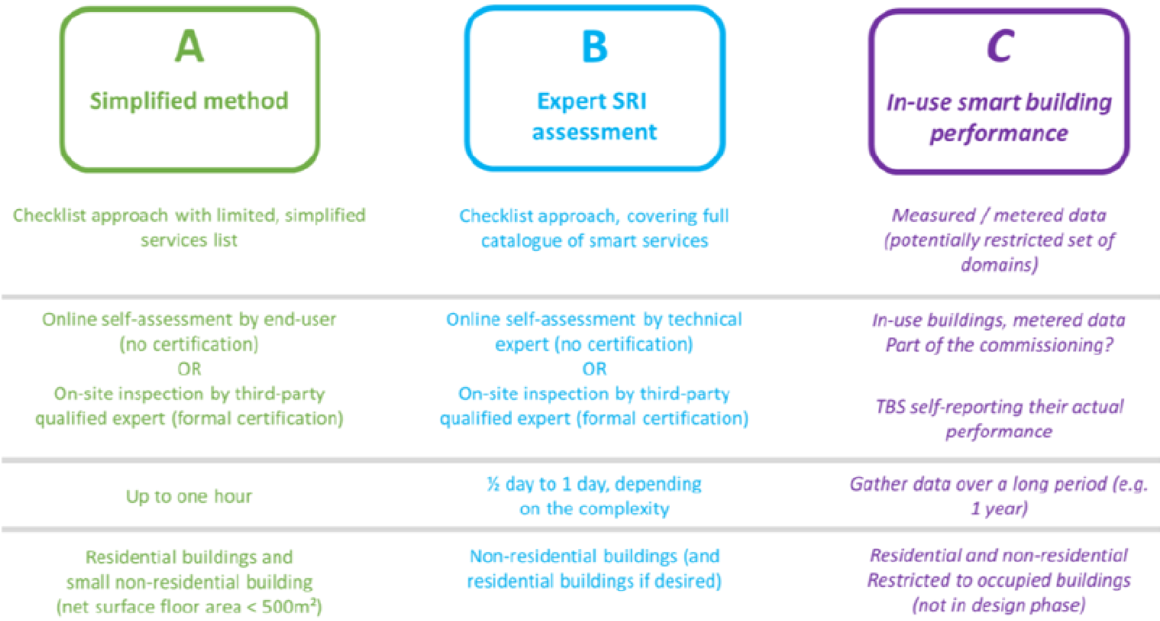


**Figure 2.14.** Overview of the three SRI evaluation methods.

# 3. Results

In this chapter, the results are addressed. Paragraph 3.1 will dive into the rule-based DSM algorithms. Paragraph 3.2 explains the results from the forecasting model(s). Paragraph 3.3 gives the results of the MPCs created in this research. Lastly, paragraph 3.4 shows the SRI scores.

## 3.1 Demand-side management (DSM) models

### 3.1.1 Naïve control

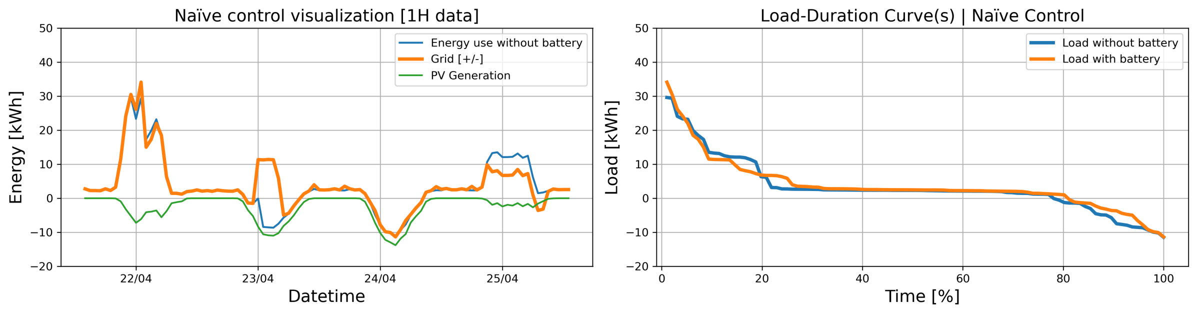


**Figure 3.1.** Results of Naïve control algorithm.

The Naïve control results are all about displaying the benefits of using algorithms and more advanced control strategies. During the weekend, a full charge is given to the battery storage system during peak solar PV production hours in order to gain the highest yield. On Monday, during office hours the BESS is discharged by a set amount, reducing the overall energy consumption of the building. In Figure 3.1 the left graph shows the energy use without control, energy going through the grid with the control activities and the PV generation. The right graph shows a load-duration curve which corresponds to all energy distributed over a percentage of the time. During the weekend of Saturday $23^{rd}$ of April, there is an increase in energy consumption as the BESS is being charged during the solar peak hours. On Monday, the discharging sequence is observed resulting in a decrease in energy use in comparison with the blue line.

The downsides of the Naïve control are that it would require manual labour to set the currents of the BESS, even during the weekend. In addition, assuming that excess solar power would occur at the weekend is based on assumptions. Therefore, this approach is not adapted to the system dynamics and mainly showcases the benefits of automated control.

### 3.1.2 MeanControl

The implemented DSM algorithm MeanControl is visualized in Figure 3.2. The results indicate an understanding of DSM procedures as some peaks are shaved and valleys are filled. The overall load duration emphasizes this as the general peaks are reduced from approximately 36 kW to 31 kW. In addition, the overall load-duration curve is flatter.

Even though peaks are reduced with the MeanControl algorithm, undesired BESS behaviour occurs during periods of excess solar power. Figure 3.3 visualized this issue occurring within the testing period of the MeanControl. The MeanControl algorithm

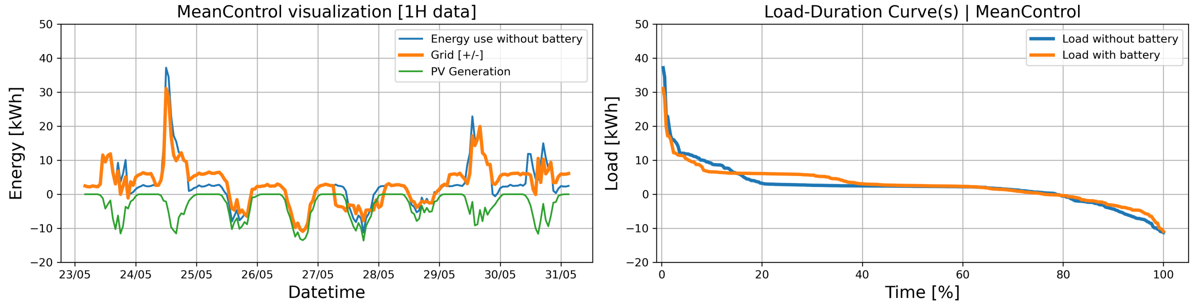


**Figure 3.2.** Results of MeanControl algorithm.

operates and acts based on live occurring events. Therefore, during some periods of the day, clouds will interfere with the accuracy of the sensors. When the MeanControl algorithm measures at the same time a cloud is passing a sensor, it recognises a demand for energy, therefore it will start discharging the BESS even though in reality this period of shade could only occur for 30 seconds. This behaviour of clouds interacting with sensors is hard to overcome, however, the Adapted-MeanControl algorithm has added logic to compensate for the frequently changing signal of the battery going from charging to discharging as is shown in figure 3.4.

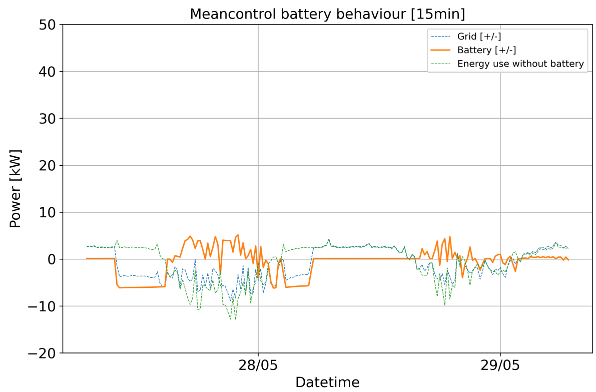


**Figure 3.3.** Battery behaviour of MeanControl algorithm.

### 3.1.3 Adapted-MeanControl

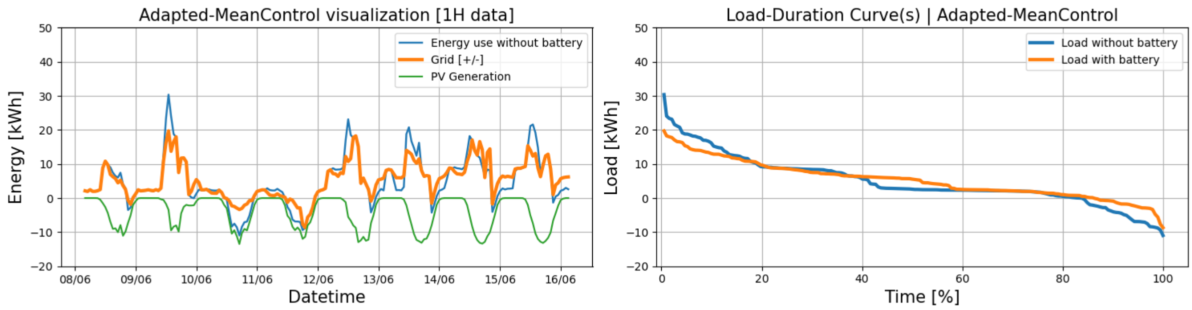


**Figure 3.4.** Results of Adapted-MeanControl algorithm.

To control the frequent charging and discharging sequence, adaptations to the existing MeanControl algorithm are created. As is discussed in Chapter 2, the Adapted-

MeanControl has the ability to understand whether the previous input is still sufficient and whether frequently changing sequences can be reduced.

In Figure 3.4, results of the testing week of the Adapted-MeanControl algorithm are presented. It is clearly visible that the peaks occurring from the EVs are penalised and shaved off using the BESS. In addition, outside office hours, the BESS is charged to increase the SOC of the BESS for new peaks occurring in the morning. It should be noted that during the weekend, the BESS is only charged with excess PV rather than using the grid. During the weekends the mean energy demand is lower and therefore excess PV is used more efficiently. The load-duration curve shows that for this week of testing, the curve is more flattened out and peaks are reduced by approximately 10 kW. However, there is still energy being fed back to the grid which indicates room for improvement. Ultimately, excess solar power is minimally fed back to the grid as peaks are reduced. Nevertheless, the load-curve flattening with the Adapted-MeanControl algorithm is sufficiently more pronounced than previous DSM algorithms. As stated earlier,

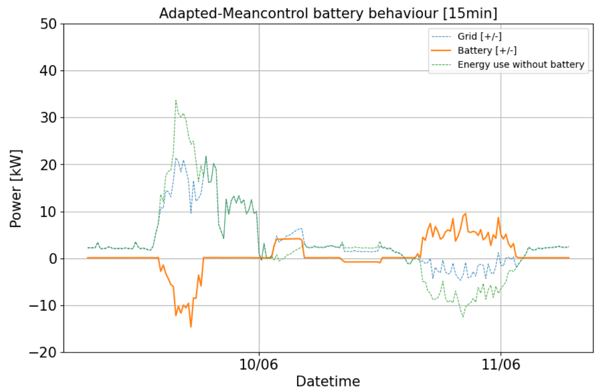


**Figure 3.5.** Battery behaviour of Adapted-MeanControl algorithm.

the Adapted-MeanControl algorithm understands whether previous inputs are still sufficient. In Figure 3.5 a clear improvement is shown in comparison with the results of the Meancontrol algorithm in Figure 3.3. A clear trend is observed where the battery charging and discharging cycles are not changing frequently. As the lifetime of the BESS mainly depends on this sequence changing and the depth of discharge of a battery, the BESS lifetime and health are more guaranteed [46].

### 3.1.4 Key performance indicators

Table 3.1 shows the results of the evaluated KPIs for the DSM algorithms. To compare the results of the DSM algorithms, it should be noted that the evaluation time is of major importance. The baseline includes data for a whole year and therefore results are more levelled out as they include seasonal change. The results of the KPIs are therefore merely an impression of the trend rather than a fully valid comparison. To achieve full scientific support, additional testing and evaluation are advised. Nevertheless, the scope of this research includes progress towards MPC and therefore, comparing MPC results with DSM algorithms is considered useful.

### 3.1.5 Conclusion

When the Power Peak Reduction is evaluated and the focus on the MeanControl and Adapted-MeanControl, it can be concluded that both algorithms understand peak be-

**Table 3.1.** KPI Evaluation DSM algorithms.

| **KPI** | **Period** | **Ideal** | **Baseline [2021]** | **NaïveCtrl** | **MeanCtrl** | **A.MeanCtrl** |
|---|---|---|---|---|---|---|
| Δ P [kW] | *Morning* | [+*] | *none* | -4.5 | 6.1 | 10.6 |
| Δ P [kW] | *Afternoon* | [+*] | *none* | 1.2 | -0.1 | -0.1 |
| Δ P [%] | *Morning* | [100%] | *none* | -15% | 16% | 35% |
| Δ P [%] | *Afternoon* | [100%] | *none* | 5% | -1% | -1% |
| FF [%] | *Horizon* | [0%] | -38% | -22% | 48% | -2% |
| SS [%] | *Horizon* | [100%] | 20% | 46% | 34% | 23% |
| SC [%] | *Horizon* | [100%] | 92% | 90% | 79% | 81% |
| FI [%] | *Horizon* | [100%] | 1% | 0% | -8% | 1% |

* Ideally, the values for Δ P should be as high as possible. Negative values indicate an increase in power demand.

haviour and can shave off these peaks. During the testing period of the Adapted-MeanControl, there were slightly higher peaks which resulted in a higher peak reduction. Moreover, it can be concluded that the valley filling is translated into a slight increase in energy consumption in the afternoon, therefore negative 'power peaks' are occurring. It should be noted, the slight increase in energy use during the afternoon compensates for the reduction in the morning.

The Flexibility Factor varies significantly amongst different algorithms and the baseline. It should be noted that -100% and 100% are the indicators of whether energy is being used during high-load hours and during off-peak hours. Therefore, approaching 0% is deemed ideal as it indicates a well maintained balance of peak shaving and valley filling. The baseline year 2021 shows that most of the energy is consumed during the high load hours. The algorithms all show deviating results, however, the Adapted-MeanControl is considered the most optimized DSM algorithm which can be confirmed by the FF KPI approaching 0%. It should be emphasized that the evaluation and testing period of the FF is up for discussion due to its relatively short time span.

The Self Sufficiency of the algorithms clearly shows improvement in comparison with the baseline. However, it should be noted that this also highly correlates with the greatness of the peaks that are shaved. When the maximum capacity for the BESS is fixed, higher SS can be achieved by finding the optimal balance between shaving off high peaks and recharging the battery. Thus, what can be observed in this research is that the Naïve control was executed in a sufficient performing manner. The MeanControl and Adapted-MeanControl both performed less ideally, however, the PPR is higher

Continuing, Self Consumption has a high correlation with the installed BESS capacity, the installed PV capacity- and generation, and the SS. Interestingly, it can be observed that the baseline year already has a high SC. Therefore, it can be concluded that most PV generation, about 90%, is used directly in the building. Therefore, it is expected that smart DSM algorithms have a higher SC yield. Nevertheless, it should be noted that the evaluation period is during the enriched solar seasons of spring and summer and the baseline is evaluated over one full year.

Lastly, the Flexibility Index is less influenced by the algorithms. However, it can be concluded that the MeanControl algorithm has 'purchased' more energy outside office hours to compensate for peaks during office hours. This is due to the set values rather than the calculated values and timing of the Adapted-MeanControl.

## 3.2 Forecasting model(s)

The forecasting model developed in this research is used as one of the two inputs for the MPC. This section will focus on the model development and the results of the final forecasting model. First, the results of the feature selection process will be elaborated. Second, the development process of the forecasting model is discussed. Last, the final model is presented in the conclusion.

It should be noted, the initial first step is to build models based on all different available years and compare the results. Therefore, a more extensive model analysis is presented in Appendix E. This section elaborates on the process of the best possible model obtained from this initial first step. In summary, Kropman has an extensive historical database. The forecasting model developed focuses on the building load with the exclusion of EVs and BESS. During the years 2018, 2019, 2020 and 2021, odd behaviour in the data was found. For the years 2018 and 2019, building components such as the chiller and the humidifier showed deviations from other years as in some cases the data was not registered. This conclusion led to the decision to deem these years unusable for model training. Moreover, during the years 2020 and 2021, the data shows significant deviations. During these years, unusual patterns in building use can be explained due to Covid-19. Nevertheless, models are developed and evaluated for these years, however, the results are less useful.

As building load is considered constant and usually good to forecast, a model is developed using data from the years 2016 and 2017. This model is used to create building load predictions for the year 2022. It should be noted, retraining the model is key to maintaining accurate results. Therefore, suggestions are made in Chapter 5.

### 3.2.1 Feature selection evaluation

After the data cleaning process discussed in Chapter 2, weather features, temporal features and lag features are evaluated. An overview of all features is presented in Table 3.2.

**Table 3.2.** Features used in initial models.

| Weather features | Temporal features | Lag features |
|---|---|---|
| GHI | Hour of day | Demand previous day |
| TEMP | Day of week | Demand previous week |
| AP | Minute of hour | |
| RH | Week of year | |
| WS | Month | |
| PWAT | Holiday | |

After an iterative process of the VIF calculation from a total of 14 features, 11 features remain and form the final model. The final features of the model are *GHI*, *TEMP*, *WS*, *Minute of hour*, *Hour of day*, *Day of week*, *Week of Year*, *Month*, *Holiday*, *Demand previous day* and *Demand previous week*.

### 3.2.2 Forecasting model development

After feature selection, the next step is completing the model development. First, hyperparameter optimization is executed. Second, the error metrics are calculated. Third, feature importance is evaluated and lastly, plots will give visual support. As discussed in Chapter 2, RandomizedSearchCV is executed over the existing hyperparameters of XGBoost. All results of the RandomizedSearchCV are given in 3.3. The column 'RandomizedSearchCV range' presents the range on which the hyperparameters are evaluated. The first value represents the starting value, the second value represents the end value and the third value represents the interval between the starting and end point of the hyperparameter. With all features and hyperparameters evaluated, a model is created

**Table 3.3.** XGBoost hyperparameter optimization results.

| Hyperparameter | Default value | RandomizedSearchCV range | Best value |
|---|---|---|---|
| learning rate ($\eta$) | 0.3 | (0.05, 0.21, 0.01) | 0.17 |
| n estimators | 100 | (50, 210, 10) | 170 |
| gamma | 0 | (0, 11, 1) | 2 |
| max depth | 6 | (2, 11, 1) | 8 |
| min child weight | 1 | (1, 11, 1) | 7 |
| subsample | 1 | (0.5, 1.1, 0.1) | 0.6 |
| colsample by tree | 1 | (0.3, 1.1, 0.1) | 0.5 |
| lambda | 1 | (0, 1.1, 0.1) | 0.3 |
| alpha | 0 | (0, 1.1, 0.1) | 0.9 |

and forecasting predictions are made on the training and test data for the years 2016 and 2017. Visual evaluation is presented in Figure 3.6 and Figure 3.7. In both figures, the actual data and the forecasting model show sufficient agreement during the day with the exception of some peaks. The training set and test set both show complimenting results indicating that overfitting and overestimating are ruled out.

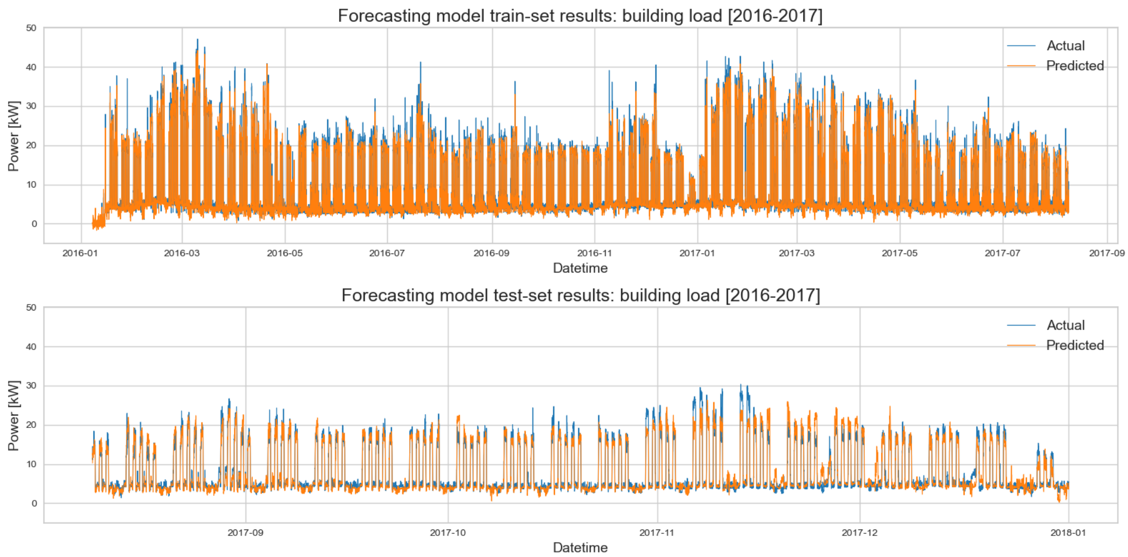


**Figure 3.6.** Visualization of forecasting results.

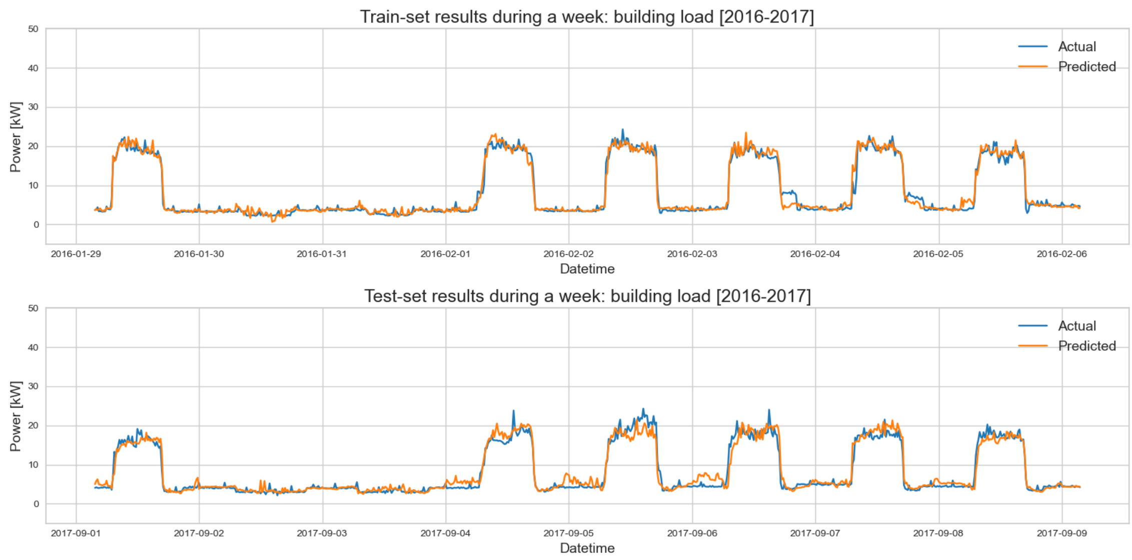


**Figure 3.7.** Visualization of forecasting results during a week.

Continuing, the evaluation of the feature importance is key to understanding the performance of a forecasting model. Therefore, the feature importance is determined using the SHAP evaluation, see paragraph 3.5.2. The results of the SHAP feature importance evaluation are visualized in Figure 3.8. As is shown in the figure, the most important features of the model are the lag features as these features represent the behaviour of the building load the most. Temporal features such as *Day of week* and *Hour of day* are also important for the model to understand patterns of employees entering and leaving the office. In addition, the weekends and holidays are well recognised by these features in combination with the *Holiday*.

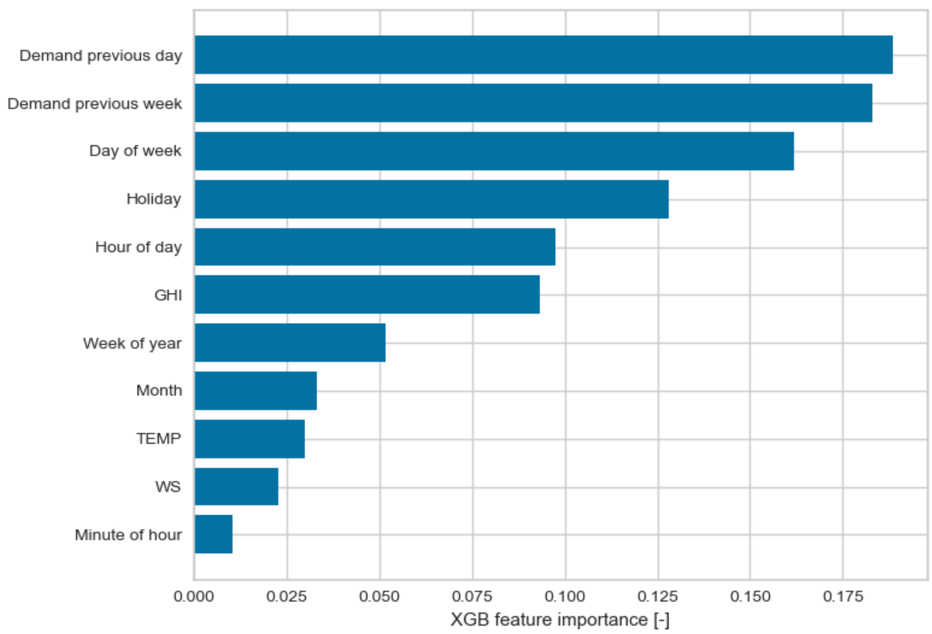


**Figure 3.8.** Visualization of SHAP feature importance.

### 3.2.3 Model implementation

The next step is fitting the model to data obtained from the year 2022. This will then be used as the final input for the MPC. Figure 3.9 visualizes the results of the model fitting to the year 2022. As is expected, deviations are observed. The forecasting models' performance has decreased, however, the visual representation of the actual building load in comparison with the predictions show agreement. It should be noted, deviations in the peak area can be explained due to physical changes to the building services. For example, the lighting in the building has undergone upgrades from regular light to smart LED lighting, lowering the overall energy used for lighting. Therefore, it is advised to keep retraining the initial final model with more recent data.

To complement the visual evaluation, error metrics are evaluated as they give a more

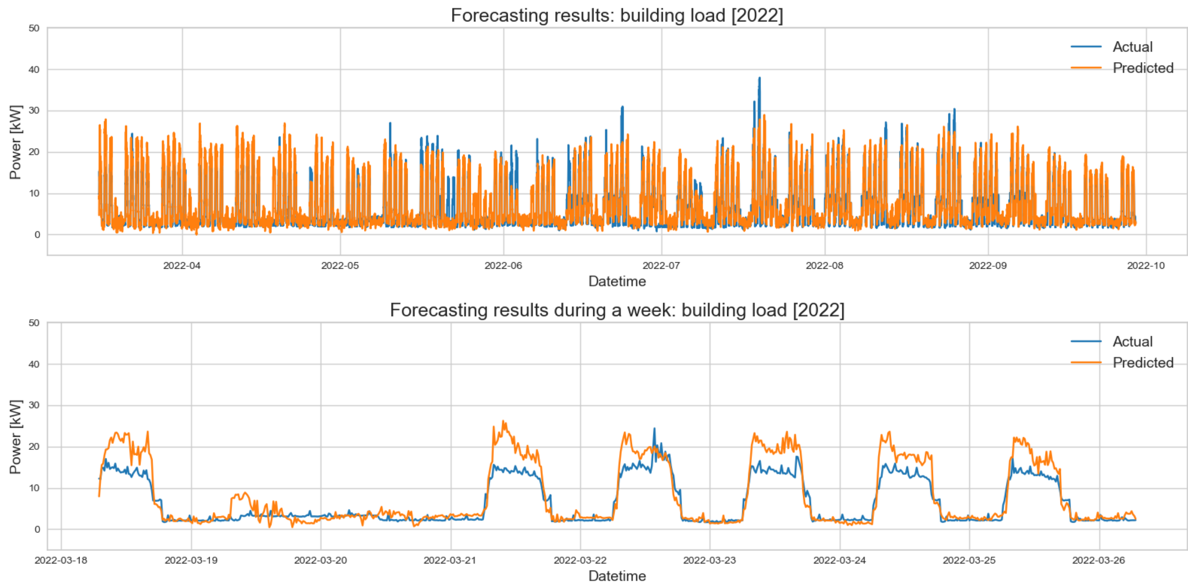


**Figure 3.9.** Visualization of forecasting results for 2022.

in-depth explanation of the performance and accuracy of the forecasting model. Table 3.4 shows the results for the MAPE and the CV-RMSE as discussed in Chapter 2. The outcomes for both the training and testing data of the XGBoost model are deemed suitable for engineering purposes as they are below 30%. The created forecasts for the year 2022 show less accurate results. However, as forecasting model improvement is not the main scope of this research, suggestions for model improvement are made in Chapter 5.

**Table 3.4.** Forecasting model error metrics evaluation.

| **Model** | **Dataset** | **MAPE [0-1]** | **CV-RMSE [0-1]** |
|---|---|---|---|
| XGB_2016_2017 | Train | 0.26 | 0.14 |
| XGB_2016_2017 | Test | 0.16 | 0.22 |
| XGB_2022 | Forecast | 0.53 | 0.48 |

## 3.3 Model predictive controller(s) (MPC)

As discussed in Chapter 2, two main MPC scenarios are evaluated. This section will explain the results of Scenario 1: MPC baseline and Scenario 2: MPC unconstrained minimum. Four additional MPC scenarios are discussed in Appendix D. Regarding the evaluation, KPIs for the MPCs are presented and compared with the Adapted-MeanControl algorithm discussed prior. In the last section, the practical implementation process of the two main scenario MPCs is discussed.

### 3.3.1 Scenario 1: MPC baseline [Ts=15 min]

The baseline MPC includes the physical constraints of the BESS. This MPC and its constraints are defined so that the outcomes are always in-line with the physical tolerance of the system. Figure 3.10 shows the load-duration curves of Scenario 1. The first observation is that, in comparison with the DSM algorithms, this MPC does not reduce the peak as would be expected. In addition, the excess solar generation is not stored in the BESS as would be expected. However, even though the load-duration curve explains the generic behaviour of the MPC, Figure 3.11 visualizes the entire horizon of the simulation. The top left graph shows the generic behaviour of the building where the building load, the grid and the PV generation are visualized. The uncontrolled grid is used in these simulations as the input for the simulation as the influence of the BESS is removed. The top right graph shows the grid data. In this graph, the difference between the uncontrolled grid and the controlled grid is visualized. It can be observed that some peaks are shaved and valleys are filled. However, frequently changing charging and discharging sequences are present. The bottom left shows the control outputs which would be sent to the BESS system. Charging and discharging is occurring on a highly frequent intervals. In addition, discharging occurs during peak periods. Therefore, it can be concluded that the MPC recognises the peaks and acts accordingly. However, the frequently changing sequence of charging and discharging is undesirable. This can be explained by the constraints definition. In this case, the minimum charging and discharging is limited to 5kW to exclude transmission losses. However, these constraints do not allow the battery to become idle. To overcome this issue, the MPC should be able to go to zero and therefore these minimum constraints have to be removed. The bottom right graph shows the SOC of the battery. This graph showcases the limits this MPC experiences as it cannot be idle and has to either charge or discharge with a 5kW minimum. This explains the saw-tooth behaviour as the model tries to minimize the power through the grid, it decides to charge and then discharge the battery in order to counter both their inputs. In theory, this would result in the lowest sum of power through the grid at the end of the horizon. However, this battery behaviour is highly undesirable as it harms the battery. Therefore, Scenario 2 is created where the minimum constraint is removed and only a maximum charging and discharging power is applied.

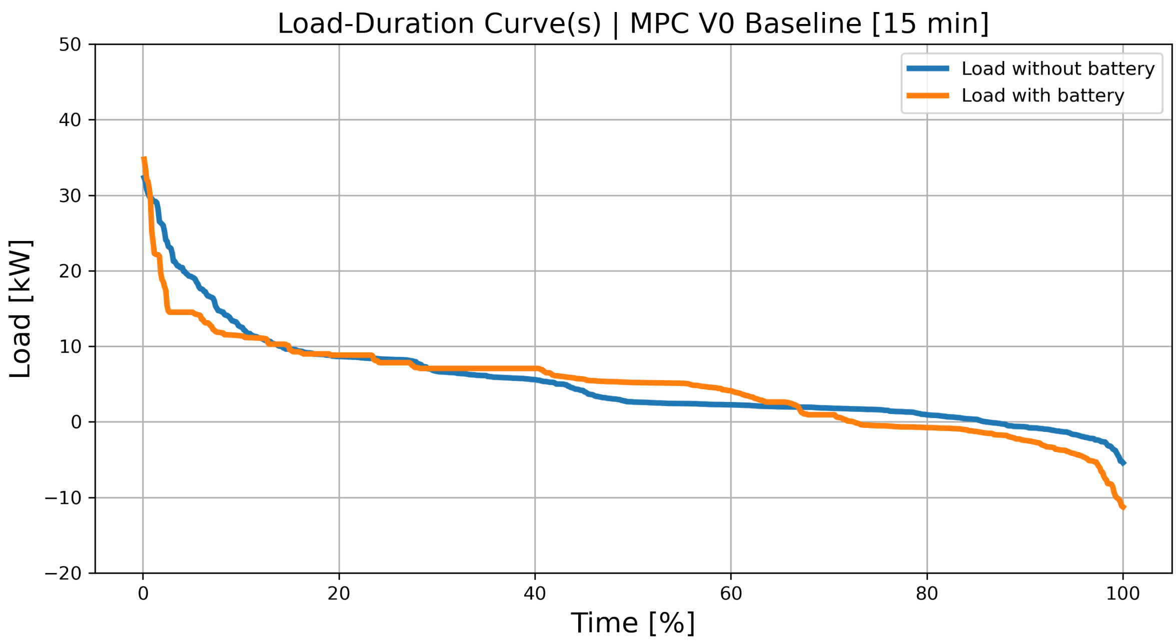


**Figure 3.10.** Visualization of load-duration curves of Scenario 1: MPC baseline.

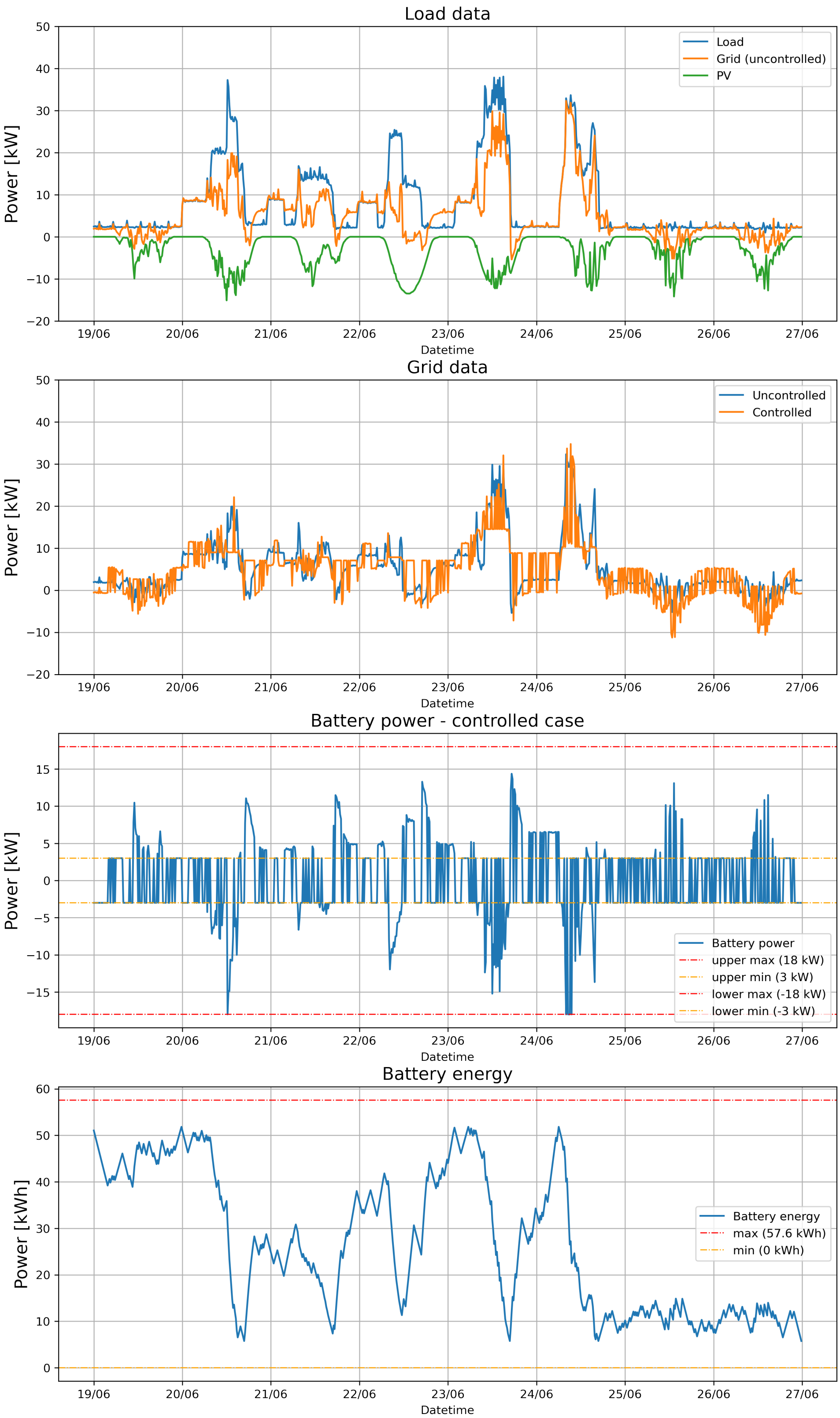


**Figure 3.11.** Results of Scenario 1: MPC baseline.

### 3.3.2 Scenario 2: MPC unconstrained minimum [Ts=15 min]

The MPC constraints are changed to allow the BESS to become idle. This is achieved by changing the minimum value for charging and discharging from 5kW to 0kW. This results in the following:

$$
\begin{aligned}
Amp_{min,old} = 3 \rightarrow Amp_{min,new} = 0 \\
kW_{min,old} = 5 \rightarrow kW_{min,new} = 0 \\
0\ kW \leq p_{charge}/p_{discharge} \leq 18\ kW
\end{aligned}
$$

It should be noted, transmission losses are occurring in the area between 0 and 5kW. Therefore, the results of this MPC scenario are merely to showcase the behaviour of the MPC. In reality, transmission losses are important to consider. Figure 3.12 shows the load-duration curves for the MPC. Now the strength of MPC is visualized as the orange curve is significantly more flat in comparison with the blue curve. Moreover, no power is fed back to the grid meaning the BESS is using the PV generation to its maximum capacity. When observing Figure 3.13 the frequently changing behaviour is no longer present. When excess PV is present, the charging power follows the PV line exactly, storing all power in the BESS. When evaluating the top right graph, a clear horizontal trend is observed during office hours. Therefore, the MPC recognises the peaks during the day and shaves these peaks using stored energy in the battery. Moreover, outside office hours the BESS is charged with energy from the grid to compensate for the peaks occurring in the morning. This demonstrates the added value of MPC in comparison with the DSM algorithms as the future is considered and the model can act accordingly.

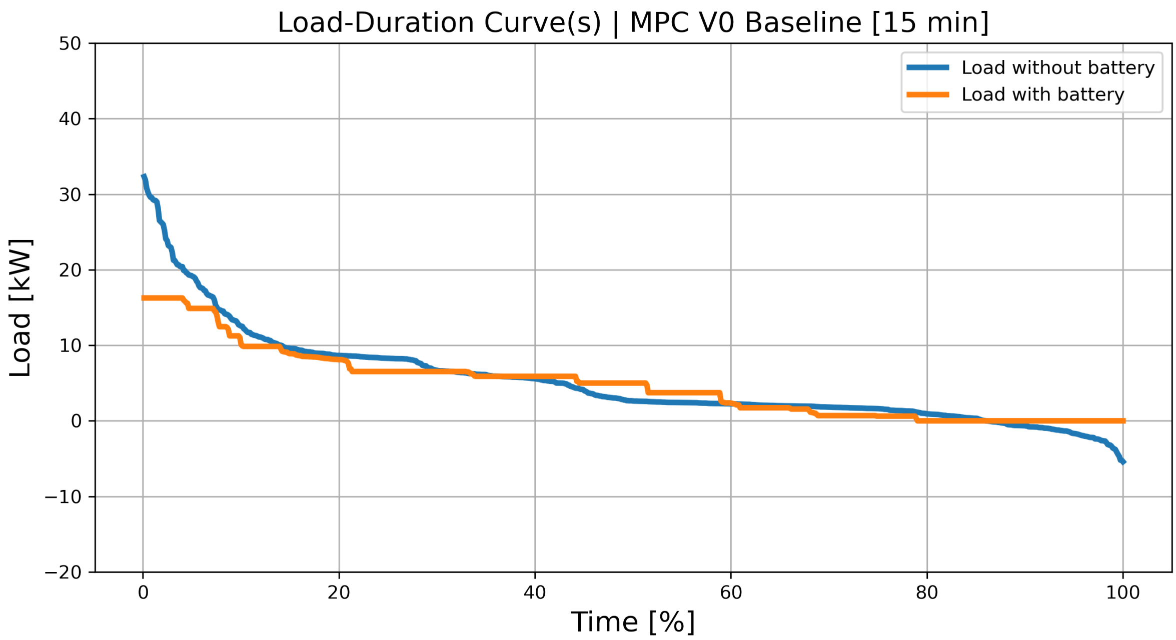


**Figure 3.12.** Visualization of load-duration curves of Scenario 2: MPC unconstrained minimum.

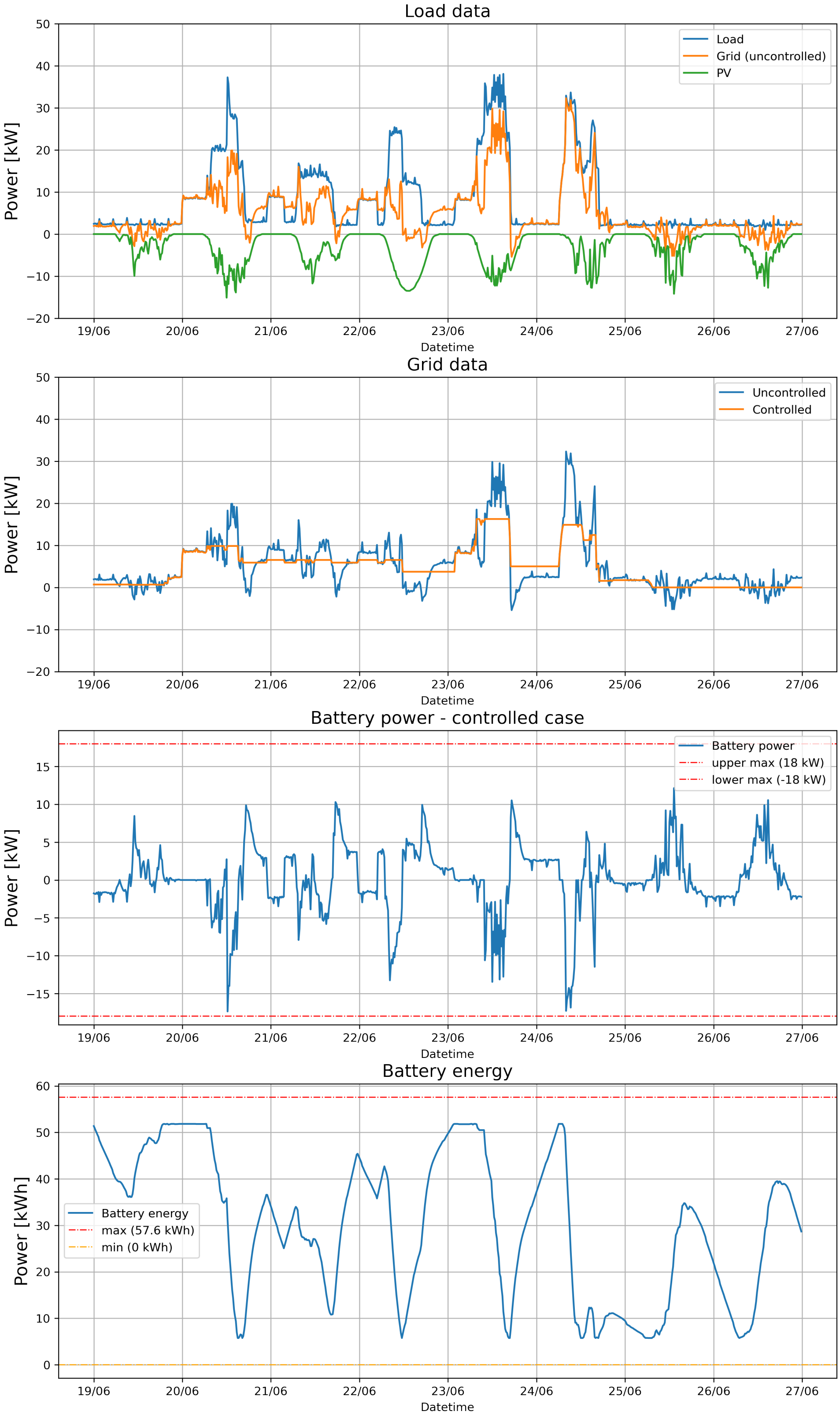


**Figure 3.13.** Results of Scenario 2: MPC unconstrained minimum.

### 3.3.3 Key performance indicators

The MPC scenarios are compared using the KPIs. To give a more extended overview of the performance of the models, the Adapted-MeanControl algorithm is added to Table 3.5. The Power Peak Reduction for Scenario 1 in comparison with the Adapted-MeanControl is lower during the morning periods and higher during the afternoon. Therefore, the MPC shows it recognises the optimization problem over the full horizon rather than acting in the moment as the Adapted-MeanControl does. Moreover, Scenario 2 outperforms both scenarios. Overall, Scenario 1 showcases a sufficient reduction during morning and afternoon peaks deeming it superior to the Adapted-MeanControl.

The Flexibility Factor of the Adapted-MeanControl and Scenario 2 show similarities. Both use the off-peak hours to charge the battery to compensate for peaks during high load hours. Scenario 1 shows less understanding of the high- and low load hours. In contrast to the other scenarios, this scenario is charging the BESS during high load hours. This is explained due to the model being unable to solve idle battery behaviour. Thus, the BESS is charged during high load hours simply because the overall energy required from the grid would be less, even if it is undesirable.

For Scenario 1 Self Sufficiency is affected by the frequently changing charging and discharging sequence. The MPC clearly tries to store as much excess PV in the BESS, however, during the afternoon the excess PV reaches the threshold of 5kW and therefore the sequences are rapidly repeated. When the Adapted-MeanControl is compared with Scenario 2, an improvement is observed as the MPC uses the excess PV to its maximum capacity. This pattern is validated when Self Consumption is evaluated. The unconstrained MPC achieves an SC ratio of 99%, clearly maximizing the PV generation and therefore minimizing the energy required from the grid. It should be noted, Scenario 1 reaches a sufficient SC as the SC of the office without any controller is at 92%.

Lastly, the Flexibility Index shows deviations in comparison with the Adapted-MeanControl. Scenario 1 has a negative FI because the BESS is often charged during peak price hours. Even though this is undesired, it cannot be resolved as the constraints would not allow it. Nevertheless, Scenario 2 showcases the saving capabilities when MPC is implemented. Approximately 9% of the cost can be saved if this MPC were to be implemented.

**Table 3.5.** KPI Evaluation MPC scenarios.

| **KPI** | **Period** | **Ideal** | **A.MeanCtrl** | **Scenario 1** | **Scenario 2** |
|---|---|---|---|---|---|
| $\Delta$ P [kW] | *Morning* | [+*] | 10.6 | 8.4 | 14.4 |
| $\Delta$ P [kW] | *Afternoon* | [+*] | -0.1 | 5.1 | 8.3 |
| $\Delta$ P [%] | *Morning* | [100%] | 35 [%] | 27% | 47% |
| $\Delta$ P [%] | *Afternoon* | [100%] | -1% | 21% | 30% |
| FF [%] | *Horizon* | [0%] | -2% | 11% | -3% |
| SS [%] | *Horizon* | [100%] | 23% | 8% | 31% |
| SC [%] | *Horizon* | [100%] | 81% | 90% | 99% |
| FI [%] | *Horizon* | [100%] | 1% | -7% | 9% |

* Ideally, the values for $\Delta$ P should be as high as possible. Negative values indicate an increase in power demand.

### 3.3.4 MPC implementation

The final part of the MPC development consists of the implementation and practical testing of both MPCs within the InsiteView environment. In contrast to the simulations, the implementation has excluded the EV load from the total building load as is mentioned in Chapter 2. The implementation consists of four main steps. First, the existing Solargis forecast with the weather data is obtained via InsiteSuite. The weather data is stored in a vector containing 96 values for the required weather features of the model. Moreover, the ML forecasting model is used to create a forecast of the building load 24 hours ahead with an interval of 15 minutes using the Solargis data as input. This will result in a vector containing 96 power values representing the building load. Second, on a local PC, the building load vector and weather data are obtained through an RPC call and loaded into the existing Jupyter Notebook. This Jupyter Notebook contains the Pyomo model and code which solves the cost function and creates a vector of outputs which of which the first value is sent to the BESS. Third, this output is sent through an RPC call to the BESS in the office where it executes this current. Last, the new SOC of the BESS is sent to the InsiteView server. Every 15 minutes this loop is executed and a new output is sent to the BESS in a receding horizon manner. The full implementation procedure is visualized in Figure 3.14.

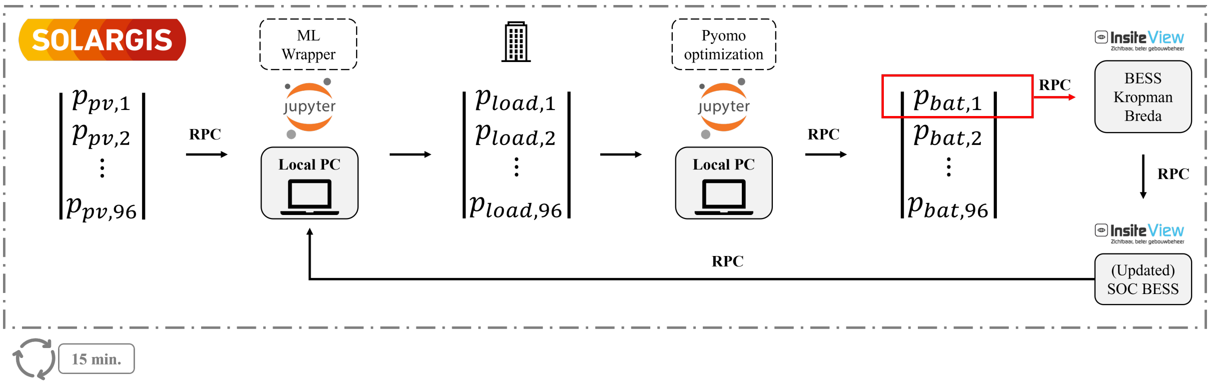


**Figure 3.14.** Visualization of MPC implementation procedure at the office building.

To further explain the MPC implementation procedure, the vector containing the 96 building load predictions is sliced to meet the current time. This ensures sending a value through RPC matches the current time of use. Thus, a slice is made in order to send the correct value to the BESS system where every 15 minutes the values are updated and 96 instances remain. It should be noted the vector will therefore always contain 96 values instead of subtracting one value after sending it. A visualization of a building load forecast vector ($p_{load}$) created at approximately 01:00 pm is given in Figure 3.15. This shows the day-ahead input for the MPC.

### 3.3.5 Conclusion

With the development of all MPCs and the final implementation, Figure 3.16 visualizes the inputs and outputs of the MPC which are sent to the BESS. The top graph shows the forecasts of the building load and PV generation, the grid with the MPC outputs implemented and the RPC outputs sent to the BESS. The bottom graph shows the BESS progression over time. It can be concluded that practical implementation of an MPC within the office is achieved. Limitations and future model improvements are discussed in Chapter 4 and Chapter 5.

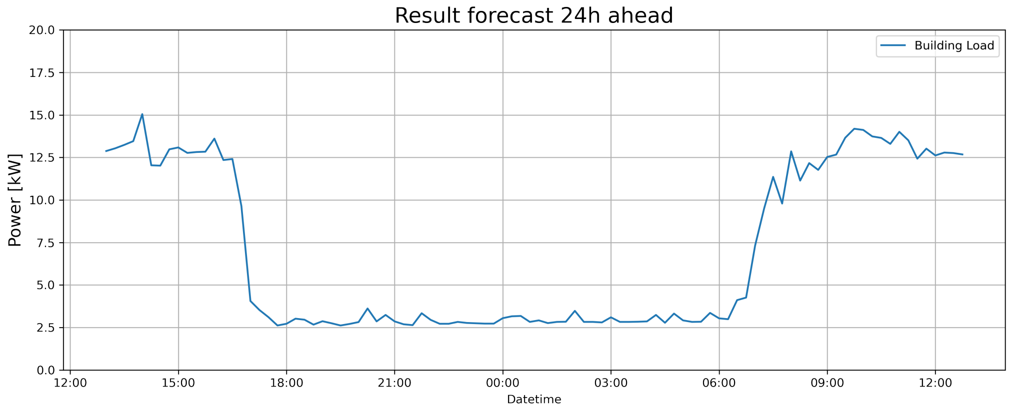


**Figure 3.15.** Visualization of the day-ahead forecast as input for the MPC.

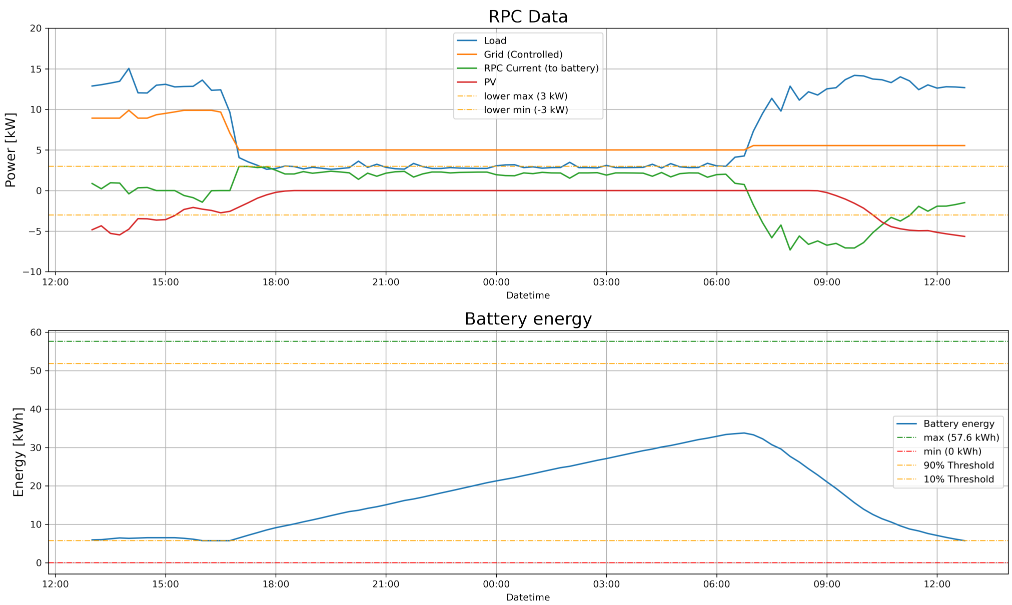


**Figure 3.16.** Visualization of RPC inputs for the MPC.

## 3.4 Smart Readiness Indicator (SRI)

To contribute to smart building technologies and functionalities, the SRI is evaluated. As stated in Chapter 2, three main methods are defined to evaluate the SRI. This research will calculate the SRI in situations before and after MPC implementation to identify the influence of an MPC on the office. Both Method A and Method B are evaluated and deviations are presented in this section. The full calculations can be found in Appendix C. The results are split into two segments of evaluation, the Impact scores and the Domain scores. The impact scores focus on the seven pillars of evaluation: *Energy efficiency*, *Energy flexibility and storage*, *Comfort*, *Convenience*, *Health, well-being and accessibility*, *Maintenance and fault prediction* and *Informant to occupants*. The Domain scores are the individual building related components: *Heating*, *Domestic hot water*, *Cooling*, *Ventilation*, *Lighting*, *Dynamic building envelope*, *Electricity*, *Electric vehicle charging*, *Monitoring and control*. To finalise this section a conclusion with the final SRI scores is presented and recommendations are made based on the SRI scores for the building.

### 3.4.1 SRI: Impact scores

The impact scores for all variants are visualized in Figure 3.17. Amongst Methods A and B there is a slight deviation visible. This is explained by the increased evaluation criteria of Method B which in some cases will refer to Method A being more on the simplistic side. When the baseline case is compared with the MPC implemented case for both methods A and B, there is a global trend indicating that an MPC improved the overall SRI score. Especially on the bar *Energy flexibility and storage*, the presence of MPC resulted in a large increase. On the other hand, it should be noted that the MPC only affected energy and control parameters, therefore it is important to evaluate the Domain scores.

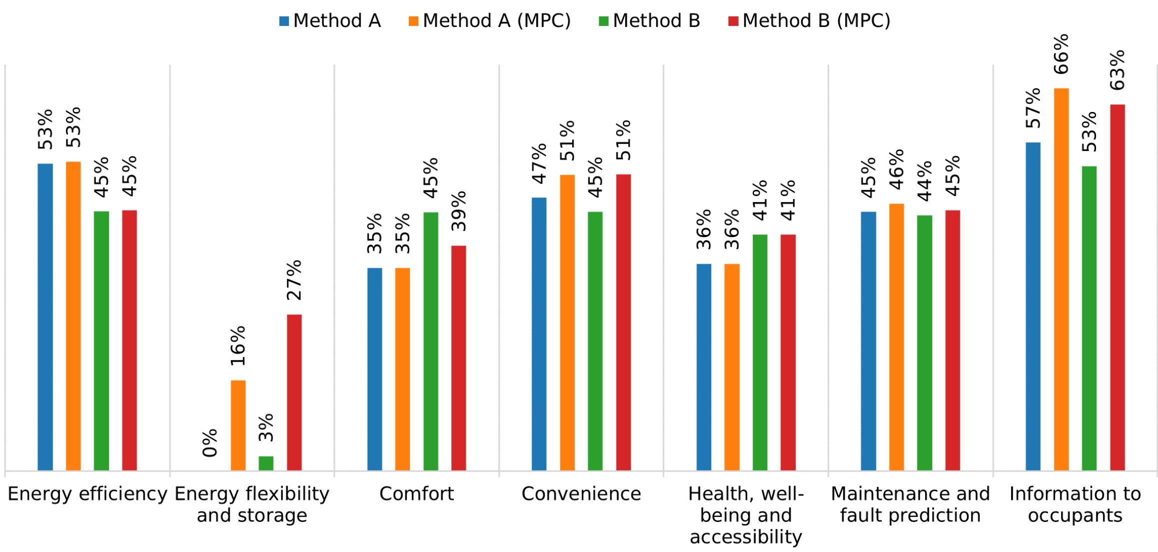


**Figure 3.17.** Impact scores for all SRI methods.

### 3.4.2 SRI: Domain scores

As is expected, the domain scores affected by the implementation of MPC are only the *Electricity* and *Monitoring and control* as is shown in Figure 3.18. For these subjects, a major improvement is observed where the increase for Method A is slightly higher in comparison with Method B. This emphasizes the general evaluation approach method of the SRI as implementing one aspect of a building might increase its performance, however, the building as a whole is evaluated with the SRI.

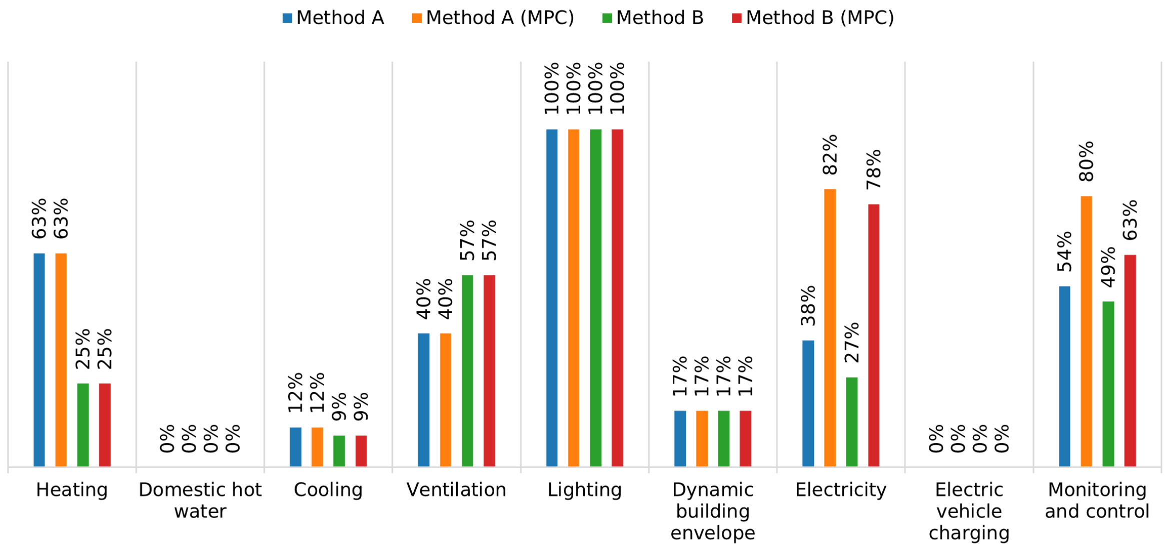


**Figure 3.18.** Domain scores for all SRI methods.

### 3.4.3 Conclusion

The final results of the four SRI calculations are presented in Table 3.6. The implementation of MPC has increased SRI scores. However, the overall SRI score for the office remains on the lower side. This has mainly to do because it is a generic office for which the SRI has multiple suggestions to improve. For each domain, a brief suggestion is given.

The heating system can increase by allowing occupants to control their desired heat on room level by showing the current heating levels and making occupants more aware of the buildings' heating schedule and profile. In addition, automated control, regulation and temperature feedback based on data is not yet implemented. Lastly, having an MPC for heating or a prediction based controller equivalent highly improves the heating flexibility towards the grid.

Domestic hot water (DHW) is not regulated and controlled in the office. Therefore, a lot of improvement can be achieved by following suggestions made by the SRI calculation as having a control regulator which automatically charges DHW at desired times. Moreover, DHW storage and renewable DHW charging using solar collectors would highly increase the SRI score.

The chiller of the office currently operates without automatic control. The cooling system operates on a constant temperature control which switches on when certain threshold values are exceeded. Suggestions in the SRI documentation are to use forecasting models to predict temperature and balance cooling control accordingly. Moreover, as is the case for heating, giving occupants the ability to control their temperature per room highly increases the score and comfort levels.

The AHU and ventilation of the office can be increased by changing the current clock and temperature control to CO2-based operation. Therefore, increased ventilation will occur in rooms with exceeding CO2 levels. In addition, indoor air quality monitoring and warning towards occupants are two motivators for comfort levels in the SRI calculation. This shows and allows occupants to realise certain CO2 levels and overrule the AHU by opening a window if necessary.

Regarding the lighting domain, the SRI already delivered a maximum score in all cases as the lighting is regulated based on occupancy levels with dynamic and adapted lighting scenes in the server.

The dynamic building envelope domain has an overall low score because window control is not considered at the office. Shading is executed by the occupants from the room rather than automatically controlled by solar sensors. Having predictive blind control based on weather forecasts would highly increase the overall SRI and is achievable when an automated blind operation is considered.

The electricity showed significant improvement with the introduction of MPC for BESS. However, the SRI suggest further increasing the domain by broadening the scope of the MPC and BESS system towards the neighbourhood level. This will give insights into the local energy market and will increase the usefulness of the MPC and BESS system towards energy flexibility at the microgrid level.

Regarding the electric vehicle charging domain, the office has four EV charging spots available. To improve the SRI score, 1- or 2-way EV charging control is to be implemented. This is in combination with occupancy presence identification when EVs arrive.

Lastly, the monitoring and control of the office increased significantly with the introduction of MPC with BESS. The final step on how this domain can be increased correlates with the increased steps for heating and cooling control. By adding MPCs or alternatives for heating and cooling operations, higher scores can be given and the overall SRI score will increase.

**Table 3.6.** Individual SRI scores of evaluation methods.

| | **Method A** | **Method A (MPC)** | **Method B** | **Method B (MPC)** |
|---|---|---|---|---|
| Score | 36% | 41% | 34% | 41% |

The implementation of MPC with BESS increased the SRI by approximately 6%. In addition, the SRI gives insights and an understanding of the steps building owners and stakeholders can take to increase a building's performance and KPIs.

# 4. Discussion

**Forecasting model**
A simplified ML model for the building load of an office is created using XGBoost from the SKlearn Python library. The building load includes a summation of HVAC, lighting and plug loads wherein the influence of EVs, PV and BESS are excluded. The forecasting model is trained on data from the years 2016 and 2017 obtained from historical databases. Due to the influence of Covid-19, data from more recent years are excluded from this research. During the training period, MAPE=26%, CV-RMSE=14% and testing period, MAPE=16%, CV-RMSE=22%; this evaluation shows a strong resemblance between predicted and actual building load. Thus, using this ML model, predictions for the year 2022 are made and used as input for the MPCs. Thorough data analysis shows various years of data of the office to be unusable, especially with two years of Covid-19 which changed the repetitive behaviour of energy usage. Therefore, the years 2016 and 2017 are used to create a forecasting model for the year 2022. As shown in Chapter 3, the accuracy of the forecasting model can be improved when the model is retrained with more recent data.

Additionally, ML models are created with XGBoost from SKlearn. During the data analysis, a choice between RandomForrest (RF) and XGBoost is made where XGBoost is chosen as this method is implemented within the ML wrapper. It should be noted that RF could show comparable, if not better outcomes. Therefore, the examination of future ML modelling methods is advised as it might increase the forecasting models' stats.

The forecasting model of the building load excludes the influence of EVs. It is visualized in the simulations that EV charging peaks are highly influential in comparison to the constant building load. Thus, it should be emphasized that to achieve higher accuracy, EV charging demand should be added to the building load, or added to the mix via a separate forecasting model. This will highly increase the practical outcomes of the MPCs as simulations showed that MPCs are capable of understanding EV behaviour.

**MPC**
The MPC cost function is a non-linear optimization problem where the power to the grid ($p_{grid}^2$) is minimized using linear constraints. The constraints represent physical limitations to the system where the control variables are the charging and discharging power of the BESS. Two MPC scenarios are evaluated within this research. Scenario 1 represents all physical limitations of the case study office. Scenario 2 has modified constraints to visualize the strength and added value of MPC compared to rule-based DSM algorithms. Rule-based algorithms conclude to be relatively fast to implement with sufficient DSM strategy outcomes. In case studies with a straightforward building layout, rule-based strategies can be sufficient solutions to increase energy flexibility. However, these strategies have no learning capabilities and increasing the complexity of these rule-based algorithms is less desirable as MPC is a more supported alternative. The MPC KPI evaluation shows the benefit of implementing MPC as power peaks are reduced by approximately 24% in Scenario 1 and 38% in Scenario 2. The flexibility factor identified the charging and discharging balance of the MPC where rule-based algorithms and MPCs both maintain a sufficient balance in relation to the energy flexibility. Self-sufficiency and self-consumption show comparable results when rule-based algorithms are compared with the MPC scenarios. However, self-consumption increases to approximately 90%, up

to almost 100% in Scenario 2 as distribution losses are neglected. The flexibility index showcases the cost saving potential of certain algorithms. In this research, the estimated price per kWh is €0.26 outside office hours and increases to €0.36 during office hours to penalise the energy drawn from the grid during peak hours. The rule-based algorithms show approximately 1% cost saving capabilities. MPC simulations show about 9% saving capabilities, however, this is without the transmission losses taken into account which would make the practical implementation less superior.

This research successfully implements MPC within an existing office in the Netherlands. ML forecasting models and Solargis weather forecasts are used to create 24-hour, day-ahead control outputs which operate on a 15-minute time sample. The MPC runs on a Jupyter Notebook which can operate on a server or local PC. The MPC sends signals to the BESS system using a sliding window with a receding horizon. This updates all MPC inputs removing as many disturbances to the system as possible.

All constraints are chosen based on the physical limitations of the system. Alternative constraint experiments are performed and discussed in Appendix D where physical aspects are removed and the validity of the model is evaluated. The main challenge with the physical system in the representation of the MPC is the minimum constraint for charging and discharging. In reality, the BESS does not allow currents below the set threshold. However, it would allow the BESS to be idle. To mathematically represent this constraint so that it would include both thresholds and the allowance to go to be idle is a complicated procedure which is outside the scope of this research. The MPC simulations show the physical limitations of the case study and demonstrate the bottlenecks of the implementation. However, including transmission losses will give a more accurate representation of reality. Therefore, regarding the implementation of MPC, both scenarios can be implemented. Nevertheless, it should be emphasized that currents sent to the system between the transmission thresholds (i.e. 0 and 5 kW) are to be penalised in reality.

The sample time of the MPC applied is 15 minutes as this is the threshold value for the Solargis forecasting model inputs. In addition, this represents the Dutch electricity grids' intra-day trading sample time which represents the real interval of operation. A brief study of sample-time alternatives is investigated, however additional motivation for the 15-minute sample time is excluded in this research.

Battery lifetime concerning battery charging and discharging sequences and the Depth of Discharge is not added to the MPCs. Therefore, it should be noted that $p_{bat,ch}$ and $p_{bat,dch}$ are optimized in regards to the cost of energy rather than to the efficiency of the BESS as a whole. Adding battery lifetime constraints to future MPC scenarios is therefore essential to obtain a generalized conclusion.

**SRI**

The SRI evaluation concludes that focus on energy flexibility and efficiency is important, however, the building and its users as a whole are equally as important. The implementation of MPC can increase the SRI score of this case study office by approximately 6%. This highly increases the electricity and controlling capabilities of buildings, nevertheless HVAC and personal comfort criteria indicate room for future improvement of the analysed case study.

# 5. Conclusion & future research

This research contributes to work package 2: Intelligent energy flexibility control strategies from the Brains4Buildings (B4B) initiative. The research provides insights into simulation and the practical implementation of MPC in office buildings. A forecasting model and MPC are developed and compared with several rule-based alternatives. The MPC is capable of achieving sufficient outcomes and practical implementation is achieved. Supported by literature, MPC is superior to rule-based alternatives. However, as is emphasized, the implementation process of a working MPC is the most important and challenging task. Therefore, this research identifies the added benefit of creating a simplified MPC, in contrast, to fully engineering an MPC before implementation. By comparing widely applied optimization problems in the literature, the optimization problem for this research is formed. The objective focuses on the cost of energy where energy from the grid is minimized. Simulations show the added benefit of implementing MPC within buildings. The energy flexibility increases as peak shaving and valley filling reduces the energy consumption during peak hours. Furthermore, MPC allows the addition of more constraints, making the building more future-proof as the scope can be broadened toward the neighbourhood level. This research focused on MPC concerning energy. The implementation of MPC highly increases the electricity and controlling capabilities of buildings, but HVAC and personal comfort are nevertheless as important. This research investigates and maps possible bottlenecks during the implementation phase. To improve the MPC within this research, suggestions for future work are presented. Ultimately, paving the way for future MPC implementations for different case studies.

**Forecasting model**

The implemented ML forecasting model for the building load is trained on data from the years 2016 and 2017. To increase the accuracy and adapt to future behaviour it is suggested to add data from the year 2022 to the training data and retrain the model. This will include new patterns occurring inside the building and therefore more accurate predictions can be made. Moreover, future research is advised on the addition of EV charging load to the building load mix. Previous research executed at Kropman regarding the same case study investigated the presence feature for occupants arriving at the building with EVs. Future research and development on this feature are advised as it will increase the robustness of the forecast. Moreover, a more accurate representation of the energy load would increase the efficiency of the MPC. Simulations show promising results when EV load predictions are taken into account, therefore future research with these implementations is recommended.

In regards to the InsiteSuite environment, it is suggested to add other applications of the SKlearn library, such as RandomForrest. As the ML wrapper uses the InsiteSuite features, it is recommended to research the future of this connection. Ultimately, having a remote environment wherein ML models can be trained and exchanged is desirable as this would allow the retraining of models and give a more broad application of ML models within InsiteSuite in general.

**MPC**

One important aspect of the MPC developed in this research is the simplicity of the model. Therefore, future research is advised to mainly focus on adding constraints to the controller(s) to achieve a more desirable outcome. The most important recommendation for future research is to investigate battery lifetime constraints to the existing MPCs. Adding these constraints will allow answers to cost related questions as well as the efficiency of BESS at different customer levels.

Currently, the MPCs operate on a receding horizon with inputs sliding over a window. An interesting addition could be researching the development of a fast controller in co-operation with the current MPC. The current MPC has a forecast of 24 hours which sends a signal every 15 minutes. Adding a feedback value obtained from another controller or input value from InsiteView could show the MPC what the *actual value* of the system is as opposed to what the forecast input predicted. This can minimize the error occurring and could overcome unexpected charging peaks. This generic feedback or control input can reduce fluctuations or errors in the system when compared with actual data.

From a customer point of view, it is interesting to investigate the translation of the MPC framework and data to the visualization within the InsiteView Next platform. As the general idea and strength of InsiteView Next are to give insight and understanding of building processes, future research is advised on how different goals or cost functions can be implemented in the InsiteView Next framework. Ultimately, customers can select a desired MPC strategy or goal with the click of a button and the graphs and tables are made to show results over time. This could allow a better understanding of the technical background towards customers and therefore improve communication between stakeholders.

**SRI**

As stated by the European Commission, Method C: In-use smart building performance, is currently unavailable as it is under development. Method C uses measured- and metered data to calculate the performance and outcomes of the SRI. Therefore, a more accurate representation of the SRI of a building can be achieved. However, as it would involve more time to derive outcomes, future research is recommended to calculate the SRI score for the case study building when the method is available. Not only will it increase the clarity of the results, but it will also contribute towards the further development of the SRI as a whole.

# 5. Bibliography

[1] IEA International Energy Agency. Tracking Buildings 2021 – Analysis - IEA, 2021. 1

[2] Marcus Gustafsson, Chiara Dipasquale, Stefano Poppi, Alessandro Bellini, Roberto Fedrizzi, Chris Bales, Fabian Ochs, Marion Sié, and Sture Holmberg. Economic and environmental analysis of energy renovation packages for European office buildings. *Energy and Buildings*, 148:155–165, 8 2017. 1

[3] Jan Ros. ENERGIETRANSITIE: ZOEKTOCHT MET EEN HELDER DOEL. Technical report, PBL Planbureau voor de Leefomgeving, Den Haag, 2015. 1

[4] IEA International Energy Agency. Statistics report Key World Energy Statistics 2021. Technical report, IEA International Energy Agency, 2021. 1

[5] Shenglin Li, Jizhong Zhu, Hanjiang Dong, Haohao Zhu, and Junwei Fan. A novel rolling optimization strategy considering grid-connected power fluctuations smoothing for renewable energy microgrids. *Applied Energy*, 309:118441, 3 2022. 1

[6] Laure Itard; Wim Zeiler; Baldiri Salcedo; Olivia Guerra Santin; Pieter Pauwels; Pauline van der Vorm; Mirjam Harmelink; Oana Trifan. Brains for Buildings (B4B), 10 2022. 1

[7] Deok Oh Woo and Lars Junghans. Framework for model predictive control (MPC)-based surface condensation prevention for thermo-active building systems (TABS). *Energy and Buildings*, 215:109898, 5 2020. 1

[8] Xiaoqing Huang, Dongliang Zhang, and Xiao Song Zhang. Energy management of intelligent building based on deep reinforced learning. *Alexandria Engineering Journal*, 60(1):1509–1517, 2 2021. 3

[9] Farhad Mofidi and Hashem Akbari. Intelligent buildings: An overview, 9 2020. 3

[10] Osama Omar. Intelligent building, definitions, factors and evaluation criteria of selection. *Alexandria Engineering Journal*, 57(4):2903–2910, 12 2018. 3

[11] Steven L. Brunton and Nathan J. Kutz. *Data-driven Science and Engineering: Machine Learning, Dynamical Systems, and Control*. Cambridge University Press, 2019. 3

[12] E. Kaiser, J. N. Kutz, and S. L. Brunton. Sparse identification of nonlinear dynamics for model predictive control in the low-data limit. *Proceedings of the Royal Society A: Mathematical, Physical and Engineering Sciences*, 474(2219), 11 2018. 3

[13] Eduardo F. Camacho and Carlos Bordons. Model Predictive Control. Technical report, Springer Science & Business Media, 2013. 4

[14] Carlos E. García, David M. Prett, and Manfred Morari. Model predictive control: Theory and practice—A survey. *Automatica*, 25(3):335–348, 5 1989. 4

[15] M. Mossolly, K. Ghali, and N. Ghaddar. Optimal control strategy for a multi-zone air conditioning system using a genetic algorithm. *Energy*, 34(1):58–66, 1 2009. 5, 6

[16] Gianluca Serale, Massimo Fiorentini, Alfonso Capozzoli, Daniele Bernardini, and Alberto Bemporad. Model Predictive Control (MPC) for enhancing building and HVAC system energy efficiency: Problem formulation, applications and opportunities. *Energies*, 11(3), 2 2018. 5

[17] Ján Drgoňa, Damien Picard, and Lieve Helsen. Cloud-based implementation of white-box model predictive control for a GEOTABS office building: A field test demonstration. *Journal of Process Control*, 88:63–77, 4 2020. 5

[18] Zakia Afroz, G. M. Shafiullah, Tania Urmee, and Gary Higgins. Modeling techniques used in building HVAC control systems: A review. *Renewable and Sustainable Energy Reviews*, 83:64–84, 3 2018. 5

[19] Jiang Jiang Wang, You Yin Jing, Chun Fa Zhang, and Jun Hong Zhao. Review on multi-criteria decision analysis aid in sustainable energy decision-making. *Renewable and Sustainable Energy Reviews*, 13(9):2263–2278, 12 2009. 6

[20] D. Mariano-Hernández, L. Hernández-Callejo, A. Zorita-Lamadrid, O. Duque-Pérez, and F. Santos García. A review of strategies for building energy management system: Model predictive control, demand side management, optimization, and fault detect & diagnosis. *Journal of Building Engineering*, 33:101692, 1 2021. 6, 9

[21] Vamsi Putta, Guangwei Zhu, Donghun Kim, Jianghai Hu, and James Braun. Comparative evaluation of model predictive control strategies for a building HVAC system. In *Proceedings of the American Control Conference*, pages 3455–3460. Institute of Electrical and Electronics Engineers Inc., 2013. 6

[22] Saran Salakij, Na Yu, Samuel Paolucci, and Panos Antsaklis. Model-Based Predictive Control for building energy management. I: Energy modeling and optimal control. *Energy and Buildings*, 133:345–358, 12 2016. 6

[23] Cheng Fan, Fu Xiao, Chengchu Yan, Chengliang Liu, Zhengdao Li, and Jiayuan Wang. A novel methodology to explain and evaluate data-driven building energy performance models based on interpretable machine learning. *Applied Energy*, 235:1551–1560, 2 2019. 6

[24] Bart Merema, Quinten Carton, Dirk Saelens, and Hilde Breesch. Implementation of MPC for an all-air system in an educational building. In *E3S Web of Conferences*, volume 246. EDP Sciences, 3 2021. 7

[25] Emrah Biyik and Aysegul Kahraman. A predictive control strategy for optimal management of peak load, thermal comfort, energy storage and renewables in multi-zone buildings. *Journal of Building Engineering*, 25:100826, 9 2019. 7

[26] Michael Dahl Knudsen, Laurent Georges, Kristian Stenerud Skeie, and Steffen Petersen. Experimental test of a black-box economic model predictive control for residential space heating. *Applied Energy*, 298:117227, 9 2021. 7

[27] Hao Qin and Xiaoxu Wang. A multi-discipline predictive intelligent control method for maintaining the thermal comfort on indoor environment. *Applied Soft Computing*, 116:108299, 2 2022. 7

[28] Clark W. Gellings. The Concept of Demand-Side Management for Electric Utilities. *Proceedings of the IEEE*, 73(10):1468–1470, 1985. 8

[29] Ellika Taveres-Cachat, Steinar Grynning, Judith Thomsen, and Stephen Selkowitz. Responsive building envelope concepts in zero emission neighborhoods and smart cities - A roadmap to implementation. *Building and Environment*, 149:446–457, 2 2019. 8

[30] Hannah Fontenot and Bing Dong. Modeling and control of building-integrated microgrids for optimal energy management – A review. *Applied Energy*, 254:113689, 11 2019. 9, 17, 18

[31] Jia Woon Lee, Mohammed Hussein Saleh Mohammed Haram, Gobbi Ramasamy, Siva Priya Thiagarajah, Eng Eng Ngu, and Yuen How Lee. Technical feasibility and economics of repurposed electric vehicles batteries for power peak shaving. *Journal of Energy Storage*, 40:102752, 8 2021. 9

[32] Bahareh Ramezani, Manuel Gameiro da Silva, and Nuno Simões. Application of smart readiness indicator for Mediterranean buildings in retrofitting actions. *Energy and Buildings*, 249:111173, 10 2021. 9

[33] Fabian Pedregosa, Gaël Varoquaux, Alexandre Gramfort, Vincent Michel, Bertrand Thirion, Olivier Grisel, Mathieu Blondel, Peter Prettenhofer, Peter Weiss, Vincent Dubourg, Jake Vanderplas, Alexandre Passos, David Cournapeau, Matthieu Brucher, Matthieu Perrot, and Édouard Duchesnay. Scikit-learn: Machine Learning in Python. Technical report, Scikit-learn, 2011. 11

[34] Michael Olusegun Akinwande, Hussaini Garba Dikko, and Agboola Samson. Variance Inflation Factor: As a Condition for the Inclusion of Suppressor Variable(s) in Regression Analysis. *Open Journal of Statistics*, 05(07):754–767, 2015. 12

[35] Tianqi Chen and Carlos Guestrin. XGBoost: A Scalable Tree Boosting System. *The 22nd ACM SIGKDD International Conference*, 2016. 12

[36] James Bergstra, James Bergstra@umontreal Ca, and Yoshua Bengio@umontreal Ca. Random Search for Hyper-Parameter Optimization Yoshua Bengio. Technical report, D epartement d Informatique et de recherche operationnelle, Montreal, 2012. 13

[37] Shalika Walker, Waqas Khan, Katarina Katic, Wim Maassen, and Wim Zeiler. Accuracy of different machine learning algorithms and added-value of predicting aggregated-level energy performance of commercial buildings. *Energy and Buildings*, 209:109705, 2 2020. 13

[38] Cheng Fan, Fu Xiao, and Yang Zhao. A short-term building cooling load prediction method using deep learning algorithms. *Applied Energy*, 195:222–233, 6 2017. 13

[39] Chengliang Fan and Yunfei Ding. Cooling load prediction and optimal operation of HVAC systems using a multiple nonlinear regression model. *Energy and Buildings*, 197:7–17, 8 2019. 13

[40] Scott M Lundberg and Su-In Lee. A Unified Approach to Interpreting Model Predictions. In I Guyon, U Von Luxburg, S Bengio, H Wallach, R Fergus, S Vishwanathan, and R Garnett, editors, *Advances in Neural Information Processing Systems*, volume 30. Curran Associates, Inc., 2017. 13

[41] Felipe Gonzalez Venegas, Marc Petit, and Yannick Perez. Active integration of electric vehicles into distribution grids: Barriers and frameworks for flexibility services, 7 2021. 18

[42] Jie Cai, Xing Jin, and Hao Zhang. Economic Model-Based Control of Sustainable Buildings with Photovoltaic (PV) and Battery Systems Considering Battery Degradation Costs. In *Proceedings of the American Control Conference*, volume 2018-June, pages 5406–5411. Institute of Electrical and Electronics Engineers Inc., 8 2018. 18

[43] William E Hart, Jean-Paul Watson, and David L Woodruff. Pyomo: modeling and solving mathematical programs in Python. *Mathematical Programming Computation*, 3(3):219–260, 2011. 20, 53

[44] Han Li, Zhe Wang, Tianzhen Hong, and Mary Ann Piette. Energy flexibility of residential buildings: A systematic review of characterization and quantification methods and applications. *Advances in Applied Energy*, 3:100054, 8 2021. 21

[45] European Commission, Directorate-General for Energy, S Verbeke, D Aerts, G Reynders, Y Ma, and P Waide. *Final report on the technical support to the development of a smart readiness indicator for buildings : final report*. Publications Office, 2020. 23

[46] Md Monirul Islam, Cihan H. Dagli, and Zeyi Sun. A Model to Estimate the Lifetime of BESS for the Prosumer Community of Manufacturers with OGS. *Procedia Computer Science*, 168:186–194, 1 2020. 27

[47] Michael L Bynum, Gabriel A Hackebeil, William E Hart, Carl D Laird, Bethany L Nicholson, John D Siirola, Jean-Paul Watson, and David L Woodruff. *Pyomo–optimization modeling in python*, volume 67. Springer Science & Business Media, third edition, 2021. 53

[48] Nanda Kishor Panda and Nikolaos G. Paterakis. A multi-objective optimization model for the quantification of flexibility in a large business park. In *SEST 2021 - 4th International Conference on Smart Energy Systems and Technologies*. Institute of Electrical and Electronics Engineers Inc., 9 2021. 53

# A. Appendix: I

## A.0.1 Meters of the office building

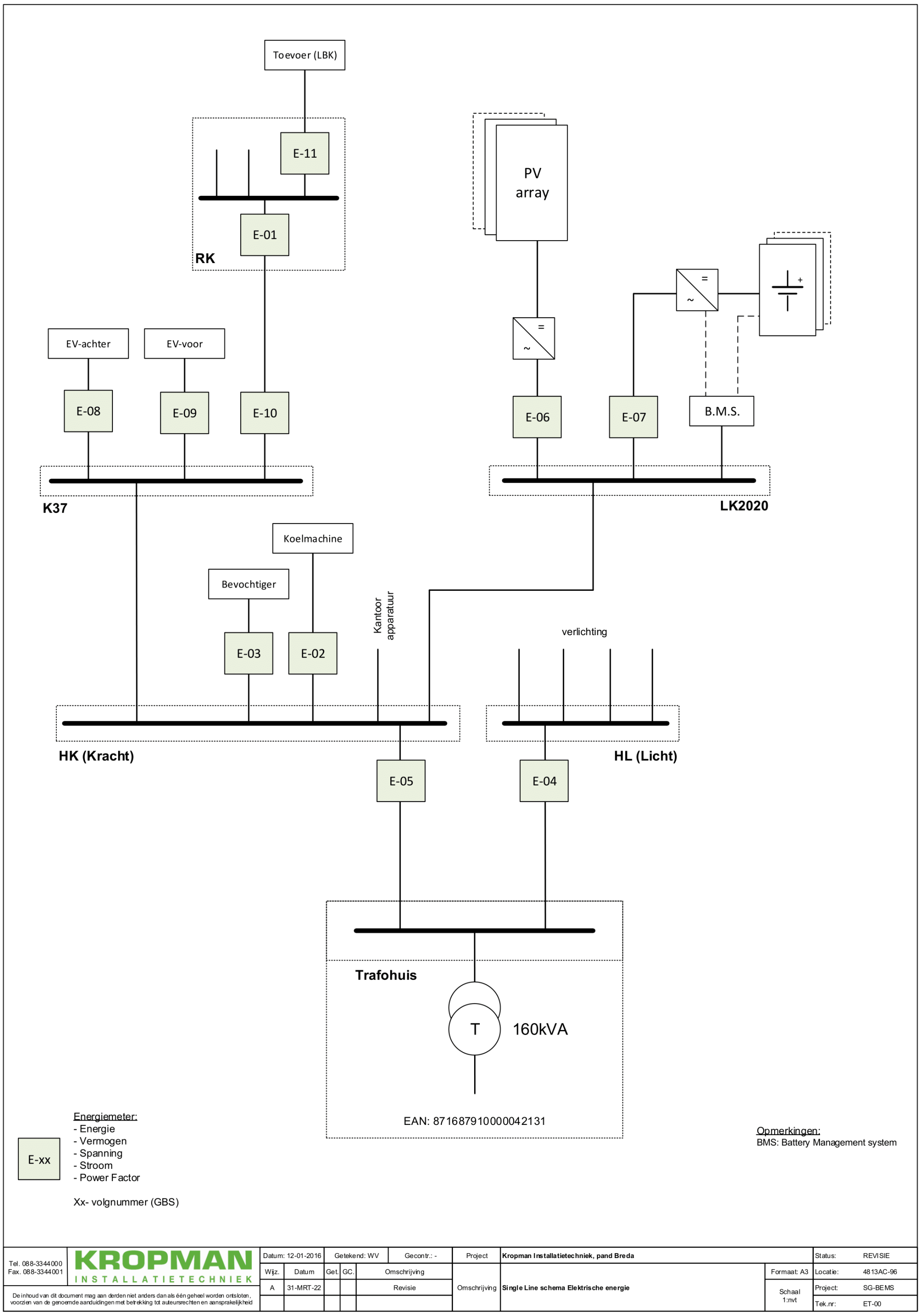


**Figure A.1.** Oneline scheme of meters in the office building.

# B. Appendix: II

### B.0.1 Pyomo explaination

Pyomo is a Python-based open-source software package that supports a diverse set of optimization capabilities for formulating, solving, and analyzing optimization models. The goal of Pyomo is to provide a platform for specifying optimization models that embodies central ideas found in modern Algebraic Modeling Languages (AMLs), within a framework that promotes flexibility, extensibility, portability, openness, and maintainability. Pyomo is an AML that extends Python to include objects for optimization modelling [43]. These objects can be used to specify optimization models and translate them into various formats that can be processed by external solvers.

When Pyomo is used for an optimization problem, the mathematical equations are to be translated to the core components of Pyomo. There are a total of seven components of which five are used in this research. A more extensive explanation for all components is given in the Pyomo book [47]. The first component is the *Var* component. This component relates to all variables in the optimization problem which can be in both continuous and discrete time. The *Objective* component contains the mathematical expression used to define the objective function. The objective function of each optimization function relates to minimizing or maximizing a certain variable in the system. The *Constraint* component is used to add restrictions to the Pyomo model. Pyomo supports equality and general inequality constraints. The *Set* component relates to a selection of the data containing numeric or symbolic elements. Individual values used in the model are represented as *Param* components. In contrast to regular *float* Python data types, the *Param* component can be mutable. To execute the optimization model, a solver is to be selected. As Pyomo uses external solvers, four different solvers are suggested within the Pyomo documentation. Out of these four solvers, *Ipopt* is selected because it can solve non-linear optimization problems.

For the optimization problem of this research, a *ConcreteModel* is created within the Pyomo environment. Two separate *Sets* are created for all time steps within the horizon of the optimization problem and an empty set for the individual parameters set for boundary values. These boundaries include battery capacity boundaries, transmission losses, initial values of the system and efficiencies. The variables created in the model are the vectors created over which the model creates outputs over the total horizon. It should be noted that $p_{pv}$ and $p_{load}$ are not added to the variable component. These vectors are disturbances which are already pre-defined therefore Pyomo cannot change values in these vectors. Furthermore, the constraints are added to the Pyomo model by creating definitions which involve the mathematical expressions linked to the created parameters and variables of the Pyomo model. These constraint definitions are then added to the model by appending the *rule* to the model via the *Constraint* component. Lastly, the objective function is mathematically defined using a definition and this objective is then added to the model completing the Pyomo environment. As a reference, previous work by Panda et al. is consulted to compare and translate the model equations within the Pyomo environment [48].

# C. Appendix: III

## C.0.1 Smart readiness indicator (SRI): full calculation

For all SRI calculations, the location of the office building is determined prior to the calculations. As the case study is an office building from The Netherlands, West Europe is the location selected for the SRI calculations. Therefore, the weighting factors within the SRI calculation are shown in Figure C.1.

| West Europe | Energy efficiency | Energy flexibility and storage | Comfort | Convenience | Health, well-being and accessibility | Maintenance and fault prediction | Information to occupants |
|---|---|---|---|---|---|---|---|
| Heating | 0.27 | 0.41 | 0.16 | 0.1 | 0.2 | 0.32 | 0.11 |
| Domestic hot water | 0.08 | 0.12 | 0.00 | 0.1 | 0 | 0.10 | 0.11 |
| Cooling | 0.13 | 0.19 | 0.16 | 0.1 | 0.20 | 0.15 | 0.11 |
| Ventilation | 0.14 | 0.00 | 0.16 | 0.1 | 0.20 | 0.17 | 0.11 |
| Lighting | 0.10 | 0.00 | 0.16 | 0.1 | 0.00 | 0.00 | 0.00 |
| Electricity | 0.02 | 0.03 | 0.00 | 0.1 | 0.00 | 0.02 | 0.11 |
| Dynamic building envelope | 0.05 | 0 | 0.16 | 0.1 | 0.20 | 0.05 | 0.11 |
| Electric vehicle charging | 0 | 0.05 | 0 | 0.1 | 0 | 0 | 0.11 |
| Monitoring and control | 0.2 | 0.2 | 0.2 | 0.2 | 0.2 | 0.2 | 0.2 |
| | *1.00* | *1.00* | *1.00* | *1.00* | *1.00* | *1.00* | *1.00* |

| IMPACT WEIGHTINGS | Energy efficiency | Energy flexibility and storage | Comfort | Convenience | Health, well-being and accessibility | Maintenance and fault prediction | Information to occupants |
|---|---|---|---|---|---|---|---|
| | 0.17 | 0.33 | 0.08 | 0.08 | 0.08 | 0.17 | 0.08 |

**Figure C.1.** SRI calculation weightings.

This appendix presents all results as given in the SRI calculation sheets. A total fo four different calculation methods are evaluated which are presented below in the following order:

1. Method A: Table C.1
2. Method A with MPC: Table C.2
3. Method B: Table C.3
4. Method B with MPC: Table C.4

### C.0.2 Method A

**Table C.1.** Individual SRI scores for evaluation Method A.

| Code | Smart ready service | Score | Elaboration |
|---|---|---|---|
| H-1a | Heat emission control | 2 | Individual room control (e.g. thermostatic valves, or electronic controller) |
| H-1c | Storage and shifting of thermal energy | 2 | HW storage vessels controlled based on external signals (from BACS or grid) |
| H-2a | Heat generator control (all except heat pumps) | 1 | Variable temperature control depending on outdoor temperature |
| H-3 | Report information regarding heating system performance | 2 | Central or remote reporting of current performance KPIs and historical data |
| DHW-1a | Control of DHW storage charging (with direct electric heating or integrated electric heat pump) | 0 | Automatic control on / off |
| DHW-1b | Control of DHW storage charging | 0 | None |
| DHW-3 | Report information regarding domestic hot water performance | 0 | None |
| C-1a | Cooling emission control | 0 | No automatic control |
| C-2a | Generator control for cooling | 0 | On/Off-control of cooling production |
| C-3 | Report information regarding cooling system performance | 2 | Central or remote reporting of current performance KPIs and historical data |
| C-4 | Flexibility and grid interaction | 0 | No automatic control |
| V-1a | Supply air flow control at the room level | 1 | Clock control |
| V-6 | Reporting information regarding IAQ | 1 | Air quality sensors (e.g. CO2) and real time autonomous monitoring |
| L-1a | Occupancy control for indoor lighting | 3 | Automatic detection (manual on / dimmed or auto off) |
| DE-1 | Window solar shading control | 0 | No sun shading or only manual operation |
| DE-4 | Reporting information regarding performance of dynamic building envelope systems | 1 | Position of each product & fault detection |
| E-2 | Reporting information regarding local electricity generation | 2 | Actual values and historical data |

| | | | |
|---|---|---|---|
| E-3 | Storage of (locally generated) electricity | 1 | On site storage of electricity (e.g. electric battery) |
| E-11 | Reporting information regarding energy storage | 2 | Actual values and historical data |
| E-12 | Reporting information regarding electricity consumption | 1 | reporting on current electricity consumption on building level |
| EV-15 | EV Charging Capacity | 3 | 10-50% or parking spaces has recharging point |
| EV-16 | EV Charging Grid balancing | 0 | Not present (uncontrolled charging) |
| EV-17 | EV charging information and connectivity | 1 | Reporting information on EV charging status to occupant |
| MC-13 | Central reporting of TBS performance and energy use | 3 | Central or remote reporting of realtime energy use per energy carrier, combining TBS of all main domains in one interface |
| MC-25 | Smart Grid Integration | 0 | None - No harmonization between grid and TBS; building is operated independently from the grid load |
| MC-30 | Single platform that allows automated control & coordination between TBS + optimization of energy flow based on occupancy, weather and grid signals | 3 | Single platform that allows automated control & coordination between TBS + optimization of energy flow based on occupancy, weather and grid signals |

### With MPC

**Table C.2.** Individual SRI scores for evaluation Method A with MPC.

| Code | Smart ready service | Score | Elaboration |
|---|---|---|---|
| H-1a | Heat emission control | 2 | Individual room control (e.g. thermostatic valves, or electronic controller) |
| H-1c | Storage and shifting of thermal energy | 2 | HW storage vessels controlled based on external signals (from BACS or grid) |
| H-2a | Heat generator control (all except heat pumps) | 1 | Variable temperature control depending on outdoor temperature |
| H-3 | Report information regarding heating system performance | 2 | Central or remote reporting of current performance KPIs and historical data |
| DHW-1a | Control of DHW storage charging (with direct electric heating or integrated electric heat pump) | 0 | Automatic control on / off |
| DHW-1b | Control of DHW storage charging | 0 | None |
| DHW-3 | Report information regarding domestic hot water performance | 0 | None |
| C-1a | Cooling emission control | 0 | No automatic control |
| C-2a | Generator control for cooling | 0 | On/Off-control of cooling production |
| C-3 | Report information regarding cooling system performance | 2 | Central or remote reporting of current performance KPIs and historical data |
| C-4 | Flexibility and grid interaction | 0 | No automatic control |
| V-1a | Supply air flow control at the room level | 1 | Clock control |
| V-6 | Reporting information regarding IAQ | 1 | Air quality sensors (e.g. CO2) and real time autonomous monitoring |
| L-1a | Occupancy control for indoor lighting | 3 | Automatic detection (manual on / dimmed or auto off) |
| DE-1 | Window solar shading control | 0 | No sun shading or only manual operation |
| DE-4 | Reporting information regarding performance of dynamic building envelope systems | 1 | Position of each product & fault detection |

| | | | |
|---|---|---|---|
| E-2 | Reporting information regarding local electricity generation | 4 | Performance evaluation including forecasting and/or benchmarking; also including predictive management and fault detection |
| E-3 | Storage of (locally generated) electricity | 4 | On site storage of energy (e.g. electric battery or thermal storage) with controller optimising the use of locally generated electricity and possibility to feed back into the grid |
| E-11 | Reporting information regarding energy storage | 4 | Performance evaluation including forecasting and/or benchmarking; also including predictive management and fault detection |
| E-12 | Reporting information regarding electricity consumption | 2 | real-time feedback or benchmarking on building level |
| EV-15 | EV Charging Capacity | 3 | 10-50% or parking spaces has recharging point |
| EV-16 | EV Charging Grid balancing | 0 | Not present (uncontrolled charging) |
| EV-17 | EV charging information and connectivity | 1 | Reporting information on EV charging status to occupant |
| MC-13 | Central reporting of TBS performance and energy use | 3 | Central or remote reporting of realtime energy use per energy carrier, combining TBS of all main domains in one interface |
| MC-25 | Smart Grid Integration | 1 | Demand side management possible for (some) individual TBS, but not coordinated over various domains |
| MC-30 | Single platform that allows automated control & coordination between TBS + optimization of energy flow based on occupancy, weather and grid signals | 3 | Single platform that allows automated control & coordination between TBS + optimization of energy flow based on occupancy, weather and grid signals |

### C.0.3 Method B

**Table C.3.** Individual SRI scores for evaluation Method B.

| Code | Smart ready service | Score | Elaboration |
|---|---|---|---|
| H-1a | Heat emission control | 2 | Individual room control (e.g. thermostatic valves, or electronic controller) |
| H-1b | Emission control for TABS (heating mode) | 0 | No automatic control |
| H-1c | Storage and shifting of thermal energy | 1 | Outside temperature compensated control |
| H-1d | Control of distribution pumps in networks | 2 | Multi-Stage control |
| H-2a | Heat generator control (all except heat pumps) | 1 | Variable temperature control depending on outdoor temperature |
| H-3 | Report information regarding heating system performance | 2 | Central or remote reporting of current performance KPIs and historical data |
| H-4 | Flexibility and grid interaction | 0 | No automatic control |
| DHW-1a | Control of DHW storage charging (with direct electric heating or integrated electric heat pump) | 0 | Automatic control on / off |
| DHW-3 | Report information regarding domestic hot water performance | 0 | None |
| C-1a | Cooling emission control | 0 | No automatic control |
| C-1b | Emission control for TABS (cooling mode) | 0 | No automatic control |
| C-1c | Control of distribution network chilled water temperature (supply or return) | 0 | Constant temperature control |
| C-1d | Control of distribution pumps in networks | 1 | On off control |
| C-1f | Interlock: avoiding simultaneous heating and cooling in the same room | 0 | No interlock |
| C-2a | Generator control for cooling | 0 | |
| C-3 | Report information regarding cooling system performance | 2 | Central or remote reporting of current performance KPIs and historical data |
| C-4 | Flexibility and grid interaction | 0 | No automatic control |
| V-1a | Supply air flow control at the room level | 1 | Clock control |

| | | | |
|---|---|---|---|
| V-1c | Air flow or pressure control at the air handler level | 1 | On off time control: Continuously supplies of air flow for a maximum load of all rooms during nominal occupancy time |
| V-2c | "Heat recovery control: prevention of overheating" | 2 | Modulate or bypass heat recovery based on multiple room temperature sensors or predictive control |
| V-2d | Supply air temperature control at the air handling unit level | 2 | Variable set point with outdoor temperature compensation |
| V-3 | Free cooling with mechanical ventilation system | 1 | Night cooling |
| V-6 | Reporting information regarding IAQ | 1 | Air quality sensors (e.g. CO2) and real time autonomous monitoring |
| L-1a | Occupancy control for indoor lighting | 3 | Automatic detection (manual on / dimmed or auto off) |
| L-2 | Control artificial lighting power based on daylight levels | 4 | "Automatic dimming including scene-based light control (during time intervals, dynamic and adapted lighting scenes are set, for example, in terms of illuminance level, different correlated colour temperature (CCT) and the possibility to change the light distribution within the space according to e. g. design, human needs, visual tasks)" |
| DE-1 | Window solar shading control | 0 | No sun shading or only manual operation |
| DE-2 | Window open/closed control, combined with HVAC system | 0 | Manual operation or only fixed windows |
| DE-4 | Reporting information regarding performance of dynamic building envelope systems | 1 | Position of each product & fault detection |
| E-2 | Reporting information regarding local electricity generation | 2 | Actual values and historical data |
| E-3 | Storage of (locally generated) electricity | 1 | On site storage of electricity (e.g. electric battery) |
| E-4 | Optimizing self-consumption of locally generated electricity | 0 | None |
| E-8 | Support of (micro)grid operation modes | 0 | None |
| E-11 | Reporting information regarding energy storage | 2 | Actual values and historical data |

| | | | |
|---|---|---|---|
| E-12 | Reporting information regarding electricity consumption | 1 | reporting on current electricity consumption on building level |
| EV-15 | EV Charging Capacity | 3 | 10-50% or parking spaces has recharging point |
| EV-16 | EV Charging Grid balancing | 0 | Not present (uncontrolled charging) |
| EV-17 | EV charging information and connectivity | 1 | Reporting information on EV charging status to occupant |
| MC-3 | Run time management of HVAC systems | 1 | Runtime setting of heating and cooling plants following a predefined time schedule |
| MC-4 | Detecting faults of technical building systems and providing support to the diagnosis of these faults | 3 | With central indication of detected faults and alarms for all relevant TBS, including diagnosing functions |
| MC-9 | Occupancy detection: connected services | 1 | Occupancy detection for individual functions, e.g. lighting |
| MC-13 | Central reporting of TBS performance and energy use | 3 | Central or remote reporting of realtime energy use per energy carrier, combining TBS of all main domains in one interface |
| MC-25 | Smart Grid Integration | 0 | None - No harmonization between grid and TBS; building is operated independently from the grid load |
| MC-28 | Reporting information regarding demand side management performance and operation | 0 | None |
| MC-29 | Override of DSM control | 0 | No DSM control |
| MC-30 | Single platform that allows automated control & coordination between TBS + optimization of energy flow based on occupancy, weather and grid signals | 3 | Single platform that allows automated control & coordination between TBS + optimization of energy flow based on occupancy, weather and grid signals |

### With MPC

**Table C.4.** Individual SRI scores for evaluation Method B with MPC.

| Code | Smart ready service | Score | Elaboration |
|---|---|---|---|
| H-1a | Heat emission control | 2 | Individual room control (e.g. thermostatic valves, or electronic controller) |
| H-1b | Emission control for TABS (heating mode) | 0 | No automatic control |
| H-1c | Storage and shifting of thermal energy | 1 | Outside temperature compensated control |
| H-1d | Control of distribution pumps in networks | 2 | Multi-Stage control |
| H-1f | Thermal Energy Storage (TES) for building heating (excluding TABS) | 0 | |
| H-2a | Heat generator control (all except heat pumps) | 1 | Variable temperature control depending on outdoor temperature |
| H-3 | Report information regarding heating system performance | 2 | Central or remote reporting of current performance KPIs and historical data |
| H-4 | Flexibility and grid interaction | 0 | No automatic control |
| DHW-1a | Control of DHW storage charging (with direct electric heating or integrated electric heat pump) | 0 | Automatic control on / off |
| DHW-1b | Control of DHW storage charging | 0 | |
| DHW-3 | Report information regarding domestic hot water performance | 0 | None |
| C-1a | Cooling emission control | 0 | No automatic control |
| C-1b | Emission control for TABS (cooling mode) | 0 | No automatic control |
| C-1c | Control of distribution network chilled water temperature (supply or return) | 0 | Constant temperature control |
| C-1d | Control of distribution pumps in networks | 1 | On off control |
| C-1f | Interlock: avoiding simultaneous heating and cooling in the same room | 0 | No interlock |
| C-2a | Generator control for cooling | 0 | On/Off-control of cooling production |

| | | | |
|---|---|---|---|
| C-3 | Report information regarding cooling system performance | 2 | Central or remote reporting of current performance KPIs and historical data |
| C-4 | Flexibility and grid interaction | 0 | No automatic control |
| V-1a | Supply air flow control at the room level | 1 | Clock control |
| V-1c | Air flow or pressure control at the air handler level | 1 | On off time control: Continuously supplies of air flow for a maximum load of all rooms during nominal occupancy time |
| V-2c | "Heat recovery control: prevention of overheating" | 2 | Modulate or bypass heat recovery based on multiple room temperature sensors or predictive control |
| V-2d | Supply air temperature control at the air handling unit level | 2 | Variable set point with outdoor temperature compensation |
| V-3 | Free cooling with mechanical ventilation system | 1 | Night cooling |
| V-6 | Reporting information regarding IAQ | 1 | Air quality sensors (e.g. CO2) and real time autonomous monitoring |
| L-1a | Occupancy control for indoor lighting | 3 | Automatic detection (manual on / dimmed or auto off) |
| L-2 | Control artificial lighting power based on daylight levels | 4 | "Automatic dimming including scene-based light control (during time intervals, dynamic and adapted lighting scenes are set, for example, in terms of illuminance level, different correlated colour temperature (CCT) and the possibility to change the light distribution within the space according to e. g. design, human needs, visual tasks)" |
| DE-1 | Window solar shading control | 0 | No sun shading or only manual operation |
| DE-2 | Window open/closed control, combined with HVAC system | 0 | Manual operation or only fixed windows |
| DE-4 | Reporting information regarding performance of dynamic building envelope systems | 1 | Position of each product & fault detection |

| | | | |
|---|---|---|---|
| E-2 | Reporting information regarding local electricity generation | 4 | Performance evaluation including forecasting and/or benchmarking; also including predictive management and fault detection |
| E-3 | Storage of (locally generated) electricity | 4 | On site storage of energy (e.g. electric battery or thermal storage) with controller optimising the use of locally generated electricity and possibility to feed back into the grid |
| E-4 | Optimizing self-consumption of locally generated electricity | 3 | Automated management of local electricity consumption based on current and predicted energy needs and renewable energy availability |
| E-8 | Support of (micro)grid operation modes | 1 | Automated management of (building-level) electricity consumption based on grid signals |
| E-11 | Reporting information regarding energy storage | 4 | Performance evaluation including forecasting and/or benchmarking; also including predictive management and fault detection |
| E-12 | Reporting information regarding electricity consumption | 2 | real-time feedback or benchmarking on building level |
| EV-15 | EV Charging Capacity | 3 | 10-50% or parking spaces has recharging point |
| EV-16 | EV Charging Grid balancing | 0 | Not present (uncontrolled charging) |
| EV-17 | EV charging information and connectivity | 1 | Reporting information on EV charging status to occupant |
| MC-3 | Run time management of HVAC systems | 1 | Runtime setting of heating and cooling plants following a predefined time schedule |
| MC-4 | Detecting faults of technical building systems and providing support to the diagnosis of these faults | 3 | With central indication of detected faults and alarms for all relevant TBS, including diagnosing functions |
| MC-9 | Occupancy detection: connected services | 1 | Occupancy detection for individual functions, e.g. lighting |
| MC-13 | Central reporting of TBS performance and energy use | 3 | Central or remote reporting of realtime energy use per energy carrier, combining TBS of all main domains in one interface |

| | | | |
|---|---|---|---|
| MC-25 | Smart Grid Integration | 0 | None - No harmonization between grid and TBS; building is operated independently from the grid load |
| MC-28 | Reporting information regarding demand side management performance and operation | 2 | Reporting information on current historical and predicted DSM status, including managed energy flows |
| MC-29 | Override of DSM control | 1 | DSM control without the possibility to override this control by the building user (occupant or facility manager) |
| MC-30 | Single platform that allows automated control & coordination between TBS + optimization of energy flow based on occupancy, weather and grid signals | 3 | Single platform that allows automated control & coordination between TBS + optimization of energy flow based on occupancy, weather and grid signals |

# D. Appendix: IV

### D.0.1 Model predictive controller additional scenarios

To complement the two MPC scenarios in the research, additional scenarios are created. Two main subjects of distinction are made. First, alternative sample times are investigated for the baseline MPC with a sample time of 15 minutes. This study is a sensitivity analysis for the sample-time component. The motivation for this additional study is to see the effects of smaller and large sample times on the initial MPC. Having a faster sample time (i.e. 5 minutes) increases the number of evaluation points in the data, therefore it is estimated to give more accurate results. However, computational time will increase. Coarsening the sample time (i.e. 60 minutes) will reduce the computational time and therefore the room for error. Second, changes to the constraints are made with a relationship to the physical system. To study the installed BESS capacity in relation to the MPC results, the maximum capacity constraint is removed. This investigates whether the installed BESS capacity is adequate for the amount of energy demand- or PV generation of the building. Additionally, a scenario on the charging constraint is made where BESS is allowed only to charge with excess PV. Charging the BESS only with PV will increase the renewable energy storage capabilities and therefore be more sustainable in regards to the grid.

In this appendix, the graphs and results are presented in the following order:

1. Scenario A: MPC baseline [Ts=5 min]: Figure D.1
2. Scenario B: MPC baseline [Ts=60 min]: Figure D.2
3. Scenario C: MPC: Infinite BESS capacity: Figure D.3

$$x^{bat,min} \leq x_k^{bat} \qquad \forall k \in N$$

4. Scenario D: MPC: Charge BESS with PV only: Figure D.4

$$p_k^{bat,ch} \leq p_{pv} \qquad \forall k \in N$$

5. KPI Evaluation additional results: Table D.1

### D.0.2 Scenario A: MPC baseline [Ts=5 min]

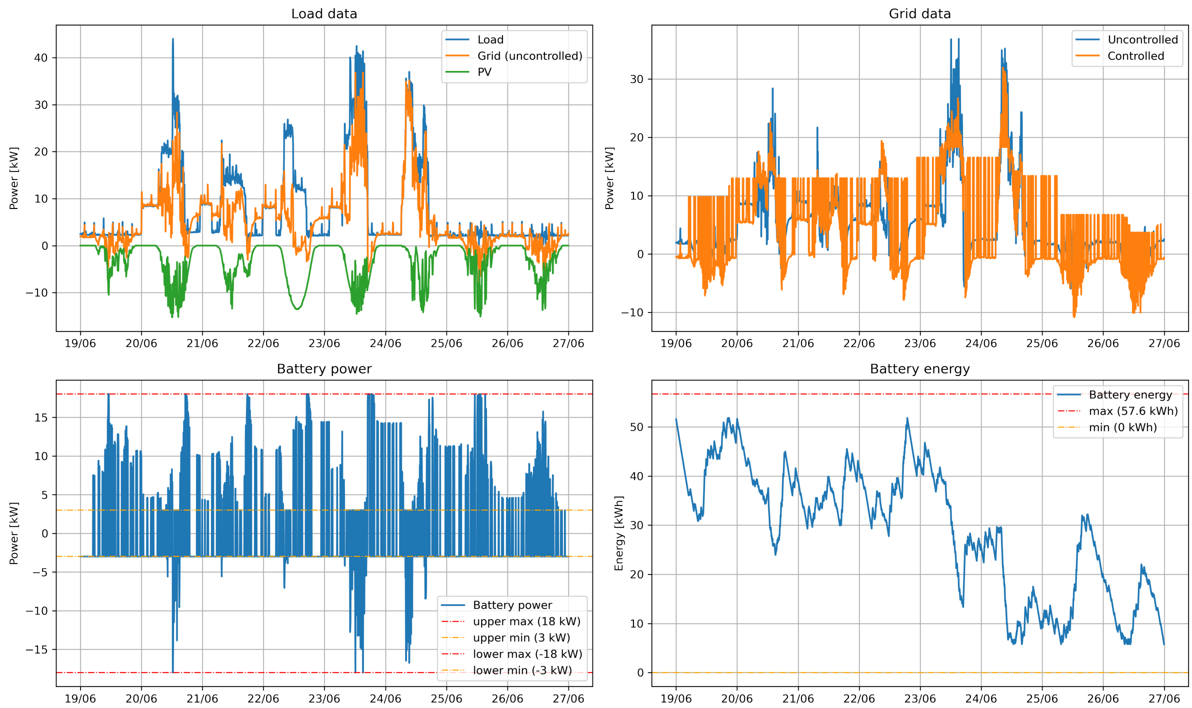


**Figure D.1.** Results of Scenario A.

### D.0.3 Scenario B: MPC baseline [Ts=60 min]

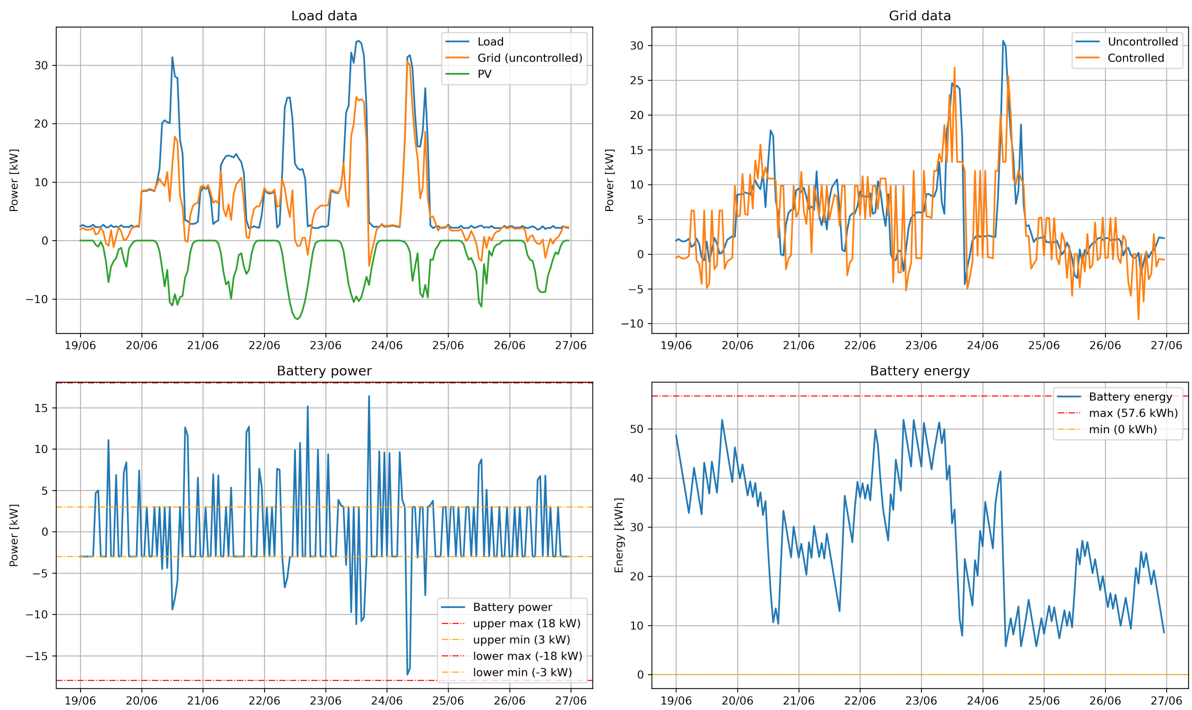


**Figure D.2.** Results of Scenario B.

### D.0.4 Scenario C: MPC: Infinite BESS capacity

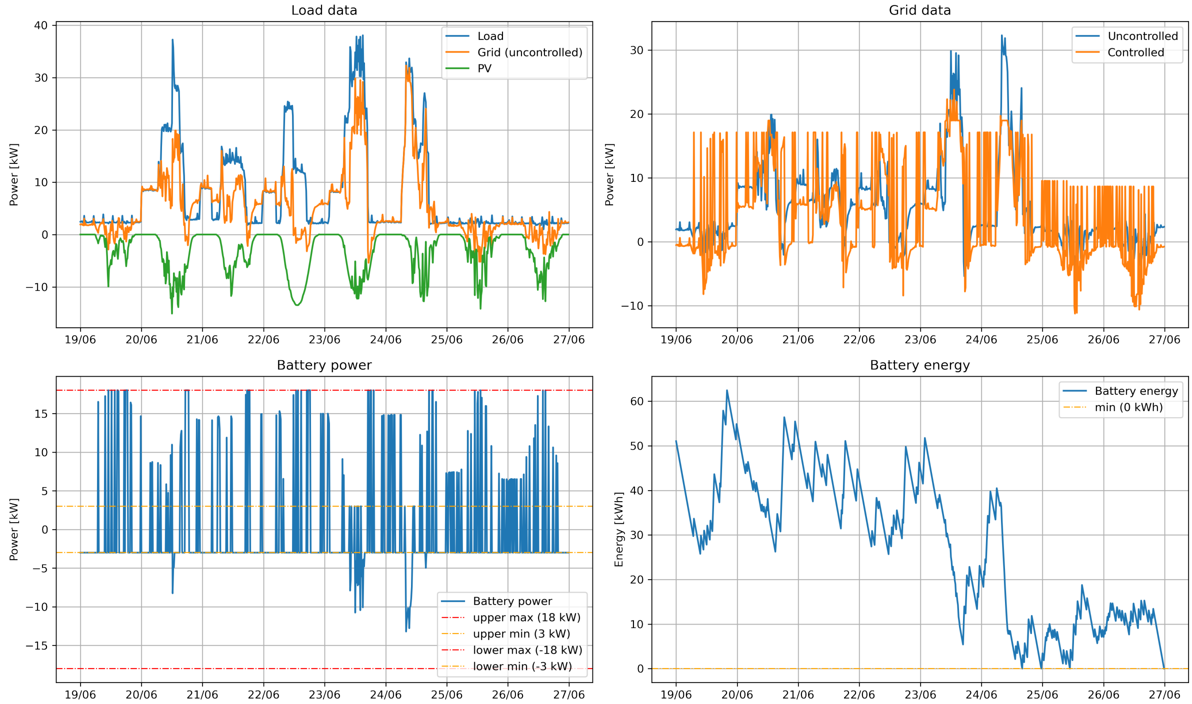


**Figure D.3.** Results of Scenario C.

### D.0.5 Scenario D: MPC: Charge BESS with PV only

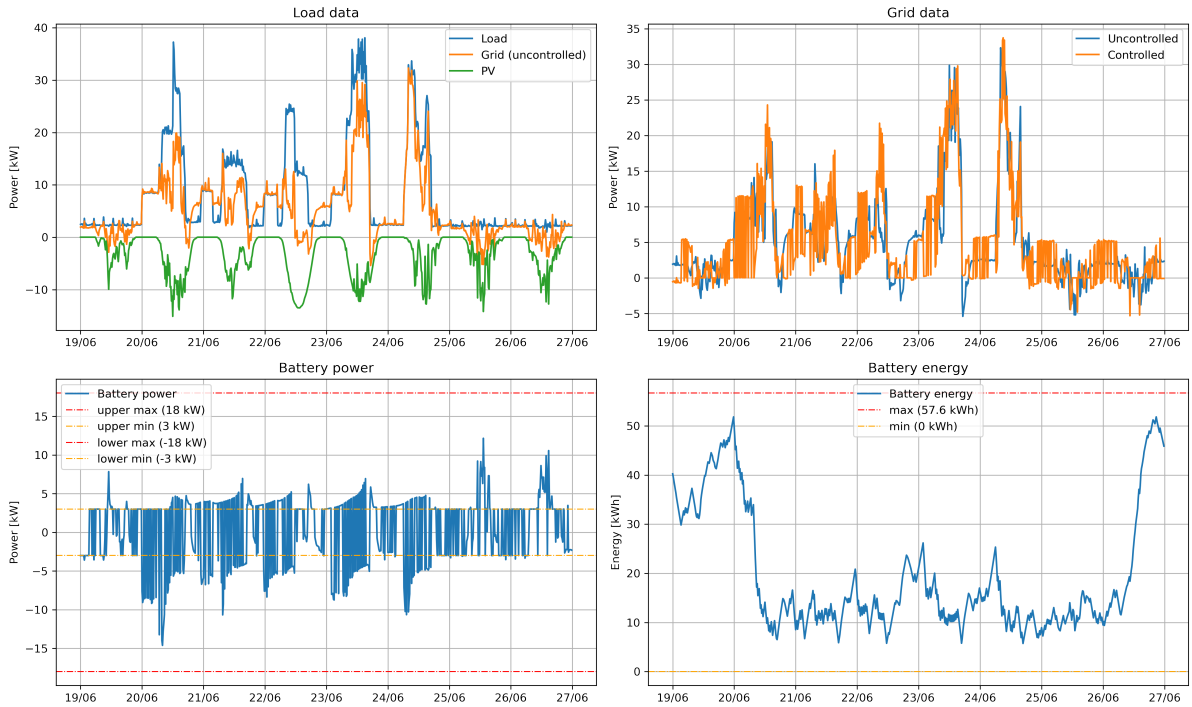


**Figure D.4.** Results of Scenario D.

**Table D.1.** KPI Evaluation.

| KPI | Period | Ideal | Scenario A | Scenario B | Scenario C | Scenario D |
|---|---|---|---|---|---|---|
| Δ P [kW] | *Morning* | [+*] | 8.4 | 5.1 | 11.3 | 1.8 |
| Δ P [kW] | *Afternoon* | [+*] | 4.2 | -2.2 | 4.4 | -0.4 |
| Δ P [%] | *Morning* | [100%] | 27% | 17% | 37% | 6% |
| Δ P[%] | *Afternoon* | [100%] | 17% | -9% | 18% | -2% |
| FF [%] | *Horizon* | [0%] | -23% | -7% | -10% | -17% |
| SS [%] | *Horizon* | [100%] | 8% | 0% | -7% | 34% |
| SC [%] | *Horizon* | [100%] | 91% | 89% | 85% | 99% |
| FI[%] | *Horizon* | [100%] | -7% | -24% | -2% | 2% |

* Ideally, the values for Δ P should be as high as possible. Negative values indicate an increase in power demand.

When the sample-time MPC scenarios are evaluated, it can be concluded that the baseline of 15 minutes is sufficient. With a sample time of 5 minutes, the BESS outputs are fluctuating even more. In the current stages of MPC development, battery life is not included. Therefore, more fluctuations in BESS behaviour are undesirable. With a sample time of 60 minutes, the interaction is too slow and coarse. The SS reduces significantly as inputs are too slow to store excess PV during the late hours of the afternoon. Therefore, the sample time of 60 minutes is less ideal.

The changed constraints resulted in interesting findings. First, increasing the installed BESS capacity is not necessary. If this were not the case, a massive increase in charging would have been observed during valley filling hours. However, the BESS is only charged until approximately 63 kWh. Therefore, increasing the BESS capacity with only 5 kWh supports the conclusion. Thus, increasing the BESS capacity is not essential in the case study. Second, when the BESS is only charged with excess PV it can be observed that during the week, the SOC of the BESS does not reach high values as the amount of excess PV is little. However, during the weekend the BESS is charged. Therefore, the SS and SC are significantly higher in comparison with the other scenarios, however, the PPR during morning and afternoon are extremely low. Thus, as a balance between all six KPIs is desirable, this study shows that charging only with PV can increase SS and SC. However, the overall score is to be evaluated and therefore additional power from the grid to compensate for the peaks in the morning is more efficient.

# E. Appendix: V

### E.0.1 Forecasting model analysis

Prior to the forecasting model development, an extensive data analysis is executed. Data from the years 2016 until 2021 is analysed and this appendix presents the most important findings. It should be noted, during the years 2020 and 2021, Covid-19 interacted with the data.

Heat maps for all individual components are created to analyse possible deviations in the data over the years. This will visually give an idea of whether changes in data registration or behaviour are occurring. As the building load shows in most cases a repetitive pattern. Investigating individual components will give insights into the behaviour of the building installations. Thus, heat maps for the years 2016, 2017, 2018 and 2022 are created to analyse possible changes in behaviour.

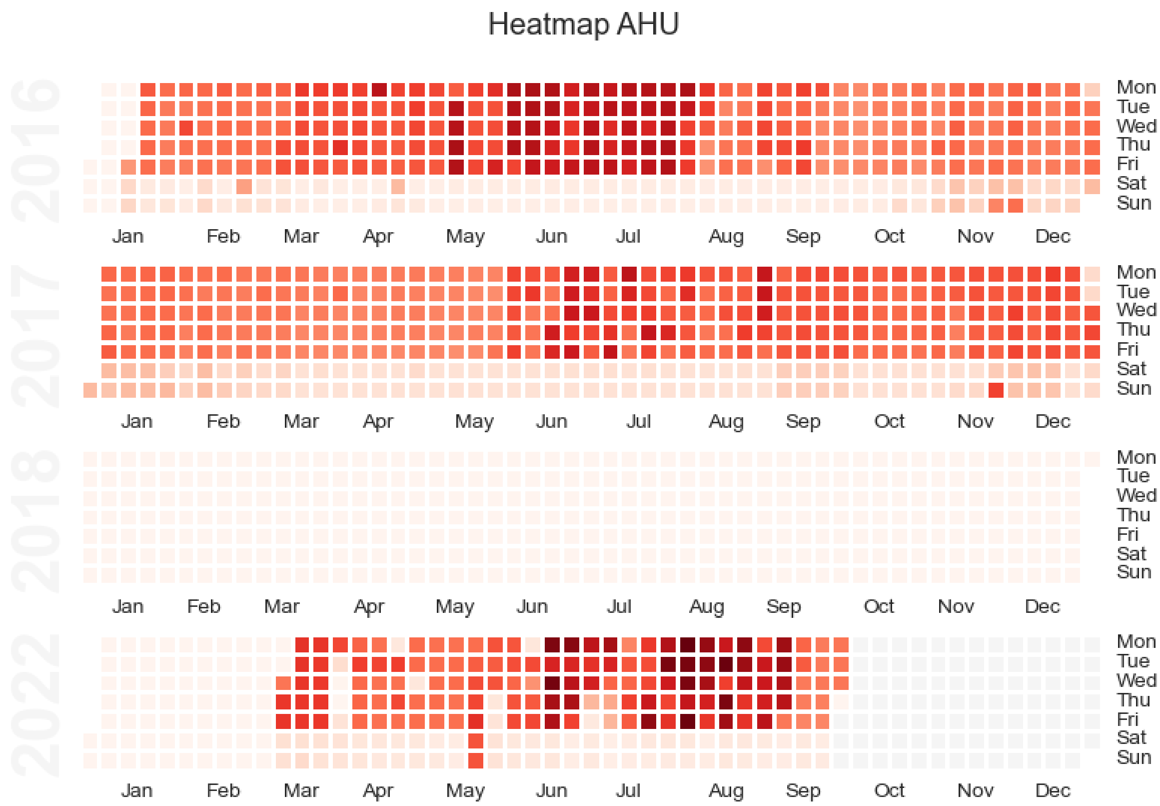


**Figure E.1.** Visualization of air handling unit data.

One big aspect which is directly visible is the data in the year 2018 is significantly lower and deviates from the pattern occurring in the previous and the current year. The results for the AHU are presented in Figure E.1.

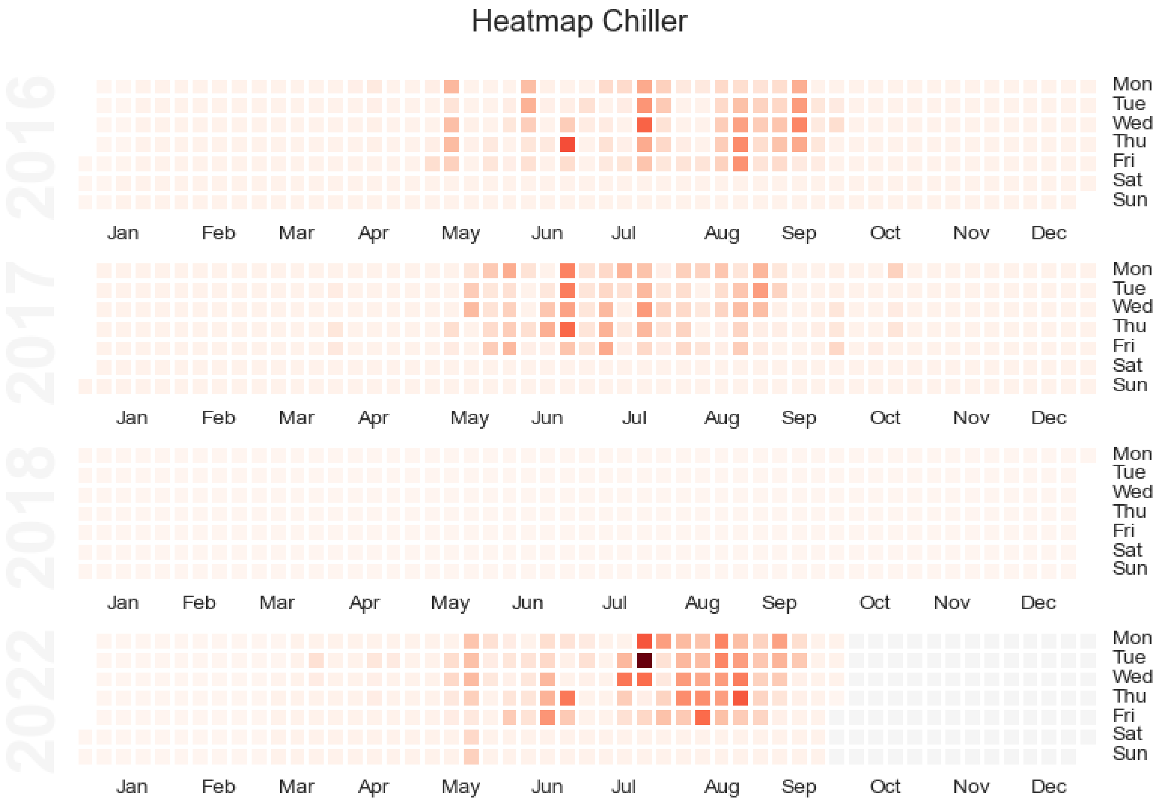


**Figure E.2.** Visualization of the chiller data.

As is the case for the AHU, the chiller data showed deviations in the year 2018. A general trend of the chiller using energy during the summer can be observed which is in line with the expectations as temperatures are higher and the building is cooled down. The results for the chiller are presented in Figure E.2.

In contrast to the chiller, the humidifier is expected to demand energy during the colder and dryer months. This is exactly the case for the years 2016 and 2017. However, in 2022 some unexpected behaviour is occurring with the humidifier as the humidifier is not showing to use as much energy as expected. Therefore, if ML models are to be trained with more recent data, this deviation is to be considered. The results for the humidifier are presented in Figure E.3.

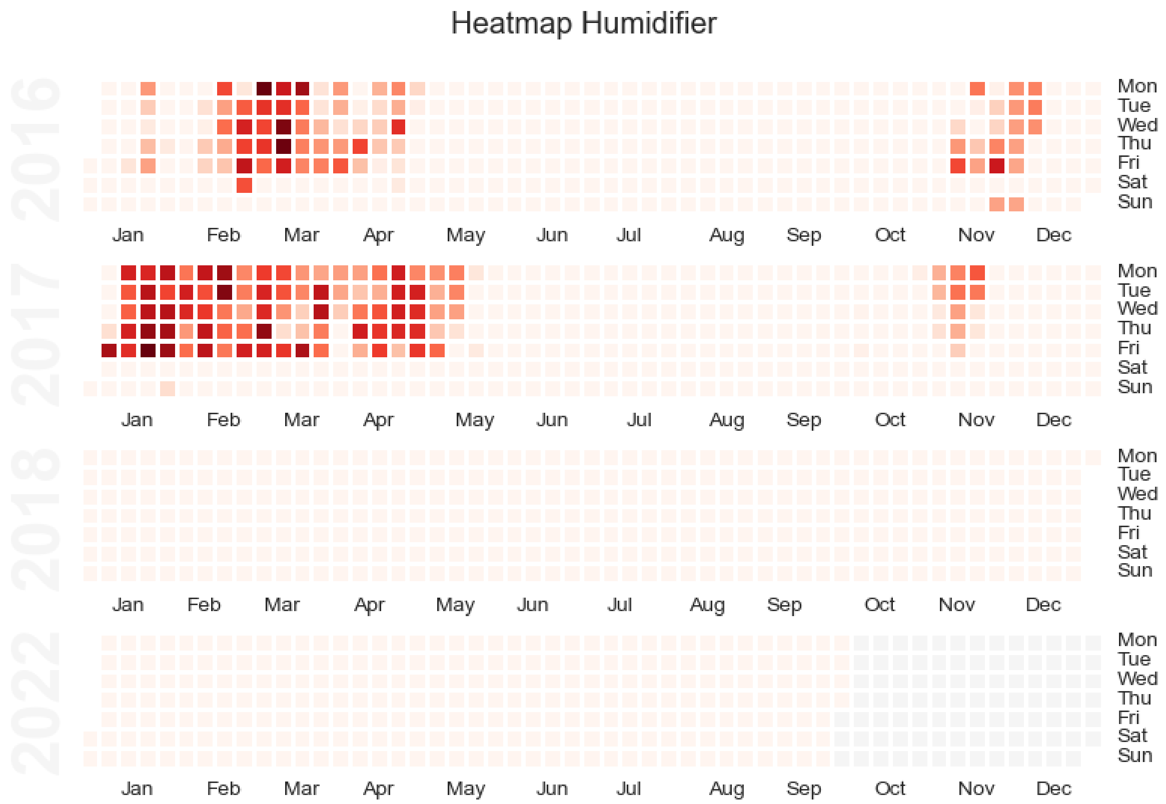


**Figure E.3.** Visualization of the humidifier data.

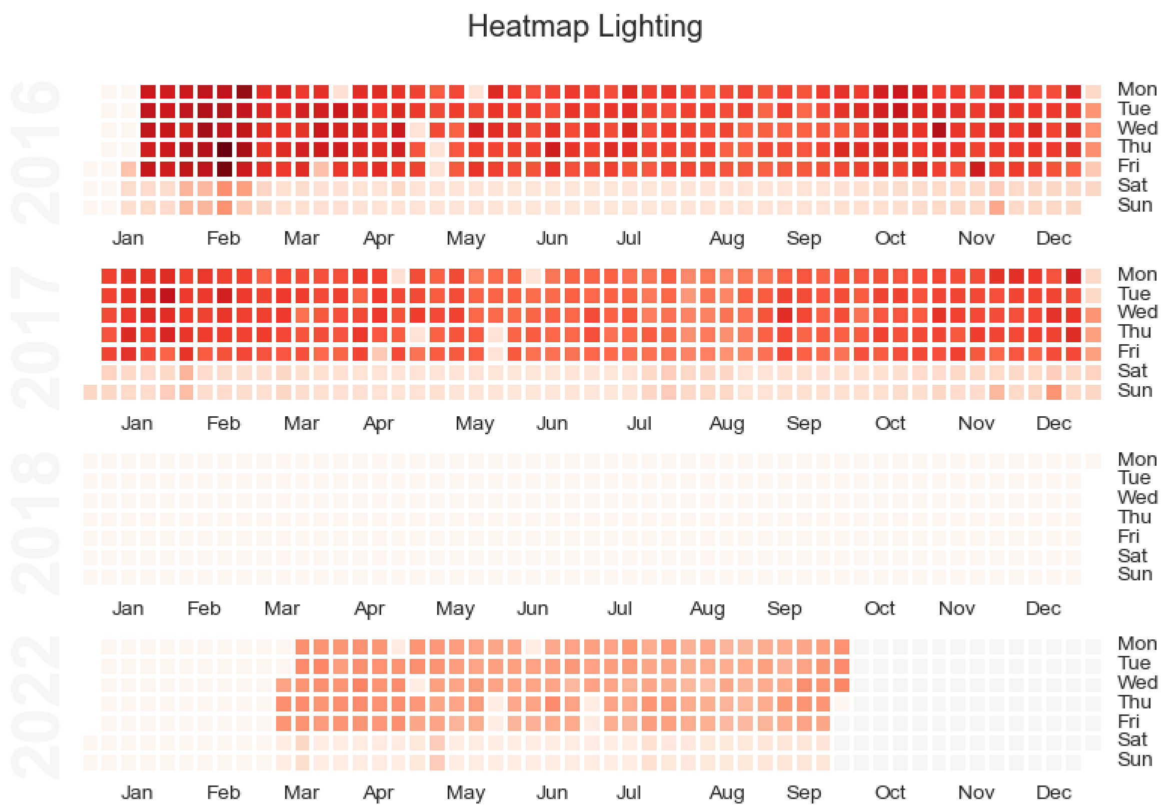


**Figure E.4.** Visualization of the lighting data.

Within the years 2016 and 2017, not much change in lighting use can be observed. The weekdays and weekends are distinguished. When more recent data from the year 2022 is investigated. A global trend is visible wherein the amount of energy used for lighting in these years is less compared to previous years. Therefore, when an ML model is created, a trend in overestimation could occur as lighting is a repeatable variable and should therefore not influence the accuracy of the forecasting model much. However, global overestimation should be considered. Moreover, excluding lighting from the overall building load mix, might result in a higher accuracy overall as historical data does not represent recent data. The results for the lighting are presented in Figure E.4.

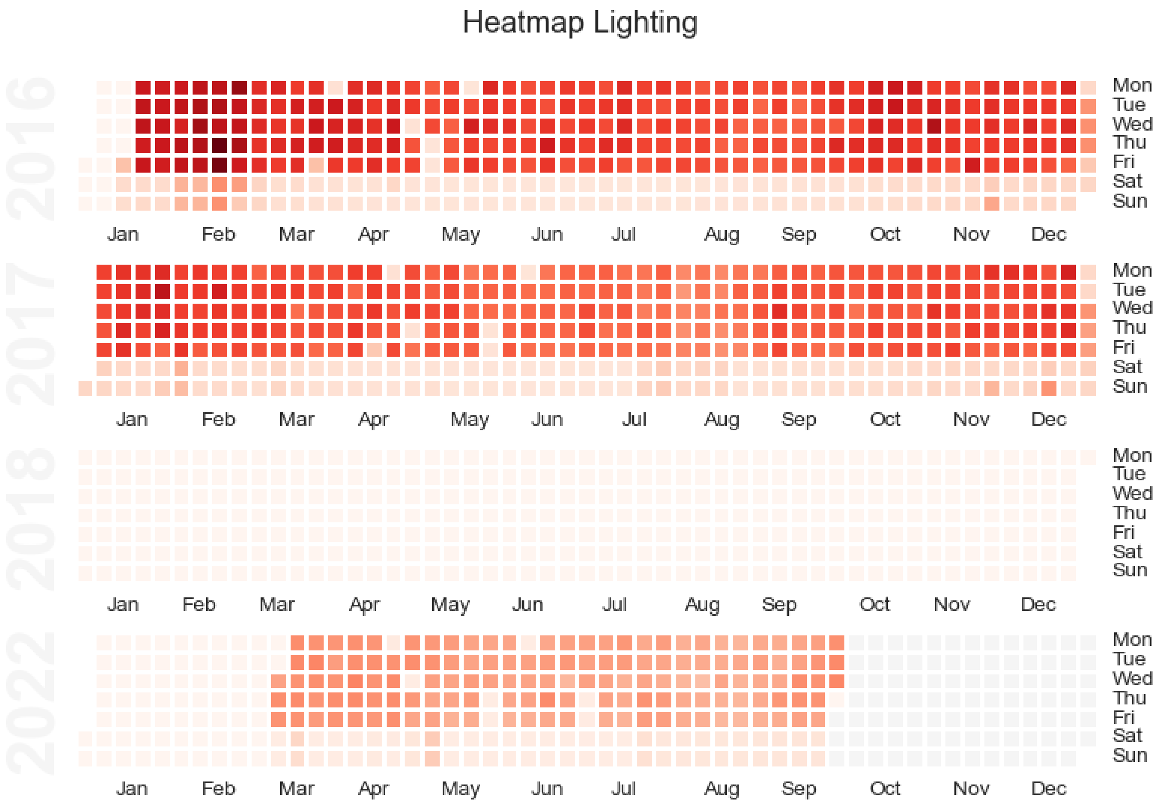


**Figure E.5.** Visualization of the humidifier data.

The power meter of the building is a summation of all meters except the lighting. The power meter in the year 2018 clearly shows no use as the data is completely different. Interestingly the missing data from the humidifier in 2022, results in lower energy demand during the colder months. The results for the power are presented in Figure E.5.

Disregarding the data analysis results, ML models are created for all logical year combinations. Figure E.6 visualizes the results as error metrics are evaluated. In summary, only the years 2016 and 2017 combined show sufficient results as other years have missing- or manipulated data. In addition, the influence of Covid-19 resulted in the years 2019, 2020 and 2021 being unusable. Thus, this analysis supported the decision of why 2016 and 2017 are used to create forecasting models for the year 2022.

| Years | Train/test | MSE | MAE | MAPE [0-1] | CV-RMSE [0-1] | CV-RMSE [%] | CV-RMSE [<30%] | CV-RSME [Deviation] |
|---|---|---|---|---|---|---|---|---|
| **2016-2017** | Train (80%) | 0.618 | 0.421 | 0.111 | 0.064 | 6% | TRUE | [-] |
| | Test (20%) | 2.213 | 1.377 | 0.200 | 0.271 | 27% | TRUE | 3% |
| **2018-2019** | Train (80%) | 1.291 | 0.727 | 0.111 | 0.155 | 16% | TRUE | [-] |
| | Test (20%) | 3.110 | 1.966 | 0.335 | 0.398 | 40% | FALSE | -10% |
| **2019-2020** | Train (80%) | 1.259 | 0.773 | 0.128 | 0.146 | 15% | TRUE | [-] |
| | Test (20%) | 2.730 | 1.560 | 0.283 | 0.335 | 34% | FALSE | -4% |
| **2020-2021** | Train (80%) | 0.875 | 0.540 | 0.090 | 0.101 | 10% | TRUE | [-] |
| | Test (20%) | 3.904 | 1.967 | 0.223 | 0.482 | 48% | FALSE | -18% |
| **2018-2020** | Train (80%) | 0.960 | 0.608 | 0.103 | 0.113 | 11% | TRUE | [-] |
| | Test (20%) | 2.654 | 1.633 | 0.300 | 0.330 | 33% | FALSE | -3% |
| **2018-2021** | Train (80%) | 1.156 | 0.722 | 0.121 | 0.136 | 14% | TRUE | [-] |
| | Test (20%) | 4.221 | 2.342 | 0.355 | 0.520 | 52% | FALSE | -22% |

**Figure E.6.** Error metrics for all forecasting models created per year.